THE ROLE OF EPENDYMOGLIAL CELLS IN THE REGENERATION OF ZEBRAFISH TELENCEPHALON

Tamara Đurović

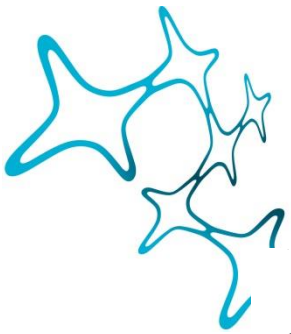

Graduate School of
Systemic Neurosciences
LMU Munich

Dissertation at the
Graduate School of Systemic Neurosciences
Ludwig-Maximilians-Universität München

April 4th, 2020

Supervisor
Prof. Dr. Jovica Ninković
Zellbiologie Department
Biomedizinisches Zentrum – BMC
Ludwig-Maximilians-Universität München

Institute of Stem Cell Research
Helmholtz Zentrum München

First Reviewer: Prof. Dr. Jovica Ninković
Second Reviewer: Dr. Leanne Godinho

Date of Submission: 04.04.2020.
Date of Defense: 30.07.2020.

Table of Contents

1. ABSTRACT 4
2. INTRODUCTION 5
2.1. Consequences of traumatic brain injury 5
2.2. Adult neurogenesis in mammalian brain 6
2.3. Neurogenic niches in the adult zebrafish brain 9
2.4. Ependymoglia behavior in physiological conditions 11
2.5. Ependymoglia behavior after the injury 14
2.6. The role of inflammation in successful zebrafish brain regeneration 17
2.7. Molecular pathways driving ependymoglia activity after an injury 18
2.8. Ahr signaling 19
3. AIMS OF THE THESIS 21
3.1. Aim of the study I 23
3.2. Aim of the study II 48
3.3. Aim of the study III 60
4. DISCUSSION 74
4.1. AhR and the stemness 78
4.2. Closing remarks 80
5. REFERENCES 82
Publications 91
Author contributions 92
Acknowledgements 95

1. ABSTRACT

Achieving successful brain regeneration in humans is currently one of the biggest challenges in the field of regeneration studies. In contrast, regeneration competent species such as the zebrafish, have a remarkable capacity for regeneration and neurogenesis after injury. Ependymoglial cells of the zebrafish brain, among which a subset act as progenitors, react to an injury and generate new neurons that subsequently migrate towards the lesion site and contribute to repair. Understanding the cellular and molecular details of regeneration in zebrafish could potentially offer targets for therapeutically relevant interventions in humans. In order to study ependymoglia behavior in depth, I developed an electroporation technique to reliably label high numbers of ependymoglial cells in vivo. Additionally, I adapted functional usage of StagR-Cas9 method in the adult zebrafish telencephalon in vivo, which allowed us to genetically manipulate multiple genes in ependymoglial cells.

I then used the developed live imaging methodology to analyze the diversity of ependymoglial response to injury in the *Tg (gfap:GFP*) zebrafish line and discovered two subpopulations of ependymoglial cells – GFP high and GFP low with their different reactions. I observed that the GFP low subpopulation directly converts to post-mitotic neurons in response to the injury and engages in restorative neurogenesis.

To understand the molecular mechanisms underlying successful regenerative neurogenesis, I focused on the behavior of the GFP low ependymoglia. I made use of the existing transcriptome analysis of this glial population and identified aryl hydrocarbon receptor (AhR) to be involved in regulation of ependymoglia behavior after injury. More specifically, inactivation of AhR signaling shortly after the injury promoted ependymoglia proliferation, whereas return of AhR to basal levels - around 7 days post-injury, promoted direct conversion of ependymoglial cells into neurons. Moreover, I was able to show that GFP low ependymoglia have high AhR signaling levels and regulate it in response to the injury. Interfering with proper regulation of AhR signaling after the injury led to inappropriate timing of generation of new-neurons and failed restorative neurogenesis.

Taken together, the core data I present in this thesis identified AhR to be an important regulator of ependymoglia behavior and their timely coordination after the injury. More precisely, AhR is a crucial factor involved in proper timing of restorative neurogenesis and successful regeneration in zebrafish, which has insofar been previously unknown.

2. INTRODUCTION

2.1. Consequences of traumatic brain injury

The brain is the highest control center of our body, and any disturbance to its inner balance has serious consequences. For instance, traumatic brain injury (TBI) is one of these such devastating disorders, being the leading cause of mortality in United States in patients below 45 years of age (Sun, 2014). Severe disability is another outcome of TBI, encompassing various psychological, cognitive, and physical impairments, such as a vegetative state or ´´unresponsive wakefulness syndrome´´, motor and sensory deficits, loss of attention and memory, depression, anxiety, and seizures (Stocchetti and Zanier, 2016). Consequently, TBI patients have difficulties leading a normal, fulfilled, life and many of them have long-term disabilities including loss of working capability and employment.

On the physiological and cellular level, a number of pathological changes accompany traumatic brain injury. Depending on the type of injury, different responses can be observed, such as wound healing and tissue repair after acute and focal injuries, or more gradually progressing tissue changes after a diffuse type of TBI. Generally, neurons and the other parenchymal cells at the site of injury undergo cell death, followed by an initial brain reaction of immune cell recruitment and initiation of debris removal. Unfortunately, mature neurons surrounding an injury do not divide, meaning that brain circuits which are damaged cannot be self-repaired. Glial cells, being the key players in the maintenance and homeostasis of the healthy CNS, also show a strong response to an injury. Processes of resident microglia and neural/glial antigen 2 positive ($NG2^+$) cells rapidly accumulate at the injury site (Burda and Sofroniew, 2014; Davalos et al., 2005; Nimmerjahn et al., 2005) and together with astrocytes, participate in reactive gliosis. Dependent on the severity of injury, reactive gliosis can range from cellular hypertrophy and proliferation, to formation of a glial scar in the most extreme cases. Scar borders are formed by reactive astrocytes, which isolate and protect surrounding healthy tissue by separating it from injured and damaged tissue. Scar-forming astrocytes play a vital role in restricting the injured area, as well as in influencing inflammatory responses, and would healing (Burda et al., 2016). In addition, despite the long held belief that scar formation inhibits axonal outgrowth and represents barrier for new synapse formation, more recent research gives opposite evidence – that astrocyte scar formation instead aids axonal regeneration, as shown after spinal cord injury (Anderson et al., 2016).

Independent from the debate on beneficial or detrimental effects of scar tissue, it is an unfortunate reality that the human brain does not successfully regenerate itself. The greatest obstacle for successful self-repair, maybe even bigger than the existence of scar

tissue, is that functional neurons and their related circuits irreversibly disappear after TBI, as mentioned above.

However, one of the biggest turning points that raised hopes toward the possibility of neuronal replacement was the discovery of neural stem cells in specialized niches. These neural stem cells give rise to newborn neurons in the adult brain, which is a contrary notion to the previously held dogma. Since this discovery, a significant amount of research effort has been devoted to understanding the consequences of TBI and establishing different approaches to replace neurons and utilize stem cells in brain repair. Currently, there are three main directions in neuronal replacement research – usage of stem cells from exogenous and endogenous sources, as well as direct neuronal reprogramming of local glial cells into neuronal fates (Grade and Götz, 2017). Although these approaches have different success and development rates, and some of them are promising, none have yet reached the stage to be broadly used in routine clinical applications.

The focus of this thesis is on natural responses of neuronal progenitors after injury, i.e. endogenous neurogenesis. Even though there is still a long way to go until broad clinical application, as will be discussed in detail below, large bodies of research suggest that there is significant potential in endogenous neuronal progenitors to generate newborn neurons. Most notably, this potential has been shown to occur outside of the traditionally known neurogenic niches found in lateral ventricles and dentate gyrus.

2.2. Adult neurogenesis in mammalian brain

As mentioned in the paragraph above, two main neurogenic niches were discovered and are traditionally known within the adult mammalian brain – the subependymal zone of the lateral ventricles (SEZ) and the subgranular zone (SGZ) of the dentate gyrus (DG) in the hippocampus (Altman and Das, 1965; Lois and Alvarez-Buylla, 1993). Both SEZ and SGZ contain neural stem cells (NSCs) embedded in a neurogenic niche, which additionally comprises of multiple cell types, such as endothelial cells, astrocytes, microglia, and progeny of NSCs. All these cells act in a synchronous manner in order to regulate constitutive adult neurogenesis in these niches (Bond et al., 2015). Under normal physiological conditions, NSCs in the SEZ proliferate and generate neuronal precursors that migrate within a path called rostral migratory stream towards the olfactory bulb, where they differentiate into granule and periglomerular neurons (Alvarez-Buylla and Garcia-Verdugo, 2002; Doetsch and Alvarez-Buylla, 1996). Neural stem cells in the SGZ give rise to intermediate progenitor cells and neuroblasts that migrate towards the dentate gyrus where they differentiate into fully functional hippocampal neurons (van Praag et al., 2002a).

Besides these two major neurogenic zones, research suggests that the adult mammalian brain harbors additional places of residence for adult NSCs, such as cerebellum, hypothalamus, substantia nigra, and amygdala (Oyarce et al., 2014). Nevertheless, these niches are less active and show lower rates of neurogenesis, and their contribution to repair still remains to be fully explored (Oyarce et al., 2014). Additionally, it has been shown that there is substantial adult neurogenesis present in humans in the striatum as well (Ernst et al., 2014). Besides humans, adult striatal neurogenesis has been observed in different species such as non-human primates, rats, and rabbits. However, striatal neurogenesis was not found in adult mice in physiological conditions (Inta et al., 2015), or if it exists, it is speculated that it is probably occurring at a very low rate (Nemirovich-Danchenko and Khodanovich, 2019). The origin of striatal progenitors is still controversial, however, there are studies showing that at least partially, progenitors are originating from SEZ (Luzzati et al., 2006).

The cortex is another highly controversial brain region regarding adult neurogenesis. Most of such studies observe no newly generated neurons in the cortex of the adult mammalian brain, done for example in adult macaque monkeys (Koketsu et al. 2003; Kornack and Rakic 2001; Liu et al. 2020), in rodents (Ehninger and Kempermann, 2003; Madsen et al., 2005) or in humans (Bhardwaj et al., 2006; Ernst et al., 2014; Spalding et al., 2005). However, some studies suggest that new neurons are generated in adult rats (Dayer et al. 2005) or monkeys (Bernier et al., 2002; Gould et al., 2001). Nevertheless, the number of these new-born neurons is rather low, or they have transient existence and their origin has yet to be established (Gould et al., 2001).

Brain damage, injuries, and different pathological states exert a strong influence on neurogenesis and migration of progenitors in the adult mammalian brain. Generally, neural progenitors are activated in SEZ after TBI and are found to proliferate and be migratory (Chang et al., 2016). However, different studies often show contradictory results.

For instance, in the damaged hippocampus under ischemic condition, where massive neuronal death has been observed, new neurons migrate from the posterior periventricular region (pPV) (Nakatomi et al., 2002) or are generated both in the pPV and locally in SGZ of the DG (Bendel et al., 2005). Similarly, in the damaged striatum, many young neurons can be observed. It has been shown in adult rats that the production of new neurons lasts for at least 4 months after striatal insult (Arvidsson et al., 2002; Thored et al., 2006). Nonetheless, their origin is still questionable. Many studies observed that the source of new neurons is SEZ (Arvidsson et al., 2002; Thored et al., 2006; Yamashita et al., 2006), yet some more recent studies reported that most of new striatal neurons induced by injury originated locally from neighboring astrocytes (Magnusson et al., 2014; Nato et al., 2015).

The situation in the cortex is not very different, with inconsistent results obtained from various studies. It is established that there is neurogenesis in the damaged cortex of the adult mammalian brain, however the origin of these cells is still open to debate and it is unclear

whether new neurons derive from SEZ/pPV or are generated locally. Some studies discovered proliferating progenitors in the damaged cortex and concluded that none or only a few new neurons migrate from the SEZ (Fukuzaki et al., 2015; Kuge et al., 2009; Ohira et al., 2010), whereas other studies could not confirm origin of new neurons from local progenitors such as astrocytes for instance (Buffo et al., 2008), and showed that most of new neurons originated in SEZ (Brill et al., 2009; Faiz et al., 2015; Magavi et al., 2000).

It is noteworthy that the difference in all the above-mentioned studies lies in the condition of the experiments, as well as the type and severity of injury induced, which is very likely the explanation for observed discrepancies between different studies. However, independently of the origin of neuronal progenitors, most of these studies agree that there is damage-induced neurogenesis occurring outside of the previously well-known neurogenic niches. Nonetheless, the question of functional relevance of these new neurons is crucial for future regenerative therapies. Predominantly, studies have shown a limitation when it comes to functional integration of new neurons and repair of lost circuits, mostly due to short and rather low survival of these neurons and lack of adequate variety of different neuronal subtypes that are generated after injury. For instance, majority of new neurons in damaged striatum die (Arvidsson et al., 2002; Dimou and Gotz, 2014; Thored et al., 2006), possibly due to inflamed surrounding tissue and unfavorable environment conditions.

Nevertheless, as already mentioned, the majority of the studies found that there is also damage-induced neurogenesis outside of the two main neurogenic niches, which raises hopes for usage of endogenous stem cells for brain repair, and represents the first step towards development of optimal therapies for the improvement of restorative neurogenesis. Therefore, more research is evidently necessary to understand the mechanisms of endogenous injury-induced neurogenesis in the adult mammalian brain. Towards this end however, further research of species that are in fact capable of self-repair, such as zebrafish, could offer valuable insights. Comparison between non-regenerative and regenerative species would shed light on the key differences and similarities between different regeneration dynamics, which is crucial for further understanding of the entire self-regenerative process.

2.3. Neurogenic niches in the adult zebrafish brain

Compared to the adult mammalian brain, zebrafish have evolved different strategies for regeneration. Similarly to its closely related species, such as bony fishes, rays, sharks, amphibians, or reptiles, zebrafish have abundantly present neurogenic niches in comparison to mammals, even in the adult stage (Dimou and Gotz, 2014). That being the case, zebrafish possess a remarkable capacity to fully regenerate brain tissue and restore lost neurons without scarring (in most injury models of zebrafish telencephalon observed until now) (Ayari et al., 2010; Barbosa et al., 2015; Baumgart et al., 2012; Becker and Becker, 2008; Cosacak et al., 2015; Kishimoto et al., 2012; Kizil et al., 2012a; Kroehne et al., 2011; März et al., 2011).

This large number of adult NSCs niches in zebrafish is spatially widespread along the entire rostro-caudal brain axis in contrast to mammals (Fig. 1). All the niches in the brain are enriched for certain type of progenitors, many of them being neuronal progenitors too. Constitutive adult neurogenesis, that relies on activity of these progenitors, occurs lifelong with an age-dependent decline (Zupanc et al., 2005; Grandel et al., 2006; Kizil et al., 2012a; Edelmann et al., 2013). Therefore, proliferation of adult neuronal progenitors contributes to continuous generation of new neurons, which are becoming part of existing circuitries. In this manner, the zebrafish brain also grows during the entire life, due to consistent turnover and overall addition of new neurons (Adolf et al., 2006; Kizil et al., 2012a; Schmidt et al., 2013).

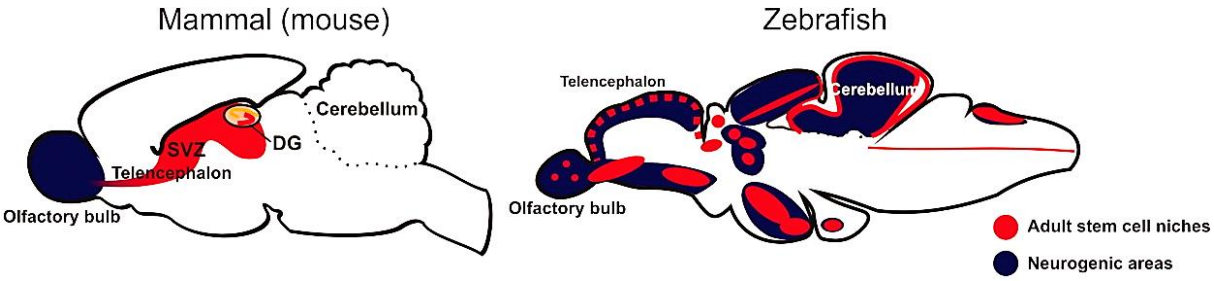

Figure 1. Neurogenic regions of the zebrafish brain in comparison to mammals. (Kizil et al. 2012) Adapted by copyright permission from John Willey and Sons and Copyright Clearance Center: *Developmental Neurobiol*ogy 72 (3): 429–61. (Kizil et al. 2012). License No: 4763040196777. (2012). https://doi.org/10.1002/dneu.20918.

Interestingly, anatomical position of most of neurogenic niches in the zebrafish brain is organized differently than in mammals (hypothalamus being the exception (Xie and Dorsky, 2017)), due to the overall variations in general brain morphology. For instance, the zebrafish telencephalon is everted, meaning that, during development, the neural tube is folding in such a manner to promote location and exposure of proliferative periventricular zones on the outer

surface of the telencephalon. This is in contrast with other vertebrates that go through the process called evagination, forming hemispheres that surround ventricles inside of the brain (Folgueira et al., 2012; Schmidt et al., 2013) (see Fig. 2).

Figure 2. Positioning of neurogenic niches in zebrafish (left) and in mammals (right) during development*. Dorsal telencephalic surface is depicted in red, place where neurogenesis occurs. Tela choroidea is represented in green. V – ventricle, Sp – subpallium.* (Folgueira et al., 2012)

Despite the different position of most of the proliferative niches, particular brain structures and regions are speculated to be homologous to mammalian regions. For instance, the central part of the dorsal telencephalon (otherwise known as dorsal pallium), is considered to be homologous to mammalian neocortex (Mueller et al., 2011), and the ventral telencephalon is considered to be homologous to the mammalian SEZ. In this brain region, different populations of slow and fast cycling cells can be found, which express PSA-NCAM (marker for migrating precursor cells) and produce neuroblasts, where some of them migrate towards the olfactory bulb (Alunni and Bally-Cuif, 2016; Glaser et al., 2007; Grandel et al., 2006). The lateral telencephalic region is, on the other hand, considered to be homologous to mammalian dentate gyrus, since it exhibits interneuron production and migration like in mammals. (Grandel et al., 2006).

Another important distinction from mammalian brain is the absence of parenchymal astrocytes in the gray and white matter of zebrafish brain and spinal cord. Instead, most regions of zebrafish brain harbor a specific type of progenitor cells residing in the rich variety of neurogenic niches. In the zebrafish telencephalon, for instance, these progenitors are called ependymoglial cells, residing at the ventricular surface (Adolf et al. 2006; Chapouton et al. 2006; Grandel et al. 2006). Ependymoglia are considered as counterparts of mammalian astrocytes in zebrafish (Alunni and Bally-Cuif, 2016).

Interestingly, the general trend of brain evolution and growing structural complexity seemed to favor astrocyte predominance over ependymoglia in adulthood (Kálmán, 2002). In parallel, higher brain complexity led to decline in regenerative capacity of those species that evolved later. The important question therefore remains – what are the characteristics of ependymoglial cells in contrast to astrocytes, which grant them remarkable regenerative capacity? Hence, further research of ependymoglial cells and their contribution to the successful regeneration existing in zebrafish is essential for understanding significant difference in the regeneration success compared to mammalian brain.

2.4. Ependymoglia behavior in physiological conditions

One of the most studied and understood regions where neurogenesis occurs in zebrafish is the telencephalon. Ependymoglial cells are widely known as cells that constitute the dorsal telencephalic neurogenic niche, among which, a subset acts as constitutively active progenitors.

As previously mentioned, owing to the everted nature of the zebrafish telencephalon, ependymoglial cells reside at the outer surface of the dorsal telencephalon, lining the ventricle and building a, so called, ventral ventricular wall (Fig. 3). The dorsal ventricular wall, also known as dorsal ependymal layer (DEL), is a continuous layer of single cells with classic, multiciliate, and cuboid ependymal morphology. The DEL spreads above and covers the entire roof of telencephalic ventricle (Lindsey et al., 2012) (see Fig. 3).

The morphology of ependymoglial cells resembles mammalian radial glia (Götz et al., 2002), with long radial processes spanning throughout the parenchyma (Fig. 3). These cells are therefore considered to be functional orthologs of mammalian ependymal cells (hence the origin of the name ependymoglia) (Zambusi and Ninkovic, 2020). One of the common features of ependymoglia is their expression of typical glial markers such as intermediate Glial Fibrillary Acidic Protein (GFAP), vimentin, S100ß, Brain Lipid Basic Protein (BLBP), and neuronal progenitor markers, Sox2 and Nestin (März et al. 2010; Kizil et al. 2012), some of which are present in astrocytes too. Additionally, ependymoglial cells and astrocytes share other characteristics, for instance, the presence of water transporting protein aquaporin-4, tight junction proteins on cell membranes and the glutamate transporter Eaat2b. Additionally, both cell types establish connections with neuronal processes through their end feet. All the above-mentioned characteristics represents evidence that ependymoglial cells embody multiple roles in the zebrafish telencephalon – specifically, that of mammalian radial glia, astrocytes, and ependymal cells altogether.

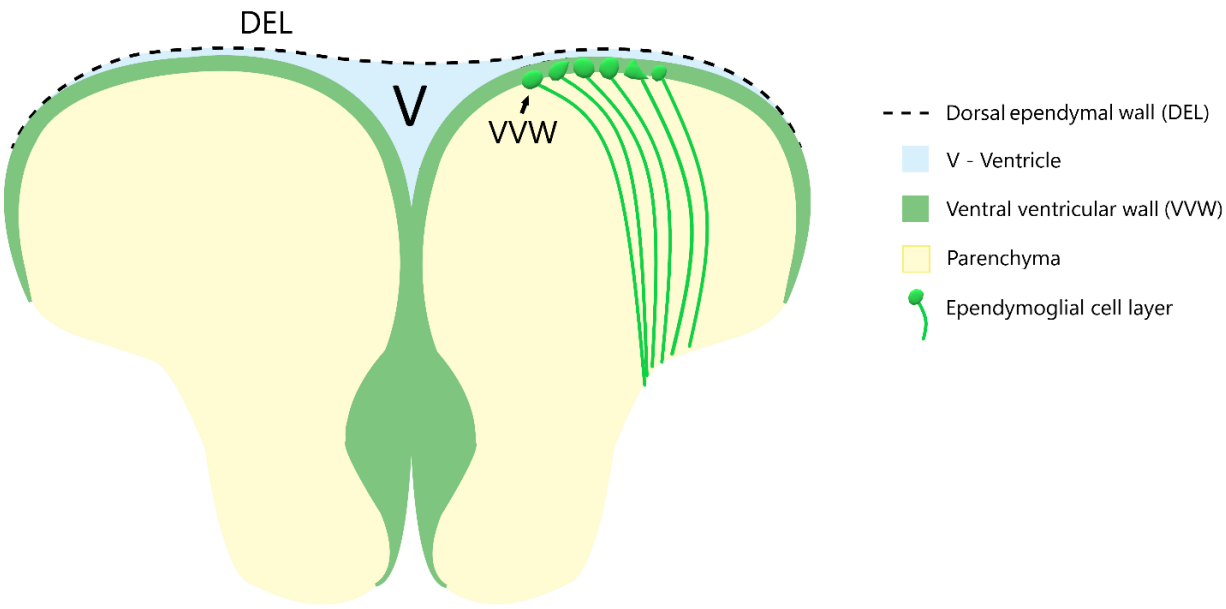

Figure 3. Scheme of coronal plane of the zebrafish telencephalon. *Position of the dorsal ependymal layer is depicted, together with ependymoglial cells constituting ventral ventricular wall (VVW) and ventricle in between.*

It is known that the entire ependymoglial cell population is not identical, and that there is a degree of heterogeneity among individual cells (Lange et al., 2020). Therefore, ependymoglial cells/progenitors are characterized as Type I and Type II progenitor cells in their quiescent and dividing state, respectively. Both Type I and Type II cells express previously mentioned glial markers and progenitor marker Sox2, however, proliferating cell nuclear antigen (PCNA) is present in dividing progenitors only. Besides ependymoglia, Type III cells are additionally present in the telencephalic neurogenic niche and these cells are referred to as neuroblasts. Neuroblasts have been classified to be in either A or B state; A state representing most probably just a transitional phase towards B state. A state neuroblasts still express lower amounts of glial markers, Nestin, Sox 2, PCNA and PSA-NCAM, whereas state B neuroblasts express only Sox 2, PCNA and PSA-NCAM (März et al., 2010; Rothenaigner et al., 2011).

Clonal analysis (Rothenaigner et al., 2011), and later *in vivo* imaging studies (Barbosa et al. 2015), showed a clear lineage relationship between progenitors I/II and III. Moreover, these studies demonstrated that HuC/D positive neurons arise from state III progenitors and that state III progenitors are originating through asymmetric divisions of type I/II progenitors.

This also raises a question about the general activity of progenitors, and indeed the same research showed that the majority of ependymoglia in the zebrafish telencephalon are in a quiescent state (approx. 60%) (Fig. 6). Dividing progenitors make up approx. 13% of the overall population observed (Rothenaigner et al., 2011; Barbosa et al., 2015) (Fig. 6). *In vivo* imaging research has found that among the dividing progenitors in the physiological condition,

there are two modes of division – symmetric gliogenic and asymmetric gliogenic (Fig. 4). During symmetric gliogenic division, one progenitor divides, giving rise to two identical progenitor cell daughters, both having gliogenic fate and typical radial process (see Fig. 4). This mode of division is very rare, accounting for only 1% of dividing progenitors (Barbosa et al., 2015).

Another mode of division, asymmetric division, gives rise to one progenitor cell and one intermediate progenitor (Barbosa et al., 2015). Intermediate progenitors further give rise to neuroblasts and newborn neurons, either directly or through proliferation, and subsequently deposit just below the ependymoglial cell layer within a span of 25µm from the ventricle (Fig. 4). This distance from the ventricle is considered to be the zone of adult constitutive neurogenesis (Barbosa et al. 2015). Asymmetric division is the predominant mode of division in the intact brain (Rothenaigner et al. 2011; Barbosa et al. 2015), simultaneously allowing self-renewal of progenitor cell pool, as well as generation of new neurons.

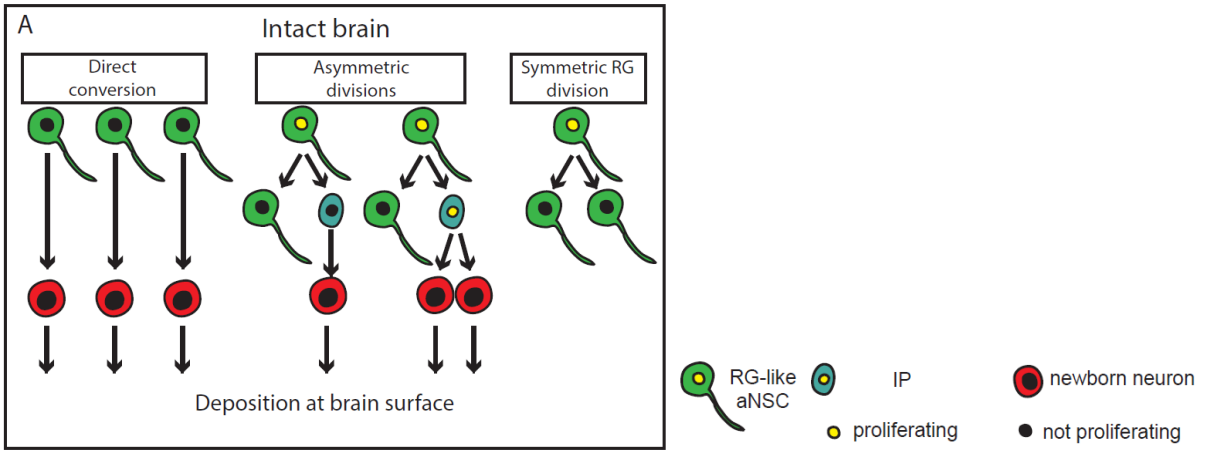

Figure 4. Behavior of ependymoglia (aNSCs) in the intact brain observed through in vivo imaging and ***clonal analysis.*** (Barbosa et al. 2015) Reprinted with permission from The American Association for the Advancement of Science: *Science* 6236 (348): 789-793. (Barbosa et al. 2015). License No: 4798771347469. (2015). DOI: 10.1126/science.aaa2729

Furthermore, Barbosa et al. 2015, observed a third, very interesting behavior, a so called direct conversion. Direct conversion was noticed for the first time using in vivo imaging technique and is characterized by ependymoglial cells directly converting or transforming into neurons, without division or an intermediate progenitor stage. During the process of direct conversion, ependymoglia are subjected to multiple transformations, represented by change in cell morphology, loss of radial process, loss of glial markers, and upregulation of pan-neuronal marker HuC/D instead (Barbosa et al. 2015). Surprisingly, the proportion of directly converting ependymoglial cells in physiological conditions is very high (17% of all

ependymoglial cells) (Barbosa et al. 2015) (Fig. 6), making it the second predominant mode of ependymoglia behavior after quiescence. Directly converted cells, like other daughter cells, accumulate just below the ependymoglia layer, within the range of 25 μm from the surface.

As previously mentioned, there is a constant cycling and transition of ependymoglial or progenitor cells between quiescent and dividing states (März et al. 2010; Chapouton et al. 2010), which makes the whole population very dynamic, and categorization of specific, distinct subpopulations challenging task. For instance, Notch receptors are one of the well-known mechanisms of progenitor pool maintenance. Notch has been found to keep ependymoglia in a quiescent state, whereas its inhibition induces proliferation (Chapouton et al. 2010; Rothenaigner et al. 2011) and in this manner Notch regulates the balance between cycling and quiescent progenitors. Additionally, Alunni et al. 2013 have shown that inhibition of Notch signaling seems to affect predominantly symmetrical and not asymmetrical divisions, and they observed that Notch1b and Notch3 receptors have distinct expression patterns – Notch 3 is present in type I and II progenitor cells, yet is absent from neuronal progenitors (type III), whereas Notch1b is present in dividing ependymoglial/progenitor cells (type II) and neuronal progenitors. Furthermore, they found Notch3 to be main player in maintenance of quiescent progenitor pool, and Notch1b to be responsible for maintenance of progenitor status in contrast (Alunni et al. 2013).

Another mechanism found to be involved in regulation of ependymoglial pools and their quiescence is dependent upon the helix-loop-helix protein Id1. Expression of Id1 in the ventricular zone has been discovered to regulate adult neurogenesis, in a similar manner to Notch3 receptor - Id1 promotes quiescent state of ependymoglia and its deletion leads to induced ependymoglial proliferation and increased neurogenesis (Viales et al., 2015). Furthermore, FgF signaling was shown to regulate division of dorsal and ventral telencephalic progenitors. Downregulation of Fgf signaling leads to a decrease in proliferation, whereas its activation leads to significant increase in proliferation both in dorsal and ventral telencephalic domains (Ganz et al., 2010).

Nonetheless, it remains unclear whether every ependymoglia cell enters the cell cycle in regular intervals, or there is a specific population of progenitor cells responsible for divisions and self-renewal of the progenitor pool, even after large-scale in vivo imaging observation of ependymoglial niche in the intact zebrafish telencephalon (Dray et al., 2015).

2.5. Ependymoglia behavior after the injury

To study regenerative potential in the zebrafish telencephalon, it was necessary to establish an injury model. In 2010, Ayari et al. established a novel stab-wound lesion model,

where a 26-gauge needle was inserted through the fish nostril into the telencephalon parenchyma (Ayari et al., 2010). This injury paradigm, commonly referred to as ´´nostril injury´´, damages only radial processes of ependymoglia residing in the parenchyma.

Over the past decade, a considerable amount of evidence confirmed that ependymoglial cells are the ones that react to injury, proliferate and generate new neurons, independent of the injury model used. In contrast with the intact brain, these newborn neurons migrate longer distances to the lesion site in parenchyma, survive long-term, integrate into the circuits and contribute to repair (Ayari et al. 2010; Kroehne et al. 2011; März et al. 2011; Kishimoto, Shimizu, and Sawamoto 2012; Baumgart et al. 2012; Barbosa et al. 2015).

The findings of Barbosa et al., 2015, unraveled in detail ependymoglia behavior after injury, and identified changes in their mode of behavior in comparison to the intact brain. Not surprisingly, the overall number of proliferating ependymoglia is doubled after an injury (Fig. 6). Interestingly, the asymmetric divisions are still a predominant mode of division among all the dividing cells (75% of all dividing progenitors). However, a new behavior was observed, the so called symmetric non-glial division, where one progenitor gives rise to two intermediate progenitors, which lose ependymoglial characteristics and obtain neuronal features (25% of all dividing progenitors) (Fig. 5). This mode of division was not observed in the intact brain. Additionally, there was no symmetric gliogenic divisions observed after injury. (Fig 5.)

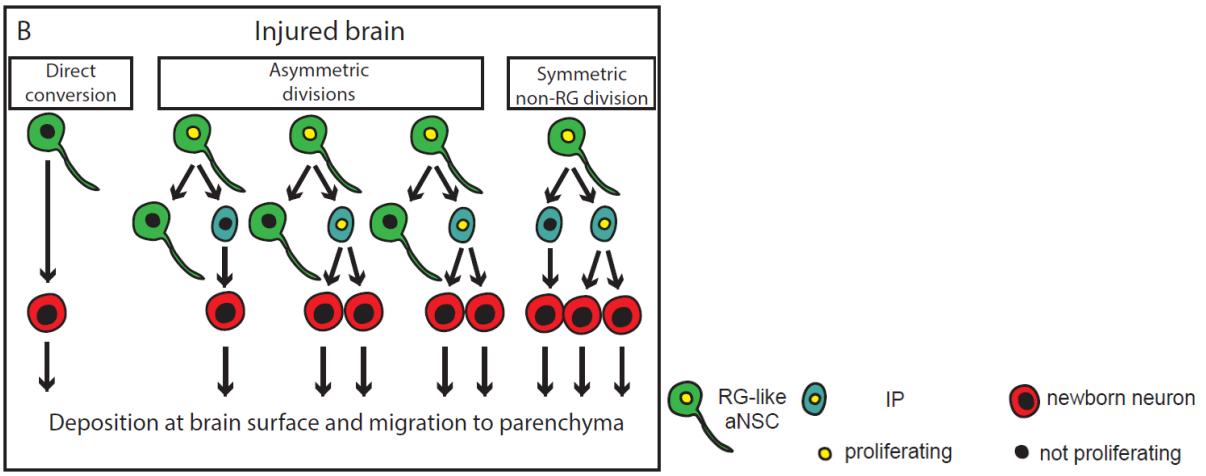

Figure 5. Behavior of ependymoglia (aNSCs) after injury observed through in vivo imaging and clonal analysis. (Barbosa et al., 2015) Reprinted with permission from The American Association for the Advancement of Science: *Science* 6236 (348): 789-793. (Barbosa et al. 2015). License No: 4798771347469. (2015). DOI: 10.1126/science.aaa2729

Furthermore, Barbosa et al., 2015 noticed that increased proliferation of progenitors was followed by increased parenchymal migration (55% in contrast to approx. 8% in the intact brain) (Fig. 6). Parenchymal migration accounts for high number of directly converted cells as well, thus the percentage of directly converted cells in Fig. 6 (approx. 3-4%) is not exact, as it is effectively much higher.

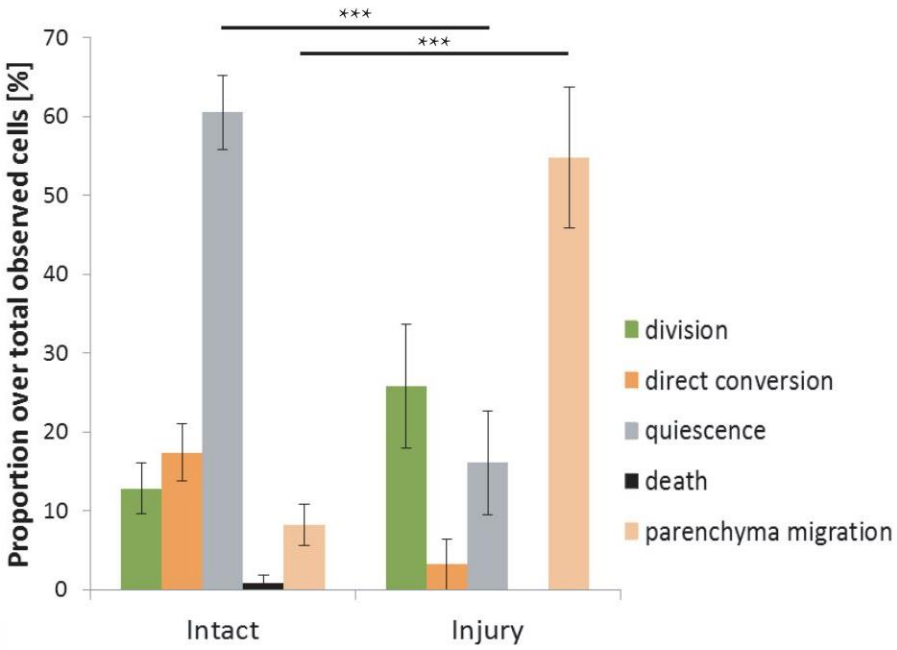

Figure 6. Proportions of different ependymoglia (aNSCs) behaviour in the intact brain and after injury over total number of cells observed through in vivo imaging. (Barbosa et al., 2015) Reprinted with permission from The American Association for the Advancement of Science: *Science* 6236 (348): 789-793. (Barbosa et al. 2015). License No: 4798771347469. (2015). DOI: 10.1126/science.aaa2729

Finally, asymmetric and symmetric non-glial divisions, as well as direct conversions after the injury, altogether increase the neuronal output at the expense of progenitors, which leads to exhaustion and depletion of progenitor pool in the long run. The lack of symmetric gliogenic divisions after injury suggests that maintenance of ependymoglial pool is not the priority in injury conditions in comparison to the intact conditions. The question of maintenance of the ependymoglial pool on both cellular and molecular levels opens new avenues for exploration of long-term regeneration potential of zebrafish.

Nevertheless, when it comes to short-term regeneration in zebrafish after injury, inflammation, together with ependymoglial cells, plays a crucial role in successful repair, which will be discussed further in the next section.

2.6. The role of inflammation in successful zebrafish brain regeneration

After a nostril injury, ependymoglia start reacting already at 2 days post injury (2 dpi) and reach their highest level of proliferation at around 7 dpi (as observed within the scope of the 7 day time frame) (Baumgart et al., 2012). Such a reaction holds similarities with reactive gliosis, reflected in the upregulation of GFAP and swelling of their processes (hypertrophy). However, ependymoglia proliferate and generate newborn neurons (Kroehne et al., 2011). Cellular bodies of ependymoglial cells were not found in the vicinity of injury site, except to some degree in the case of large injury (Baumgart et al., 2012), which is in stark contrast to astrocytes in mice.

Additionally, type III cells or neuronal progenitors have also been observed to proliferate in ventricular zone around 2 dpi. Two different populations of these progenitors were identified - neuronal progenitors positive for PSA-NCAM and another population which is negative for PSA-NCAM, and the reason might be that they are still in the process of maturation towards neuronal fate and therefore did not start expressing PSA-NCAM marker yet (Baumgart et al., 2012). Importantly, constitutive neurogenesis is not disrupted during recruitment of neuronal progenitors for restorative neurogenesis, as the number of newborn neurons in ventricular zone stays the same as in the intact brains (Baumgart et al., 2012).

Nevertheless, ependymoglia are not the only cell type reacting to injury, nor the only cell type responsible for successful regeneration dynamics. Microglia, being one of the first cell types to react to injury in mice, is the first cell type that becomes active in zebrafish too, and is found to proliferate already at 24h post-injury and reaches its proliferation peak at 2 dpi. Apart from proliferation, microglia accumulate around the lesion site and display a transformed morphology which ranges from finely branched, in the intact brain, to phagocytic and activated after injury. Nevertheless, activation and increased proliferation of microglia is complete by 7 dpi, suggesting their initial role in cleaning up cellular debris and phagocytosis of apoptotic cells (Hanisch and Kettenmann, 2007). Correspondingly, oligodendrocyte cells have been detected surrounding the injury site and proliferating (Kroehne et al., 2011), however this activation decreases quickly and is back to normal levels at 7 dpi (Baumgart et al., 2012).

Fast clearance of microglia and oligodendroglia from the injury site, and in the absence of ependymoglial accumulation, is presumably one of the main reasons for successful regeneration in zebrafish in contrast to mammals. Nevertheless, success of regeneration in the zebrafish is tightly linked with acute inflammation that arises at the injury site. For instance, several studies have shown that chemokine signaling acts as regulator of neural stem cell activation in the intact and injured brain (Diotel et al., 2010; Kizil et al., 2012b; Cosacak et al., 2015). In contrast to mammals, the zebrafish creates an environment that has a pro-regenerative effect (Kyritsis et al., 2012). Injury-induced molecular programs lead to activation

of leukocytes and microglia cells, which are inactive in the intact brain. Acute inflammation was further shown to be necessary for the activation and proliferation of ependymoglial cells, subsequent neurogenesis, and successful brain regeneration (Kyritsis et al., 2012). Specifically, the transcription factor Gata3 was found to be important for regenerative neurogenesis, as will be discussed later in more detail.

Communication between the immune system and ependymoglial cells still requires better understanding. Signaling factors that initiate ependymoglial activity, or molecular mechanisms that are triggered as a consequence of inflammation in ependymoglia are only partially understood. Additionally, given the contradictory evidence in mammals about both beneficial and undesirable effects of inflammation on neural stem cells, it seems that zebrafish employs a more efficient dynamic (Kizil et al., 2015). The key for the successful cooperation between immune system and ependymoglial cells after injury in zebrafish might lie in the proper integration of time dependent cues driving the behavior of ependymoglia cells. More complete understanding of how zebrafish manages different variables in space and time after injury may help us understand how we could stimulate a regenerative response in mammals.

2.7. Molecular pathways driving ependymoglia activity after an injury

When it comes to the short-term recovery of the zebrafish telencephalon, many molecular mechanisms have been proposed. Some of them are molecular signatures already active in the intact brain, which keep the same dynamic after injury, while others have different functions from those in the healthy brain. For instance, helix-loop-helix protein id1, regulates ependymoglial proliferative response after injury by promoting their quiescence and maintenance of neural stem cell pool, the same as in the intact brain (Viales et al., 2015). Likewise, expression of Notch3 receptor continuously supports ependymoglia quiescence even after the injury (Alunni et al., 2013). On the other hand, FgF signaling is required for ependymoglial proliferation in an injury-dependent context (Kizil, et al. 2012), similarly to the intact brain, however it acts through different molecular pathways. Furthermore, expression of Notch1 receptor controls ependymoglial proliferation and neurogenesis after injury (Kishimoto et al., 2012), in contrast to its role in the intact brain (Chapouton et al., 2010).

As previously mentioned, the transcription factor Gata3 was found to be required for regenerative neurogenesis and injury induced proliferation of ependymoglia in zebrafish (Kizil et al. 2012). Gata3 is induced by lesion and acute inflammation in proliferating and non-proliferating ependymoglia, but its expression was first noticed in quiescent ependymoglia cells after 12h, which would become proliferative at 3dpi and give rise to new neurons. Interestingly, there is a subpopulation of proliferating ependymoglia that is not expressing

Gata3, suggesting that these cells might be constitutive progenitors and that Gata3 might delineate only ependymoglia recruited as the response to injury (Kizil et al. 2012).

Despite all the proposed mechanisms, our current molecular understanding of the regenerative process in zebrafish remains inadequately understood, especially the question of how different behavior of ependymoglia would be timely regulated post-injury. Therefore, which molecular mechanisms are responsible for proper timely orchestration of different cell type reactions during the entire regeneration process continues to be an important question, that has not been investigated until recently.

2.8. Ahr signaling

AhR is a ligand-binding transcription factor, belonging to the family of basic helix-loop-helix (bHLH) proteins. AhR is in the subgroup of bHLH-PAS, characterized by two PAS domains, PAS A and PAS B (Bersten et al., 2013; Mulero-Navarro and Fernandez-Salguero, 2016) (Fig. 7).

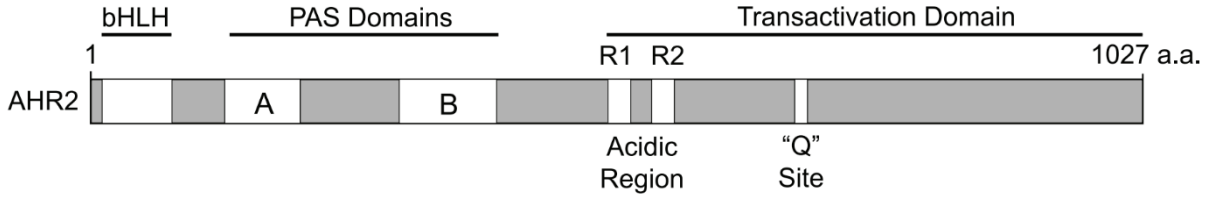

Figure 7. Domains of zebrafish aryl hydrocarbon receptor (AhR). (Lanham et al., 2011)

AhR is known as an environmental sensor, which mediates xenobiotic induced toxicity and reacts to a broad spectrum of xenobiotics. AhR resides in the cytoplasm, and upon ligand binding, it translocates to the nucleus, where it dimerizes with ARNT, another member of bHLH-PAS subgroup. This dimer subsequently binds to xenobiotic responsive elements, upstream of target genes, such as typical detoxification enzymes, for example, cytochrome oxidases P450 (cyp1a1, cyp1a2, cyp1b1 and others) (Bersten et al., 2013; Mulero-Navarro and Fernandez-Salguero, 2016).

Apart from perceiving the state of the environment, an increasing body of evidence shows its expression in immune system, inflammation and infection, and researchers are

trying to unravel its response to physiological ligands (Stockinger et al., 2014). Additionally, AhR has been found to be implicated in many other processes, such as cell differentiation, pluripotency or stemness and more general, homeostasis and stress response (Furness et al., 2007; Ko and Puga, 2017; Mulero-Navarro and Fernandez-Salguero, 2016). Furthermore, it is becoming increasingly evident that AhR also plays a role in promoting self-renewal and regeneration (Casado, 2016).

In the context of neurogenesis, AhR is found to be expressed in adult mouse brain neural progenitor cells (NPCs) of the hippocampus, where its deletion negatively altered hippocampal neurogenesis and neural progenitor cell proliferation (Latchney et al., 2013). In contrast, in a stroke model of mice, specific AhR knockout and inhibition from neural progenitor cells and their lineages, led to reduced astrogliosis, suppressed inflammation, increased NPCs proliferation and overall improved behavioral deficits compared to controls (Chen et al., 2019).

The AhR receptor is recently attracting increased scientific attention due to its involvement in multiple important processes in both healthy and compromised brains. We have found AhR receptor to be significantly downregulated in the injured zebrafish telencephalon, and an ability to regulate ependymoglia proliferation, direct conversion and neurogenesis (Di Giaimo, Durovic et al., 2018), which will be elaborated further on.

3. AIMS OF THE THESIS

Achieving successful brain regeneration in humans is to date one of the biggest challenges within regenerative medicine. The discovery of neural stem cells (NSCs) that reside in the adult brain raised hopes for regenerative therapies, however the first attempts to use existing NSCs for repair in mammalian brain largely failed. Regeneration-competent species, such as zebrafish, generate new neurons that are engaged in repair and are able to accomplish remarkably successful brain regeneration, even at the adult stage. Therefore, one of the main aims in the field is to understand the underlying basis of this regeneration process, and more specifically, restorative neurogenesis in the adult zebrafish brain to better apply such mechanics in humans.

Despite many important contributions in the last decade, the behavior of ependymoglial cells in the zebrafish brain that leads to neurogenesis, as well as the underlying molecular mechanisms governing neurogenesis and regeneration, are yet to be fully elucidated. Throughout my thesis, I predominantly aimed to investigate and obtain a more complete understanding of molecular mechanisms involved in restorative neurogenesis, which are responsible for specific behavior of ependymoglial cells in the zebrafish telencephalon.

To this end, the first objective was to adapt and develop techniques which would facilitate reliable labelling and manipulation of ependymoglial cells in the adult zebrafish telencephalon. First, I aimed at further improving an electroporation method, which was previously established in our laboratory, in order to increase the efficiency and number of ependymoglial cells being labelled. This electroporation protocol enabled reliable labelling of a high number of ependymoglial cells through in vivo delivery of plasmid DNA and facilitated investigation of ependymoglial behavior. Next, there was the necessity of a straightforward and practical method which would allow genetic manipulation of multiple genes in ependymoglial cells. Breunig et al., 2018 established the StagR technique, a single step method enabling packaging of multiple gRNAs in a single vector, and I adapted its functional utilization for gene ablation in the adult zebrafish telencephalon in vivo.

With the aid of the aforementioned techniques, a further objective was to answer the question of molecular mechanisms underpinning ependymoglial behavior during restorative neurogenesis. Previous research from Barbosa et al., 2015 shed light on the specifics of ependymoglial response to injury and discovered three modes of ependymoglial behavior in this condition: two division modes, asymmetric and symmetric non – gliogenic mode and third mode called direct conversion. Additionally, there are many studies that previously unraveled different molecular mechanisms responsible for proliferative behavior of ependymoglial cells after injury. Nevertheless, how the different modes of ependymoglial behavior are timely

regulated to provide new neurons after injury, and what molecular mechanisms are at play in order to successfully respond to injury conditions, remained unresolved. Therefore, the main objective of my thesis was to understand the regulation of ependymoglial reaction to an injury and, further, to identify the molecular signature that is involved in synchronization of their timely behavior. To this end, we found AhR that is highly expressed in ependymoglial cells after injury to be an important regulator of ependymoglia behavior and their timely coordination, and that is plays a crucial role in ensuring proper and successful restorative neurogenesis.

3.1. Aim of the study I

The aim of the study I was to investigate:

The role of aryl hydrocarbon receptor (AhR) in ependymoglial cells after injury, its timely regulation of restorative neurogenesis, and the effects this entails for regeneration of zebrafish telencephalon.

The Aryl Hydrocarbon Receptor Pathway Defines the Time Frame for Restorative Neurogenesis

Rossella Di Giaimo *, **Tamara Durovic ***, Pablo Barquin, Anita Kociaj, Tjasa Lepko, Sven Aschenbroich, Christopher T. Breunig, Martin Irmler, Filippo M. Cernilogar, Gunnar Schotta, Joana S. Barbosa, Dietrich Trumbach, Emily Violette Baumgart, Andrea M. Neuner, Johannes Beckers, Wolfgang Wurst, Stefan H. Stricker, and Jovica Ninkovic.

* The authors contributed equally to the manuscript

Di Giaimo, Durovic et al., 2018, Cell Reports 25, 3241–3251 December 18, 2018

https://doi.org/10.1016/j.celrep.2018.11.055

For this paper I performed one half of all experiments and analyzed all the data coming from those experiments. More specifically, Fig. 1 (C, D, E, F), Fig. 2 (A, B, C, D), entire Fig. 3, Fig. 4 (A, B, G, H), and entire Suppl. Fig. 3 were done by me. I also contributed to the writing process, together with Prof. Dr. Jovica Ninković and Prof. Dr. Rossella Di Giaimo. The contribution of other authors is written in the paper.

Report

Cell Reports

The Aryl Hydrocarbon Receptor Pathway Defines the Time Frame for Restorative Neurogenesis

Graphical Abstract

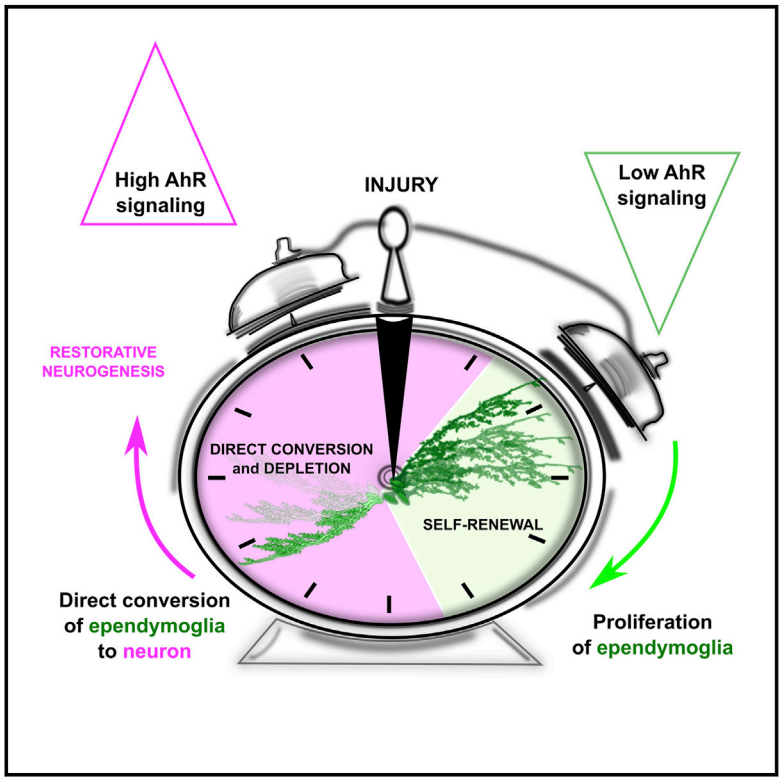

Authors

Rossella Di Giaimo, Tamara Durovic, Pablo Barquin, ..., Wolfgang Wurst, Stefan H. Stricker, Jovica Ninkovic

Correspondence

ninkovic@helmholtz-muenchen.de

In Brief

Zebrafish have a high capacity to replace lost neurons after brain injury. Di Giaimo et al. identify the aryl hydrocarbon receptor (AhR) as a crucial regulator of restorative neurogenesis timing in the zebrafish brain. Interference with timely AhR regulation after injury leads to aberrant restorative neurogenesis.

Highlights

- Aryl hydrocarbon receptor (AhR) pathway is crucial for brain regeneration
- High AhR levels promote conversion of ependymoglia to neurons during regeneration
- Low AhR levels promote ependymoglial proliferation in the injured brain
- AhR levels set the proper timing of restorative neurogenesis

Di Giaimo et al., 2018, Cell Reports *25*, 3241–3251
December 18, 2018
https://doi.org/10.1016/j.celrep.2018.11.055

CellPress

Cell Reports
Report

The Aryl Hydrocarbon Receptor Pathway Defines the Time Frame for Restorative Neurogenesis

Rossella Di Giaimo,[1,2,17] Tamara Durovic,[1,3,17] Pablo Barquin,[4] Anita Kociaj,[1,3] Tjasa Lepko,[1,3] Sven Aschenbroich,[1,3] Christopher T. Breunig,[5,6] Martin Irmler,[7] Filippo M. Cernilogar,[8] Gunnar Schotta,[8,9] Joana S. Barbosa,[1,18] Dietrich Trümbach,[10] Emily Violette Baumgart,[1] Andrea M. Neuner,[5,6] Johannes Beckers,[7,11,12] Wolfgang Wurst,[10,13,14,15] Stefan H. Stricker,[5,6] and Jovica Ninkovic[1,16,19,*]

[1]Institute of Stem Cell Research, Helmholtz Center Munich, 85764 Neuherberg, Germany
[2]Department of Biology, University of Naples Federico II, 80134 Naples, Italy
[3]Graduate School of Systemic Neurosciences, Biomedical Center of LMU, 82152 Planegg, Germany
[4]Universidad Pablo de Olavide, Sevilla, 41013 Sevilla, Spain
[5]MCN Junior Research Group, Munich Center for Neurosciences, 82152 Munich, Germany
[6]Epigenetic Engineering, Institute of Stem Cell Research, Helmholtz Center Munich, 85764 Neuherberg, Germany
[7]Institute of Experimental Genetics, Helmholtz Zentrum München, 85764 Neuherberg, Germany
[8]Division of Molecular Biology, Biomedical Center, Faculty of Medicine, LMU Munich, 82152 Planegg, Germany
[9]Munich Center for Integrated Protein Science (CiPSM), 82152 Planegg, Germany
[10]Institute of Developmental Genetics, Helmholtz Zentrum München, 85764 Neuherberg, Germany
[11]German Center for Diabetes Research (DZD), 85764 Neuherberg, Germany
[12]Technische Universität München, Chair of Experimental Genetics, 85354 Freising-Weihenstephan, Germany
[13]Munich Cluster for Systems Neurology SYNERGY, 82152 Planegg, Germany
[14]German Center for Neurodegenerative Diseases (DZNE), 82152 Planegg, Germany
[15]Chair of Developmental Genetics, Technische Universität München, 85354 Freising-Weihenstephan, Germany
[16]Department for Cell Biology and Anatomy, Biomedical Center of LMU, 82152 Planegg, Munich, Germany
[17]These authors contributed equally
[18]Present address: Institute of Animal Pathology, Vetsuisse Faculty, University of Bern, Bern, Switzerland
[19]Lead Contact
*Correspondence: ninkovic@helmholtz-muenchen.de
https://doi.org/10.1016/j.celrep.2018.11.055

SUMMARY

Zebrafish have a high capacity to replace lost neurons after brain injury. New neurons involved in repair are generated by a specific set of glial cells, known as ependymoglial cells. We analyze changes in the transcriptome of ependymoglial cells and their progeny after injury to infer the molecular pathways governing restorative neurogenesis. We identify the aryl hydrocarbon receptor (AhR) as a regulator of ependymoglia differentiation toward post-mitotic neurons. *In vivo* imaging shows that high AhR signaling promotes the direct conversion of a specific subset of ependymoglia into post-mitotic neurons, while low AhR signaling promotes ependymoglial proliferation. Interestingly, we observe the inactivation of AhR signaling shortly after injury followed by a return to the basal levels 7 days post injury. Interference with timely AhR regulation after injury leads to aberrant restorative neurogenesis. Taken together, we identify AhR signaling as a crucial regulator of restorative neurogenesis timing in the zebrafish brain.

INTRODUCTION

Regeneration in the mammalian CNS is largely limited (Dimou and Götz, 2014) and restricted to either demyelinated axon repair (Dimou and Götz, 2014) or, in very few cases, neuronal repair (Arvidsson et al., 2002; Chen et al., 2004; Ernst et al., 2014). Neuronal replacement in mammals is limited to brain areas in close proximity to neurogenic zones (Brill et al., 2009). However, a large number of young neurons originating from the neurogenic zones fail to mature and integrate at the injury site and instead die (Arvidsson et al., 2002; Brill et al., 2009). In contrast, the zebrafish CNS has the capacity to regenerate brain tissue after injury (Becker and Becker, 2015). This regeneration also includes the replacement of lost neurons (restorative neurogenesis) (Barbosa et al., 2015; Baumgart et al., 2012; Kishimoto et al., 2012; Kroehne et al., 2011; Kyritsis et al., 2012). Tremendous regeneration capacity coincides with the wide spread of ependymoglial cells producing different neuronal subtypes in the zebrafish brain throughout their lifetime (Kyritsis et al., 2012). Notably, ependymoglial cells lining the ventricular surface in the adult zebrafish telencephalon generate new neurons that are recruited to the injury site (Barbosa et al., 2015; Baumgart et al., 2012; Kishimoto et al., 2012; Kyritsis et al., 2012). Importantly, a considerable proportion of these additionally generated neurons fully differentiate into the appropriate neuronal subtypes and survive for more than 3 months (Baumgart et al., 2012; Kroehne et al., 2011). The activation of ependymoglial cells to produce additional neurons is preceded by the activation of microglial cells involved in the initial wound healing process. Importantly, the initial inflammation does not only remove cellular debris but also induces restorative neurogenesis (Kyritsis et al., 2012), suggesting a biphasic regeneration process in the zebrafish brain. During the first phase, activated glial cells restrict the

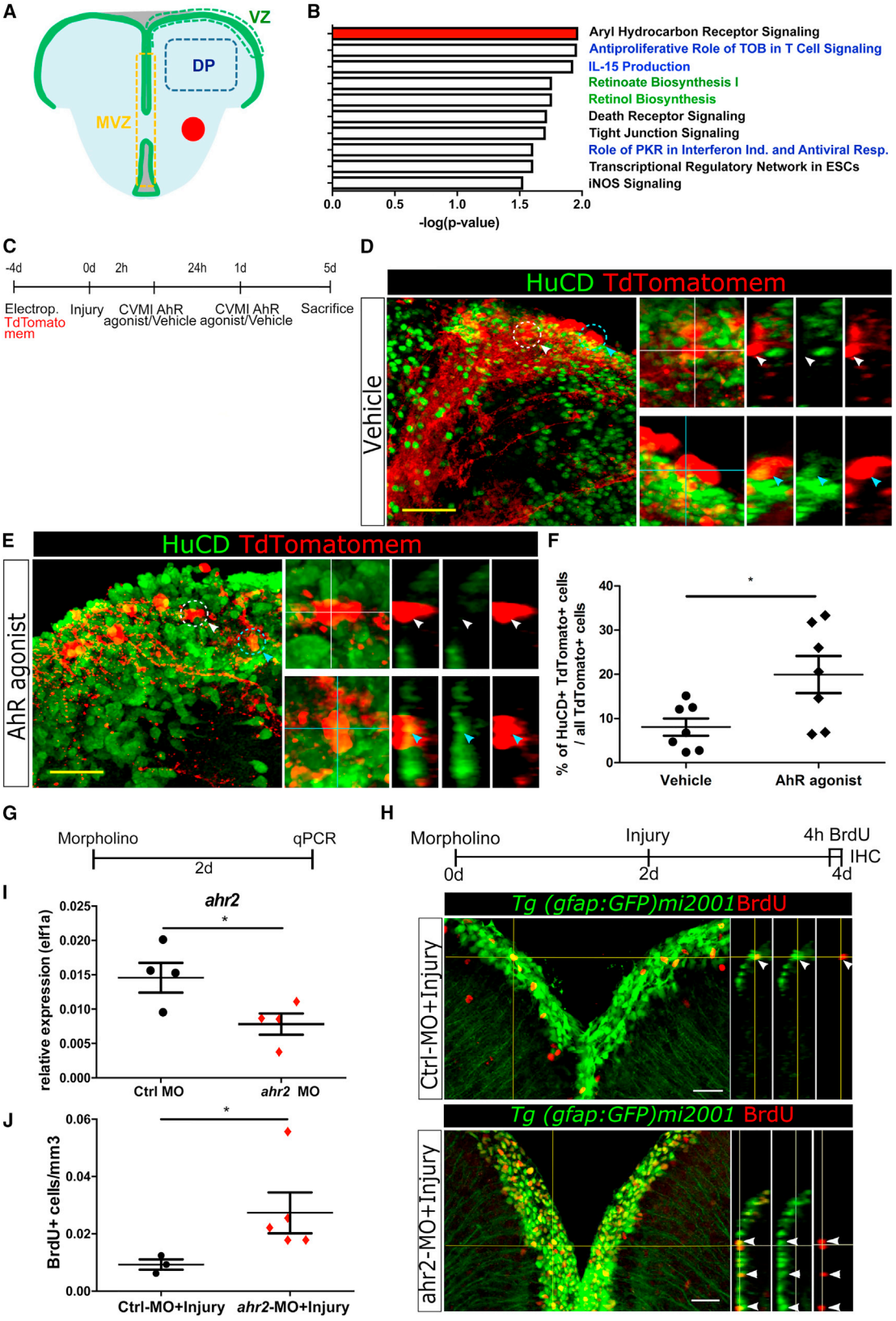

(legend on next page)

initial damage and clear cellular debris. The following second phase promotes the production of new neurons from the ependymoglia that are necessary for tissue restoration (Kyritsis et al., 2012). This delay in restorative neurogenesis relative to the initial inflammatory phase therefore stands as a crucial mechanism to allow correct zebrafish brain regeneration. For this reason, understanding the specific molecular programs underlying the timely production of new neurons is critical to implement regeneration from endogenous glial cells in the mammalian brain. Despite their importance, these mechanisms, which are involved in the temporal control of restorative neurogenesis from ependymoglial cells, are not well understood. Therefore, we aim to identify them using both longitudinal analysis of injury-induced transcriptome changes in ependymoglial niches and the cell-type-specific manipulation of these pathways.

RESULTS

To define the molecular pathways controlling restorative neurogenesis initiation in the dorsal neurogenic zone (VZ) of the zebrafish telencephalon (Barbosa et al., 2015), we aimed to identify injury-induced changes in the transcriptome specific for the VZ. To this end, we compared changes in the transcriptome in laser-dissected tissue from 3 different telencephalic areas from intact and stab-wound injured brains (Barbosa et al., 2016) using the Affymetrix Zebrafish Gene 1.x ST array (Figure 1A). We compared injury-induced changes in the VZ to changes in the brain parenchyma (DP), which is free of neuronal progenitors, to reveal a signature specific for this cell type. Moreover, a comparison with the medial neurogenic zone (MVZ) was performed to extract pathways specific for progenitors in the VZ engaged in the repair process. Non-supervised hierarchical clustering of injury-induced changes at 2 and 7 days after injury in these 3 different areas revealed several clusters of co-regulated genes. These clusters were either specific to the VZ (clusters 1 and 2), shared between neurogenic niches (clusters 3 and 4), or changed in all 3 analyzed areas (clusters 5 and 6; Figures S1A and S1B; Table S1). We reasoned that the molecular signature controlling the early response of the ependymoglia should be upregulated specifically in the dorsal neurogenic zone at 2 dpi, correlating with the first signs of ependymoglia reaction to injury (Baumgart et al., 2012), and should chase out at 7 dpi, as represented by cluster 1 (Figure S1A). We observed 192 genes specifically upregulated in the VZ at 2 dpi (Figure S1B). Ingenuity Pathway Analysis (IPA) of these genes revealed significant over-representation of several metabolic (green) and immune-system-related (blue) pathways (Figure 1B; Table S1). However, the most significantly regulated pathway was the aryl hydrocarbon receptor (AhR) signaling pathway (Figure 1B), placing it as our prime candidate for further analysis. We therefore analyzed the expression of AhR-signaling-regulated genes after injury and observed an upregulation of Irf9, Nfkbie, and Tgfb1 specifically at 2 dpi (Figure S1C), which was indicative of reduced AhR signaling. Taken together, our data revealed a specific inhibition of AhR signaling in the dorsal neurogenic zone at 2 dpi that then chases out at 7 dpi, suggesting its role in the initial control of restorative neurogenesis.

To address the importance of AhR signaling levels in restorative neurogenesis, we either potentiated AhR signaling with a high-affinity AhR agonist, β-naphthoflavone (BNF; Berghard et al., 1992), or decreased it by morpholino-mediated knockdown. AhR is a ligand-dependent transcription factor that is restrained in the cytoplasm by a chaperone complex when inactive (Hestermann and Brown, 2003). Upon ligand binding, AhR translocates to the nucleus and activates the transcription of its downstream targets (Hestermann and Brown, 2003). BNF induces AhR translocation to the nucleus without a natural ligand and therefore activates AhR signaling (Soshilov and Denison, 2014). To minimize systemic effects, we injected 10 μg/g of body mass of BNF in the telencephalic ventricle using cerebroventricular microinjections (CVMIs) (Figure 1C). We first analyzed the efficiency of CVMI-administered BNF to activate AhR signaling based on the expression levels of cytochrome P450 1B1 oxidase (Cyp1b1), a transcriptional reporter for AhR signaling (Soshilov and Denison, 2014). Notably, we detected more than 2-fold higher levels of Cyp1b1 in the injured brains in BNF-treated animals compared to the vehicle treatment (Figure S1D). We then assessed the number of new neurons generated from ependymoglial cells (Figures 1C–1F). To follow both ependymoglia and their progeny, including newly generated neurons, we labeled ependymoglia by electroporation of a plasmid encoding for membrane-localized TdTomato

Figure 1. Levels of AhR Signaling Define the Balance between Ependymoglial Proliferation and Differentiation

(A) Schematic representation of the laser-microdissected areas used for transcriptome analysis.

(B) Histogram depicting canonical pathways (Ingenuity) enriched in the gene set specifically upregulated in the dorsal VZ at 2 dpi.

(C) Scheme showing the experimental outline to assess the influence of AhR potentiation on restorative neurogenesis.

(D and E) Confocal images showing the fate of TdTomatomem-labeled cells in AhR agonist-treated (E) and vehicle-treated (D) brains 5 days after injury. High magnification images with orthogonal projections depict representative TdTomatomem+/HuC/D− (white circle) and TdTomatomem/HuC/D double-positive (blue circle) cells. White arrowhead indicates HuC/D-negative and blue arrowhead HuC/D-positive cells. Scale bars, 50 μm.

(F) Dot plot showing the proportion of HuC/D and TdTomatomem double-positive cells among all TdTomatomem-labeled cells in AhR agonist- and vehicle-treated brain.

(G) Scheme depicting the experimental procedure to assess the efficiency of morpholino-mediated AhR knockdown in ependymoglia.

(H) Scheme of the experimental procedure used to analyze ependymoglia proliferation after morpholino-mediated knockdown and confocal images with orthogonal projections showing examples of proliferating, BrdU-positive ependymoglia (white arrowhead) in the injured brains after control or ahr2-specific morpholino treatment. Scale bars, 20 μm.

(I) Dot plot showing ahr2 expression in ependymoglia.

(J) Dot plot depicting the number of proliferating ependymoglia after reducing AhR signaling.

Single dots represent individual animals indicating biological replicates in all dot plots. Lines show mean ± SEM. *$p \leq 0.05$ (Mann-Whitney test). VZ, dorsal neurogenic zone (50 um width from the ventricular surface); MVZ, medial neurogenic zone; DP, brain parenchyma (DP areas were chosen far from the injury sites [red circle in A]).

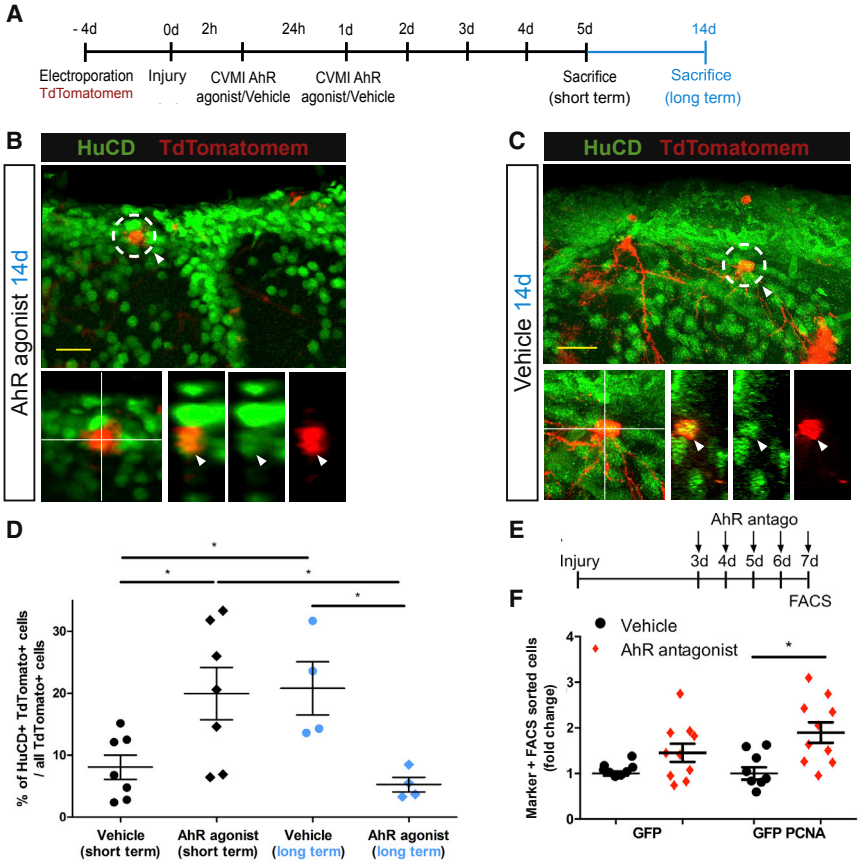

Figure 2. AhR Signaling Regulates the Timing of the Restorative Neurogenesis that Is Crucial for the Survival of Newborn Neurons

(A) Schematic representation of the experimental procedure used to follow ependymoglial progeny after injury and the activation of AhR signaling.

(B and C) Micrographs depicting HuC/D and TdTomatomem double-positive cells without radial morphology in AhR agonist-treated (B) or vehicle-treated (C) brains 14 days after injury. Dashed white circles indicate representative cells that are magnified in the lower panel with orthogonal projections. Images are presented as full z-projections of the confocal z stack. Scale bars, 20 μm.

(D) Dot plot showing the percentage of double-positive HuC/D and TdTomatomem cells among all TdTomatomem-positive cells after treatment with AhR agonist or vehicle at 5 dpi (short term) and 14 dpi (long term).

(E) Scheme showing the experimental outline to assess the impact of low AhR levels on ependymoglial proliferation.

(F) Dot plot depicting the change in the number of PCNA-positive ependymoglia in injured telencephalon treated with vehicle or AhR antagonist. Single dots represent individual animals indicating biological replicates in all dot plots. Lines show mean ± SEM. *$p \leq 0.05$ (Mann-Whitney test).

(TdTomatomem) red fluorescent protein (Barbosa et al., 2015) (Figure 1C), allowing the long-term tracing of the ependymoglial lineage (Barbosa et al., 2015, 2016). Elevated AhR signaling in the injured brain increased the number of newborn, HuC/D-positive neurons derived from the electroporated ependymoglial cells compared to the vehicle treatment (Figures 1D–1F). Conversely, the morpholino-mediated knockdown of aryl hydrocarbon receptor 2 (ahr2; Figures 1G and 1I), a major mediator of AhR signaling in zebrafish (Bello et al., 2004), increased the ependymoglia proliferation compared to control morpholino (Figures 1H and 1I). Taken together, our data suggest a role for AhR signaling levels in controlling ependymoglial behavior after injury, with high levels of AhR signaling promoting neurogenesis from the zebrafish ependymoglia and low AhR signaling triggering their proliferation and/or self-renewal.

To assess the importance of this regulation, we followed the fate of new neurons added after AhR potentiation using TdTomatomem-based fate mapping. We analyzed the fate of progeny at 5 (short-term tracing) and 14 days (long-term tracing) after injury (Figure 2A). As expected, the proportion of new TdTomatomem+ HuC/D+ neurons significantly increased after AhR potentiation compared to the vehicle-treated animals in short-term tracing. The proportion of TdTomatomem+ and HuC/D+ neurons increased further at 14 days compared to 5 days after vehicle treatment (Figures 2B–2D). Surprisingly, we observed that the number of TdTomatomem+, HuC/D+ neurons after AhR potentiation was significantly lower at 14 dpi (long-term tracing, Figure 2D) compared to 5 dpi (Figure 2D), suggesting impaired survival of additional neurons generated due to the inappropriate regulation of AhR signaling. To complement this analysis of precocious activation of AhR signaling, we interfered with the return of AhR signaling to basal levels after the initial decrease following injury and analyzed the proliferation of ependymoglia. To achieve the precise timing of interference with AhR signaling, we used a pharmacological approach and locally administered 6 μM AhR antagonist (AhR Antagonist II, SR1-CAS) using CVMI. Administration of the antagonist efficiently decreased AhR signaling, as measured by Cyp1b1 expression (Figure S2A). AhR levels were then kept low by the daily administration of the agonist starting at day 3 after injury, and the number of actively cycling, PCNA$^+$ ependymoglia was determined at 7 dpi using intracellular fluorescence-activated cell sorting (FACS) (Figures 2E, 2F, and S2C), as previously described (Barbosa et al., 2016). We chose to analyze samples at 7 dpi because this is the time point when the expression of Cyp1b1 is again increased to basal levels observed in the intact brain (Figure 4E). The number of proliferating ependymoglia significantly increased (Figures 2E and 2F) after antagonist treatment compared to the vehicle control. This increase correlates with our hypothesis that low AhR levels allow the proliferation of ependymoglia after injury. Our data, therefore, suggest a role of AhR in regulating the balance between the proliferation and differentiation of ependymoglia to ensure the proper timing of restorative neurogenesis.

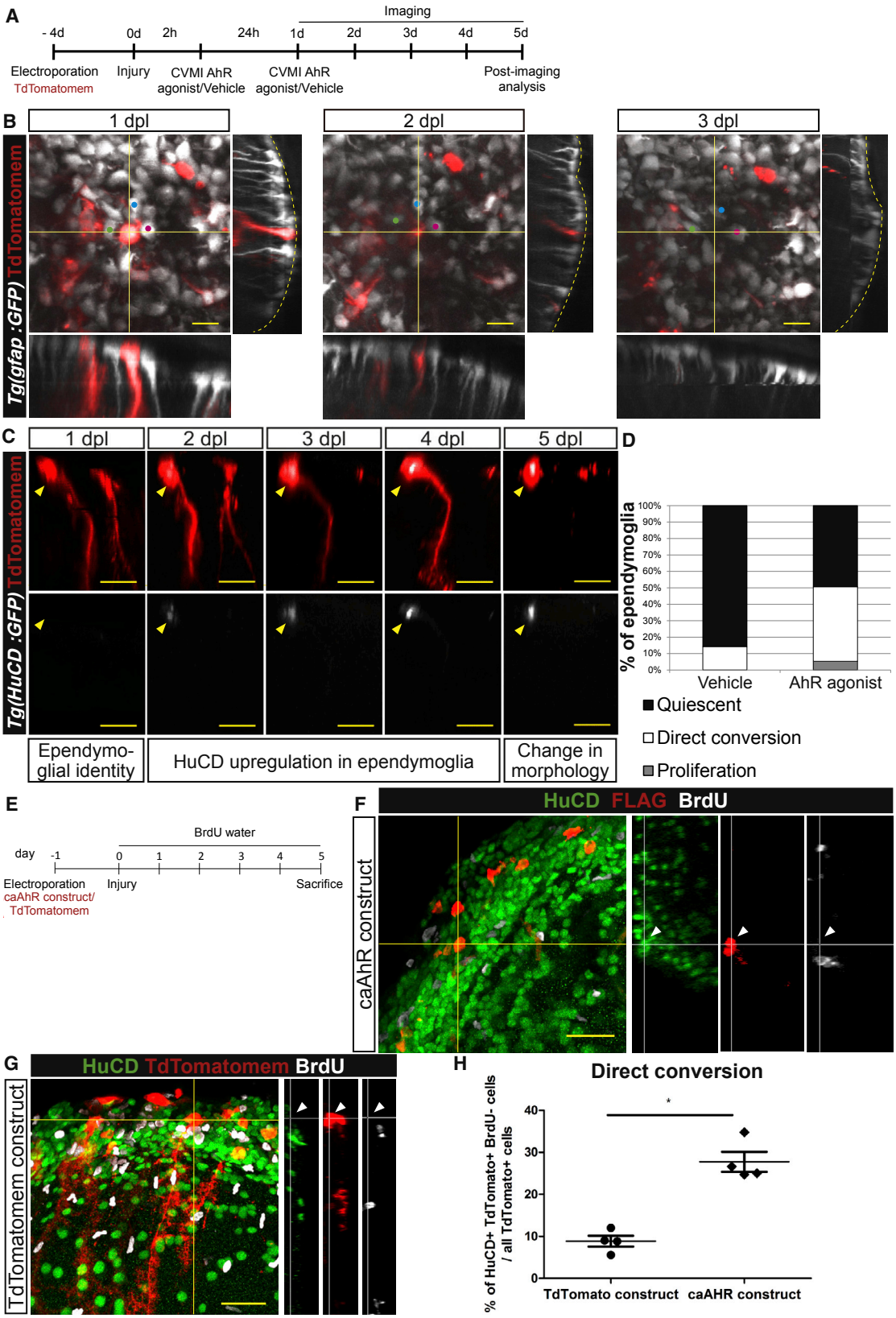

(legend on next page)

Restorative neurogenesis in zebrafish is achieved by both an increase in the number of dividing neuronal progenitors (Barbosa et al., 2015) and an increase in the direct conversion of ependymoglia into post-mitotic neurons (Barbosa et al., 2015). To assess the direct conversion of ependymoglia after injury and AhR signaling activation, we sparsely labeled ependymoglia by the electroporation of TdTomatomem (Barbosa et al., 2015) and followed individual labeled ependymoglia and their progeny for 5 days by live imaging (Figures 3A, 3B, S3A, and S3B). The identity of the followed cells was then assessed by post-imaging staining for neuronal marker HuC/D. This allowed the re-identification of previously imaged cells (Figures S3E–S3G). We electroporated plasmids in the *Tg(gfap:GFP)*mi2001 transgenic line expressing GFP in all ependymoglia (also retained in 25% of their progeny) to identify the ependymoglia identity by GFP expression and the radial morphology, as previously described (Barbosa et al., 2015, 2016). The direct conversion of ependymoglia into neurons was then characterized by the loss of radial morphology, migration out of the ependymoglial layer toward the brain parenchyma (Figures 3B and S3F), and the expression of the post-mitotic marker HuC/D prior to a change in radial morphology (Figure 3C; Figure S3G). In line with our previous observation (Barbosa et al., 2015), only a few ependymoglial cells divided (Figure 3D; Figures S3A and S3B), and the vast majority (85%) of labeled ependymoglia in vehicle-treated injured telencephalons remained quiescent. These ependymoglia cells did not change their identity within a 5-day imaging period (Figures 3D and S3A), whereas 14.2% of labeled cells directly converted (Figures 3B–3D). In contrast, after AhR signaling enhancement, 45% of labeled ependymoglial cells directly converted into post-mitotic neurons (Figure 3D). This increase in direct conversion was associated with the depletion of ependymoglia present in the dorsal neurogenic niche, as we observed a significant increase in the dorsal surface free of gfap:GFP-positive ependymoglia in BNF-treated brains compared to the vehicle treatment (Figures S3H and S3I; Videos S1 and S2). We did not observe any difference in terminal deoxynucleotidyl transferase-mediated deoxyuridine triphosphate nick end labeling (TUNEL)-positive cells at the dorsal telencephalon area between the BNF and vehicle treatment (Figures S3C and S3D). Therefore, we concluded that direct conversion causes ependymoglial depletion rather than cell death. Taken together, our data suggest that AhR signaling enhancement after injury leads to increased neurogenesis via the direct conversion and depletion of ependymoglia.

Restorative neurogenesis in zebrafish is tightly associated with the activation of microglia and monocyte infiltration (Kyritsis et al., 2012), and AhR signaling regulates monocyte extravasation (Rothhammer et al., 2016). Therefore, we next wondered if increased AhR signaling levels would promote the direct conversion of ependymoglia in a cell-autonomous manner. To assess this hypothesis, we potentiated AhR signaling in a cell-autonomous manner by electroporating the constitutively active AhR construct (caAhR) in ependymoglia (Figure S3J). The caAhR construct is generated by fusing the N-terminal portion of zebrafish ahr2 lacking a PAS B domain with the transactivation domain of mouse AhR that activates the canonical AhR pathway independently of the ligand binding (Soshilov and Denison, 2014). We co-electroporated caAhR with TdTomatomem for long-term fate mapping and kept the animals in the BrdU bath to label all dividing cells over a 5-day experiment (Figure 3E). Since the electroporation initially labels virtually only ependymoglia (Figure S3J; see also Barbosa et al., 2015), we reasoned that TdTomatomem+, BrdU+, and post-mitotic neuronal marker HuC/D+ cells represent new neurons being generated from proliferating progenitors, while TdTomatomem+, HuC/D+, and BrdU− cells arose from the direct conversion of ependymoglia without cell division (Figures 3F and 3G). Similar to live imaging, we observed that 10% of cells electroporated with the control plasmid acquired neuronal identity (HuC/D+) without BrdU incorporation. However, the cells electroporated with caAhR showed a 3-fold increase in direct conversions (Figure 3H). All in all, our analysis indicates that the AhR levels regulate the direct conversion of ependymoglia in a cell-autonomous manner.

Increased levels of AhR in the injured brain promoted the direct conversion of up to 45% of all ependymoglia, prompting us to hypothesize that only a subset of ependymoglia respond to the AhR levels in a given condition. Indeed, live imaging of ependymoglia in the *Tg(gfap:GFP)mi2001* transgenic line (Bernardos and Raymond, 2006) revealed two states of gfap:GFP+ ependymoglial cells (GFP^{low} and GFP^{high}) based on the GFP expression levels (Figure 4A). Approximately 25% of the ependymoglial progeny remain GFP+ (Barbosa et al., 2015) due to GFP protein stability. Therefore, to exclude that GFP^{low} state represents ependymoglial progeny, we analyzed the morphology of GFP+ cells in confocal stacks from live imaging and in non-stained

Figure 3. High AhR Signaling Induces Direct Conversion of Ependymoglia into Post-Mitotic Neurons

(A) Schematic representation of the experimental procedure used to follow the cell fate of ependymoglia after injury and the activation of AhR signaling using *in vivo* imaging.

(B) 2-photon images with orthogonal projections of the same TdTomatomem-labeled ependymoglia in a Tg(*gfap:GFP*)*mi2001* line followed for 5 days, depicting direct conversion. Yellow line delineates the ventricular surface.

(C) 2-photon images with orthogonal projections of the same TdTomatomem-labeled ependymoglia in the Tg(*HuC:GFP*) line followed for 5 days, depicting different phases of direct conversion including the upregulation of the HuC/D marker.

(D) Histogram representing the behavior of ependymoglial cells in the injured vehicle and AhR agonist-treated brains observed using live imaging.

(E) Schematic representation of the experimental procedure used to follow direct conversion after cell-autonomous enhancement of AhR signaling in the injured brains.

(F and G) Micrographs with orthogonal projections depicting the fate of ependymoglial progeny after caAhR construct (F) or TdTomatomem control construct (G) electroporation at 5 days after brain injury.

(H) Dot plot showing the percentage of ependymoglial direct conversion (HuC/D and TdTomatomem double-positive cells negative for BrdU) after caAHR for TdTomatomem construct electroporation. Single dots represent individual animals indicating biological replicates. Lines show mean ± SEM. *$p \leq 0.05$ (Mann-Whitney test). Scale bars, 30 μm.

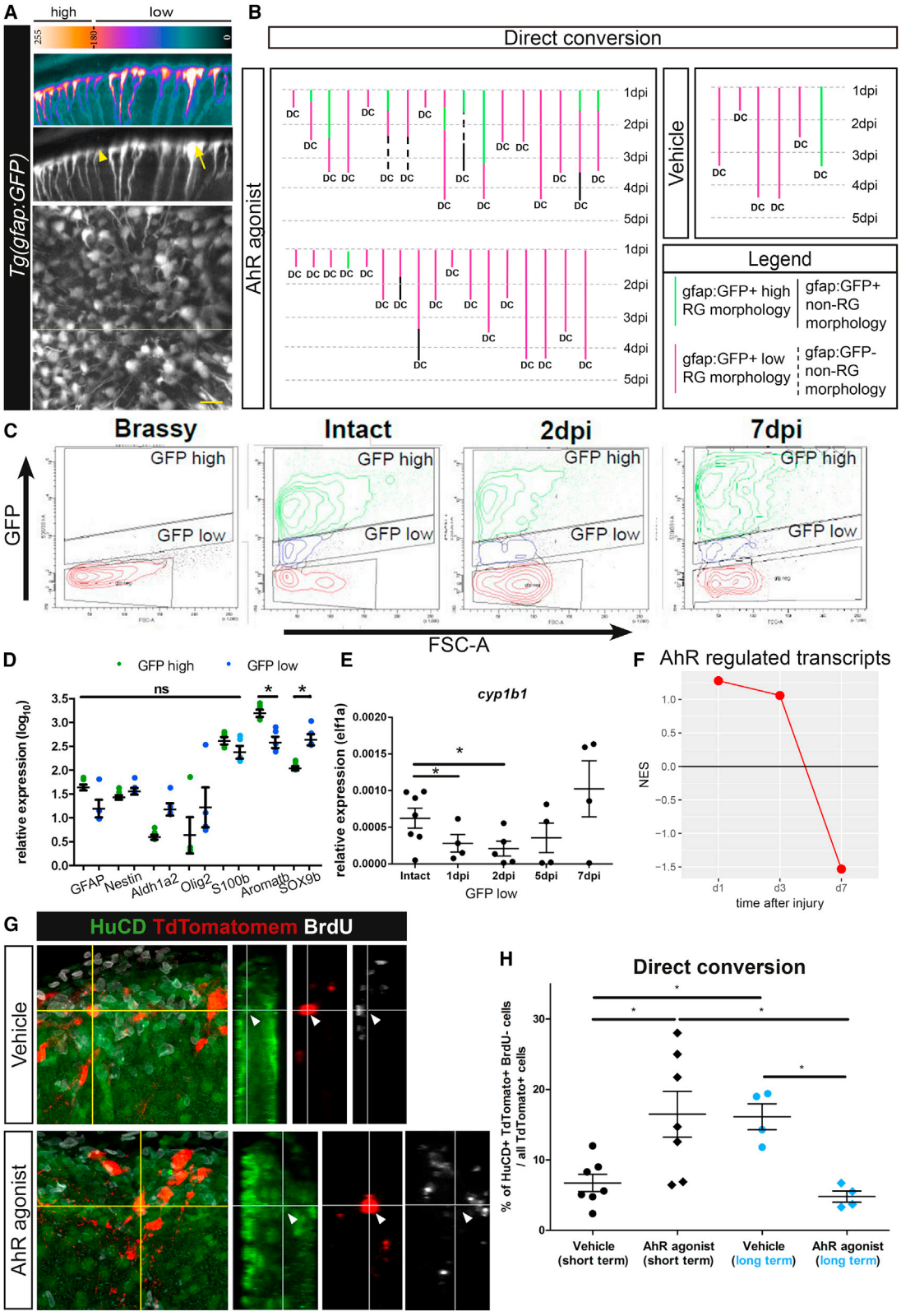

(legend on next page)

brain sections of the dorsal VZ in *Tg(gfap:GFP)mi2001* animals. We observed ependymoglial cells with radial morphology expressing both low and high GFP levels (arrow depicting GFP^{high} and arrowhead depicting the GFP^{low} in Figure 4A). Moreover, the FACS-based analysis of GFP levels in the *Tg(gfap:GFP)mi2001* transgenic line revealed two distinct GFP+ states based on the contour diagram plot in both intact and injured brains (Figure 4C). Cells from both states express comparable levels of typical ependymoglial markers such as Gfap, Nestin, and S100b, as detected by RT-qPCR performed on FACS-purified GFP+ cells (Figure 4D), therefore demonstrating the ependymoglial nature. However, the two ependymoglial states show different expression levels of other glial genes, such as Sox9b and Aromatase B, suggesting that the transcriptomic signatures of cells belonging to different states are not completely identical (Figure 4D). Notably, an analysis of their transcriptomes revealed clear clustering according to the GFP expression levels (Figure S4A) and the enrichment of distinct biological processes (Figures S4B and S4C). The GFP^{high} state is enriched in processes linked to cell proliferation, while processes related to cellular migration and differentiation are significantly enriched in the GFP^{low} state. However, these ependymoglial states are plastic with regard to GFP levels; some GFP^{high} cells achieved the GFP^{low} phenotype and vice versa within 5 days of *in vivo* live imaging in both intact and injured brains (Figure 4B). Nevertheless, 97% of all ependymoglia that directly convert into post-mitotic HuC/D+ neurons acquire the GFP^{low} phenotype before conversion (pink line in Figure 4B).

Therefore, we next set out to analyze the level of AhR signaling in the FACS-purified GFP^{low} population using the expression of AhR target gene Cyp1b1 as a readout. Importantly, we detected a downregulation of Cyp1b1, one of the major AhR targets, at 2 dpi in the GFP^{low} population that returns back to the intact brain basal levels at 7 dpi (Figure 4E). This regulation is parallel to the transcriptional upregulation of the Mcm7, Ccna2, and Nfkbie (Figures S4D–S4F) genes, showing inverse correlation to the activation state of AhR signaling (Marlowe et al., 2004). In contrast, these transcriptional changes could not be observed in GFP^{high} ependymoglia, with the exception of Nfkbie (Figures S3A–S3C). In line with the regulation of AhR signaling targets, we further observed significantly higher levels of aryl hydrocarbon receptor 2 (ahr2) transcript in the GFP^{low} ependymoglia both in the intact and injured telencephalon (Figure S4G). Therefore, we performed RNA sequencing (RNA-seq) and compared the total transcriptomic changes in FACS-purified GFP^{low} ependymoglia at 1, 3, and 7 dpi to the intact brain. A multidimensional scaling plot showed a rapid reaction of GFP^{low} ependymoglia to injury with large differences in the overall transcriptomic signature already at 1 dpi (Figure S4H). The gene set enrichment analysis revealed AhR pathway (gene set defined based on the Ingenuity database) regulation in GFP^{low} ependymoglia at 1 and 3 days after injury compared to the intact brain, but not at 7 dpi (Figure 4F), in line with our Cyp1b1-based monitoring of signaling activity (Figure 4E). Moreover, we identified a significant downregulation (false discovery rate [FDR] < 0.05) of 3 pathways immediately after injury (1 dpi), including epithelial-mesenchymal transition (EMT) (Figure S4I), a process already linked to the level of AhR signaling (Rico-Leo et al., 2013). Therefore, these data suggest that the AhR-regulated EMT process could control the direct conversion of ependymoglia into the post-mitotic neurons during the repair process. Interestingly, the GFP^{low} population of ependymoglia specifically upregulates GATA3 (Figure S4J), a transcription factor implicated in restorative neurogenesis (Kyritsis et al., 2012), further corroborating the prime role of the GFP^{low} population in restorative neurogenesis. Notably, neurons generated by direct conversion are mostly susceptible to the AhR signaling levels, as we observed that these neurons fail to survive long term after precocious AhR activation (Figures 4G and 4H).

Taken together, we have identified a population of ependymoglial cells that generate new neurons in the zebrafish telencephalon by direct conversion and revealed the AhR signaling pathway that was thus far unknown in this context.

DISCUSSION

Brain injury in zebrafish induces a specific temporal sequence of cellular events starting with the accumulation of neutrophils and

Figure 4. AhR Signaling Is Regulated in the Population of Ependymoglia Undergoing Direct Conversion

(A) Micrograph with orthogonal projection and pixel intensity image depicting the surface of the ependymoglial cell layer in the Tg(*gfap:GFP*)*mi2001* line. The signal is obtained using *in vivo* imaging. Note that two different states of ependymoglia cells can be distinguished based on the following levels of GFP expression: GFP^{high} (arrow) and GFP^{low} (arrowhead).

(B) Lineage trees of ependymoglia cells undergoing direct conversion in the injured brains after AhR agonist or vehicle treatment. Every line in the box represents a single ependymoglia cell followed during the 5-day-period of *in vivo* imaging.

(C) FACS plots depicting the definition of the sorting gates (Brassy background) and sorting of gfap:GFP^{high} and GFP^{low} ependymoglia in intact and injured telencephalons based on the contour plots.

(D) Dot plot showing the real-time expression of glial genes in GFP^{high}- and GFP^{low}-sorted cells from intact brains. Single dots represent individual animals indicating biological replicates. Each biological replicate is the mean of 4 technical replicates. Lines show mean ± SEM. *$p \leq 0.05$ (unpaired t test).

(E) Dot plot depicting the expression of Cyp1b1 in GFP^{low} ependymoglia-sorted cells from intact brains and after injury. Single dots represent individual animals indicating biological replicates. Each biological replicate is the mean of 4 technical replicates. Lines show mean ± SEM. *$p \leq 0.05$ (repeated one-way ANOVA with Bonferroni post hoc test).

(F) Gene set enrichment analysis (GSEA) plot depicting AhR pathway regulation at 1, 3, and 7 days after injury in the GFP^{low} ependymoglial subpopulation.

(G) Micrographs with orthogonal projections depicting HuC/D and TdTomatomem double-positive cells negative for BrdU lacking radial morphology in AhR agonist- or vehicle-treated brains 5 days after injury. Images are presented as full z-projections of the confocal z stack.

(H) Dot plot showing the percentage of neurons generated by direct conversion (double-positive HuC/D and TdTomatomem cells negative for BrdU) among all TdTomatomem-positive cells after treatment with AhR agonist or vehicle at 5 dpi (short term) and 14 dpi (long term). Single dots represent individual animals indicating biological replicates. Lines show mean ± SEM. *$p \leq 0.05$ (Mann-Whitney test).

DC, direct conversion; NES, normalized enrichment score.

microglia at the injury site. This accumulation is followed by the activation of oligodendrocyte progenitors within the first 24 hr after injury. Interestingly, the ependymoglial cells generating new neurons are fully activated somewhat later (Baumgart et al., 2012; Kroehne et al., 2011). This indicates an indirect activation of the ependymoglial cells. Notably, monocyte invasion and inflammation have been shown to be necessary for the activation of ependymoglia in zebrafish (Kyritsis et al., 2012) to generate long-term surviving neurons. The transcriptome analysis presented here further supports a role of immune cells in regulating neurogenesis, as we observed a number of pathways involved in the immune cell reaction to be specifically upregulated shortly after brain injury. However, most of these changes chase out toward 7 days after injury despite the significant increase in the proliferation of ependymoglial cells at this time point. These data suggest a paradigm in which initial changes in AhR levels prevent the premature engagement of ependymoglia cells primed to directly convert during the initial inflammatory phase. Notably, we were able to show that the interference with this timing by precociously activating AhR signaling leads to aberrant neurogenesis because additional new neurons generated in these conditions fail to survive. As ongoing inflammatory processes and astrogliosis prevent the survival and full differentiation of adult neural stem cell progeny in the mammalian brain after stroke (Dimou and Götz, 2014), our data raise the possibility that the mammalian central nervous system lost the capacity to precisely time the generation of new neurons and, therefore, regeneration capacity. The implementation of such a regulatory system in the injured mammalian brain might be the key to achieve successful regeneration.

Our analysis suggests that the appropriate regulation of AhR signaling after injury is necessary for the proper timing of restorative neurogenesis relative to the inflammatory phase of regeneration. The inhibition of AhR shortly after injury blocks the direct conversion of ependymoglia into neurons, while high levels of AhR achieved at 7 dpi promote direct conversion. The activity of the AhR pathway is controlled by a number of environmental factors including dioxins, polychlorinated biphenyls, polycyclic aromatic hydrocarbons (Stanford et al., 2016), tryptophan metabolites, and the cytokine network, suggesting a role of AhR signaling in sensing the environment after the injury. Indeed, the kynurenine pathway activated after traumatic brain injury (Yan et al., 2015) potentiates the AhR (Bersten et al., 2013), possibly via controlling tryptophan metabolism. The kynurenine pathway regulated in microglia in response to injury (Yan et al., 2015) could therefore provide endogenous ligands responsible for the translocation of AhR to the nucleus and could control the direct conversion in response to injury. The major AhR signaling mediator, AhR, is the nuclear receptor promoting the transcription of a spectrum of genes involved in the cell cycle, tissue homeostasis, early cell differentiation, and stress response (Bersten et al., 2013). The transcriptional activity of AhR is controlled by its shuffling between the nucleus and cytoplasm in a ligand-dependent manner (Bersten et al., 2013). Therefore, low AhR stability due to the PAS domain (Bersten et al., 2013) and ligand-dependent translocation to the nucleus allow the fast and dynamic AhR-mediated control of cellular behavior during wound healing and regenerative neurogenesis, including direct conversion. Interestingly, adult neurogenesis in the dentate gyrus of the hippocampus influenced by activity is dependent on AhR signaling (Latchney et al., 2013). Moreover, AhR signaling regulates the differentiation of hematopoietic progenitors (Boitano et al., 2010), suggesting an emerging concept that AhR levels allow the synchronization of the current demands implied by the environment, such as injury and the stem cell output.

STAR★METHODS

Detailed methods are provided in the online version of this paper and include the following:

- KEY RESOURCES TABLE
- CONTACT FOR REAGENT AND RESOURCE SHARING
- EXPERIMENTAL MODEL AND SUBJECT DETAILS
  - Zebrafish lines
- METHOD DETAILS
  - Stab-wound injury
  - Plasmids
  - Plasmid electroporation and cerebroventricular microinjections of drugs or morpholinos
  - *In vivo* imaging
  - Injected drugs
  - Morpholinos
  - Tissue preparation and immunohistochemistry
  - Laser capture microdissection
  - Microarray and Bioinformatics analysis
  - FACS sorting
  - RNA sequencing and Bioinformatic analysis
  - Real time q-PCR
  - BrdU labeling experiments
  - Cell death assay (TUNEL)
- QUANTIFICATION AND STATISTICAL ANALYSIS
  - Ependymoglia surface measuring (quantifications)
- DATA AND SOFTWARE AVAILABILITY
  - Software
  - Data

SUPPLEMENTAL INFORMATION

Supplemental Information includes four figures, two tables, and two videos and can be found with this article online at https://doi.org/10.1016/j.celrep.2018.11.055.

ACKNOWLEDGMENTS

We are particularly grateful to Dr. Magdalena Götz (Ludwig-Maximilians-University, Munich) for her valuable support toward this study and her experimental suggestions. We would also like to thank Dr. Judith Fischer and Andrea Steiner-Mezzadri (Helmholtz Zentrum Munich) for their great help with the FACS. A special thanks to Dr. Filippo Calzolari for his support and suggestions. Additionally, we thank Sarah Hubinger and Anke Bettenbrock for excellent technical assistance, all the members of the fish regeneration group, and the members of the Götz lab for discussions. We thank Magdalena Götz and Tara Comber for critical readings of the manuscript. This work was supported by the German Research Foundation Collaborative Research Centre (CRC) 870 to J.N. and W.W. and SPP1738 and SPP1757 to J.N.; the Helmholtz Portfolio Theme "Metabolic Dysfunction and Common Disease" (J.B.); the Helmholtz Alliance "Imaging and Curing Environmental Metabolic Diseases"

(ICEMED) (J.B. and J.N.); and the German Federal Ministry of Education and Research (BMBF) through the Joint Project HIT-Tau (01EK1605C to W.W. and D.T.). A SD confocal microscope was used (DFG INST 86/1581-1 FUGG).

AUTHOR CONTRIBUTIONS

R.D.G. and J.N. conceived the project and experiments. R.D.G., T.D., A.K., M.I., F.M.C., J.B., E.V.B., P.B., C.T.B., A.M.N., and S.H.S. performed the experiments and analyzed the data; M.I., G.S., and D.T. performed the bioinformatics analyses. R.D.G., J.N., and T.D. wrote the manuscript with inputs from P.B., A.K., M.I., F.M.C., G.S., J.B., D.T., E.V.B., J.S.B., and W.W.

DECLARATION OF INTERESTS

The authors declare no competing interests.

Received: November 28, 2017
Revised: October 10, 2018
Accepted: November 13, 2018
Published: December 11, 2018

REFERENCES

Arvidsson, A., Collin, T., Kirik, D., Kokaia, Z., and Lindvall, O. (2002). Neuronal replacement from endogenous precursors in the adult brain after stroke. Nat. Med. *8*, 963–970.

Barbosa, J.S., Sanchez-Gonzalez, R., Di Giaimo, R., Baumgart, E.V., Theis, F.J., Götz, M., and Ninkovic, J. (2015). Neurodevelopment. Live imaging of adult neural stem cell behavior in the intact and injured zebrafish brain. Science *348*, 789–793.

Barbosa, J.S., Di Giaimo, R., Götz, M., and Ninkovic, J. (2016). Single-cell in vivo imaging of adult neural stem cells in the zebrafish telencephalon. Nat. Protoc. *11*, 1360–1370.

Baumgart, E.V., Barbosa, J.S., Bally-Cuif, L., Götz, M., and Ninkovic, J. (2012). Stab wound injury of the zebrafish telencephalon: a model for comparative analysis of reactive gliosis. Glia *60*, 343–357.

Becker, C.G., and Becker, T. (2015). Neuronal regeneration from ependymoradial glial cells: cook, little pot, cook!. Dev. Cell *32*, 516–527.

Bello, S.M., Heideman, W., and Peterson, R.E. (2004). 2,3,7,8-Tetrachlorodibenzo-p-dioxin inhibits regression of the common cardinal vein in developing zebrafish. Toxicol. Sci. *78*, 258–266.

Berghard, A., Gradin, K., and Toftgård, R. (1992). The stability of dioxin-receptor ligands influences cytochrome P450IA1 expression in human keratinocytes. Carcinogenesis *13*, 651–655.

Bernardos, R.L., and Raymond, P.A. (2006). GFAP transgenic zebrafish. Gene Expr. Patterns *6*, 1007–1013.

Bersten, D.C., Sullivan, A.E., Peet, D.J., and Whitelaw, M.L. (2013). bHLH-PAS proteins in cancer. Nat. Rev. Cancer *13*, 827–841.

Boitano, A.E., Wang, J., Romeo, R., Bouchez, L.C., Parker, A.E., Sutton, S.E., Walker, J.R., Flaveny, C.A., Perdew, G.H., Denison, M.S., et al. (2010). Aryl hydrocarbon receptor antagonists promote the expansion of human hematopoietic stem cells. Science *329*, 1345–1348.

Brill, M.S., Ninkovic, J., Winpenny, E., Hodge, R.D., Ozen, I., Yang, R., Lepier, A., Gascón, S., Erdelyi, F., Szabo, G., et al. (2009). Adult generation of glutamatergic olfactory bulb interneurons. Nat. Neurosci. *12*, 1524–1533.

Chen, J., Magavi, S.S.P., and Macklis, J.D. (2004). Neurogenesis of corticospinal motor neurons extending spinal projections in adult mice. Proc. Natl. Acad. Sci. USA *101*, 16357–16362.

Dimou, L., and Götz, M. (2014). Glial cells as progenitors and stem cells: new roles in the healthy and diseased brain. Physiol. Rev. *94*, 709–737.

Dobin, A., Davis, C.A., Schlesinger, F., Drenkow, J., Zaleski, C., Jha, S., Batut, P., Chaisson, M., and Gingeras, T.R. (2013). STAR: ultrafast universal RNA-seq aligner. Bioinformatics *29*, 15–21.

Ernst, A., Alkass, K., Bernard, S., Salehpour, M., Perl, S., Tisdale, J., Possnert, G., Druid, H., and Frisén, J. (2014). Neurogenesis in the striatum of the adult human brain. Cell *156*, 1072–1083.

Fischer, J., Beckervordersandforth, R., Tripathi, P., Steiner-Mezzadri, A., Ninkovic, J., and Götz, M. (2011). Prospective isolation of adult neural stem cells from the mouse subependymal zone. Nat. Protoc. *6*, 1981–1989.

Hestermann, E.V., and Brown, M. (2003). Agonist and chemopreventative ligands induce differential transcriptional cofactor recruitment by aryl hydrocarbon receptor. Mol. Cell. Biol. *23*, 7920–7925.

Huber, A.B., Kania, A., Tran, T.S., Gu, C., De Marco Garcia, N., Lieberam, I., Johnson, D., Jessell, T.M., Ginty, D.D., and Kolodkin, A.L. (2005). Distinct roles for secreted semaphorin signaling in spinal motor axon guidance. Neuron *48*, 949–964.

Kelsh, R.N., Brand, M., Jiang, Y.J., Heisenberg, C.P., Lin, S., Haffter, P., Odenthal, J., Mullins, M.C., van Eeden, F.J., Furutani-Seiki, M., et al. (1996). Zebrafish pigmentation mutations and the processes of neural crest development. Development *123*, 369–389.

Kishimoto, N., Shimizu, K., and Sawamoto, K. (2012). Neuronal regeneration in a zebrafish model of adult brain injury. Dis. Model. Mech. *5*, 200–209.

Kroehne, V., Freudenreich, D., Hans, S., Kaslin, J., and Brand, M. (2011). Regeneration of the adult zebrafish brain from neurogenic radial glia-type progenitors. Development *138*, 4831–4841.

Kyritsis, N., Kizil, C., Zocher, S., Kroehne, V., Kaslin, J., Freudenreich, D., Iltzsche, A., and Brand, M. (2012). Acute inflammation initiates the regenerative response in the adult zebrafish brain. Science *338*, 1353–1356.

Latchney, S.E., Hein, A.M., O'Banion, M.K., DiCicco-Bloom, E., and Opanashuk, L.A. (2013). Deletion or activation of the aryl hydrocarbon receptor alters adult hippocampal neurogenesis and contextual fear memory. J. Neurochem. *125*, 430–445.

Livak, K.J., and Schmittgen, T.D. (2001). Analysis of relative gene expression data using real-time quantitative PCR and the 2(-Delta C(T)) Method. Methods *25*, 402–408.

Love, M.I., Huber, W., and Anders, S. (2014). Moderated estimation of fold change and dispersion for RNA-seq data with DESeq2. Genome Biol. *15*, 550.

Marlowe, J.L., Knudsen, E.S., Schwemberger, S., and Puga, A. (2004). The aryl hydrocarbon receptor displaces p300 from E2F-dependent promoters and represses S phase-specific gene expression. J. Biol. Chem. *279*, 29013–29022.

McCurley, A.T., and Callard, G.V. (2008). Characterization of housekeeping genes in zebrafish: male-female differences and effects of tissue type, developmental stage and chemical treatment. BMC Mol. Biol. *9*, 102.

Mootha, V.K., Lindgren, C.M., Eriksson, K.F., Subramanian, A., Sihag, S., Lehar, J., Puigserver, P., Carlsson, E., Ridderstrale, M., Laurila, E., et al. (2003). PGC-1alpha-responsive genes involved in oxidative phosphorylation are coordinately downregulated in human diabetes. Nat. Genet *34*, 267–273.

Park, H.C., Kim, C.H., Bae, Y.K., Yeo, S.Y., Kim, S.H., Hong, S.K., Shin, J., Yoo, K.W., Hibi, M., Hirano, T., et al. (2000). Analysis of upstream elements in the HuC promoter leads to the establishment of transgenic zebrafish with fluorescent neurons. Dev. Biol. *227*, 279–293.

Prasch, A.L., Teraoka, H., Carney, S.A., Dong, W., Hiraga, T., Stegeman, J.J., Heideman, W., and Peterson, R.E. (2003). Aryl hydrocarbon receptor 2 mediates 2,3,7,8-tetrachlorodibenzo-p-dioxin developmental toxicity in zebrafish. Toxicol. Sci. *76*, 138–150.

R Development Core Team (2009). R: A Language and Environment for Statistical Computing (R Foundation for Statistical Computing).

Rainer, J., Sanchez-Cabo, F., Stocker, G., Sturn, A., and Trajanoski, Z. (2006). CARMAweb: comprehensive R- and bioconductor-based web service for microarray data analysis. Nucleic Acids Res. *34*, W498–W503.

Rico-Leo, E.M., Alvarez-Barrientos, A., and Fernandez-Salguero, P.M. (2013). Dioxin receptor expression inhibits basal and transforming growth factor β-induced epithelial-to-mesenchymal transition. J. Biol. Chem. *288*, 7841–7856.

Rothhammer, V., Mascanfroni, I.D., Bunse, L., Takenaka, M.C., Kenison, J.E., Mayo, L., Chao, C.C., Patel, B., Yan, R., Blain, M., et al. (2016). Type I interferons and microbial metabolites of tryptophan modulate astrocyte activity and central nervous system inflammation via the aryl hydrocarbon receptor. Nat. Med. *22*, 586–597.

Soshilov, A.A., and Denison, M.S. (2014). Ligand promiscuity of aryl hydrocarbon receptor agonists and antagonists revealed by site-directed mutagenesis. Mol. Cell. Biol. *34*, 1707–1719.

Stanford, E.A., Ramirez-Cardenas, A., Wang, Z., Novikov, O., Alamoud, K., Koutrakis, P., Mizgerd, J.P., Genco, C.A., Kukuruzinska, M., Monti, S., et al. (2016). Role for the Aryl Hydrocarbon Receptor and Diverse Ligands in Oral Squamous Cell Carcinoma Migration and Tumorigenesis. Mol. Cancer Res. *14*, 696–706.

Subramanian, A., Tamayo, P., Mootha, V.K., Mukherjee, S., Ebert, B.L., Gillette, M.A., Paulovich, A., Pomeroy, S.L., Golub, T.R., Lander, E.S., and Mesirov, J.P. (2005). Gene set enrichment analysis: a knowledge-based approach for interpreting genome-wide expression profiles. Proc. Natl. Acad. Sci. USA *102*, 15545–15550.

Xu, C., Volkery, S., and Siekmann, A.F. (2015). Intubation-based anesthesia for long-term time-lapse imaging of adult zebrafish. Nat. Protoc. *10*, 2064–2073.

Yan, E.B., Frugier, T., Lim, C.K., Heng, B., Sundaram, G., Tan, M., Rosenfeld, J.V., Walker, D.W., Guillemin, G.J., and Morganti-Kossmann, M.C. (2015). Activation of the kynurenine pathway and increased production of the excitotoxin quinolinic acid following traumatic brain injury in humans. J. Neuroinflammation *12*, 110.

STAR★METHODS

KEY RESOURCES TABLE

REAGENT or RESOURCE	SOURCE	IDENTIFIER
Antibodies		
Chicken Anti-Green Fluorescent Protein	Aves Labs	Cat# GFP_1020; RRID: AB_10000240
Rat Anti-BrdU	Abcam	Cat# ab6326; RRID: AB_305426
Rabbit Anti-Red Fluorescent Protein	Rockland	Cat# 600-401-379; RRID: AB_2209751
Rabbit Anti-HuC/HuD	Abcam	Cat# AB_210554; https://www.abcam.com/huchud-protein-antibody-ab210554.html
Mouse Anti-Human HuC/HuD neuronal protein	Molecular Probes	Cat# A-21271; RRID:AB_221448
Mouse Anti-FLAG M2 antibody	Sigma Aldrich	Cat# F1804-1MG
BABB clearing protocol	Huber et al., 2005	N/A
Chemicals, Peptides, and Recombinant Proteins		
β-naphthoflavone (BNF)	Sigma-Aldrich	Cat# N3633
AhR antagonist	Calbiochem	Cat# 182705
Dimethylsulfoxid (DMSO)	Sigma-Aldrich	CAS: 67-68-5
Fast Green FCF	Sigma-Aldrich	Cat# F258-25G
MS222	Sigma-Aldrich	Cat# A5040-25G
DAPI	Sigma Aldrich	Cat# 10236276001
BrdU	Sigma Aldrich	Cat# B5002
Aqua Poly/mount	Polysciences Inc	Cat# 18606-5
SYBR Green	QIAGEN	Cat# 204057
Critical Commercial Assays		
ApopTag Red *In Situ* Apoptosis Detection Kit	EMD Millipore	S7165
POL-membrane slides	Leica Microsystems	11505188
RNeasy Plus Micro Kit	QIAGEN	7404
Ovation Pico WTA System V2	NuGen	3302-12
Encore Biotin Module	NuGen	4200-12
Zebrafish 1.0 ST arrays	Affymetrix	902007
PicoPure RNA Isolation Kit	Thermo Fisher	KIT0204
SMART-Seq v4 Ultra Low Input RNA Kit	Clontech	634888
MicroPlex Library Preparation Kit v2	Diagenode	C05010012
Maxima first strand synthesis kit	Thermo Scientific	K1671
Deposited Data		
Microarray data	This study	GenBank: GSE102400
RNA-seq data	This study	GenBank: GSE121404
Experimental Models: Organisms/Strains		
Tg(gfap:gfp)mi2001	Bernardos and Raymond, 2006	ZFIN ID: ZDB-PUB-060616-45
Tg(HuC:GFP)	Park et al., 2000	ZFIN ID: ZDB-PUB-001205-14
Brassy	Kelsh et al.,1996	ZFIN ID: ZDB-PUB-970210-32

(*Continued on next page*)

Continued

REAGENT or RESOURCE	SOURCE	IDENTIFIER
Oligonucleotides		
ahr2 Morpholino: MO-ahr2 TGTACCGAT ACCCGCCGACATGGTT	Gene Tools	Prasch et al., 2003
Morpholino: Standard control morpholino	Gene Tools	N/A
Primers for Real time qPCR see Table S2	This paper	N/A
Software and Algorithms		
ImageJ	National Institutes of Health	https://imagej.nih.gov/ij/
Fiji	Laboratory for Optical and Computational Instrumentation	https://fiji.sc/; RRID: SCR_002285
Imaris V 6.3 software	Bitplane	http://www.bitplane.com/
Imaris V 8.4.1 software	Bitplane	http://www.bitplane.com/
FW10-ASW software	Olympus	https://www.olympus-lifescience.com/en/support/downloads/#!dlOpen=%23detail847249651
GraphPad Prism 7	GraphPad Software	https://www.graphpad.com/
Expression console (v.1.2)	Thermofisher	https://www.thermofisher.com/us/en/home/life-science/microarray-analysis/microarray-analysis-instruments-software-services/microarray-analysis-software/affymetrix-expression-console-software.html
R Development Core	N/A	https://www.r-project.org
CARMAweb	N/A	https://carmaweb.genome.tugraz.at/carma/
Ensembl Genome browser 90	N/A	http://www.ensembl.org//useast.ensembl.org/index.html?redirectsrc=//www.ensembl.org%2Findex.html
QIAGEN's Ingenuity Pathway Analysis (IPA®)	QIAGEN	https://www.qiagenbioinformatics.com/
STAR	Dobin et al., 2013	https://github.com/alexdobin/STAR
DeSeq2	Love et al., 2014	https://bioconductor.org/packages/release/bioc/html/DESeq2.html
Gene Set Enrichment Analysis	Subramanian et al., 2005; Mootha et al., 2003	http://software.broadinstitute.org/gsea/index.jsp
Molecular Signatures Database	Subramanian et al., 2005	http://software.broadinstitute.org/gsea/msigdb/index.jsp

CONTACT FOR REAGENT AND RESOURCE SHARING

Further information and requests for resources and reagents should be directed to and will be fulfilled by the Lead Contact, Prof. Jovica Ninkovic (ninkovic@helmholtz-muenchen.de).

EXPERIMENTAL MODEL AND SUBJECT DETAILS

Zebrafish lines

Transgenic zebrafish lines that were used are *Tg(gfap:gfp)mi2001* (Bernardos and Raymond, 2006) and *Tg(HuC:GFP)* (Park et al., 2000) crossed with *brassy.* We also used non-transgenic strains AB/EK hybrid and *brassy* (Kelsh et al., 1996).

All experiments were done with 3-5 months old animals, as in this age range we do not observe any age-associated differences. Control and treated animals were littermates in individual experiments. We did at least 3 independent biological replicates in every experiment (the exact number of analyzed animals is specified in every dot plot) and analysis was done blindly.

All animals were kept under standard, husbandry conditions and experiments were performed according to the handling guidelines and regulations of EU and the Government of Upper Bavaria (AZ 55.2-1-54-2532-0916).

METHOD DETAILS

Stab-wound injury

Stab wound injury (nostril injury type) was performed in both telencephalic hemispheres as previously described (Baumgart et al., 2012). Stab-wound injuries were made using a 100 × 0.9 mm glass capillary needle (KG01, A. Hartenstein). All needles were pulled

on a Narishige Puller (model PC-10) using a ''One-stage'' pull setting at a heater level of 63.5°C. The resulting dimensions of the needle used to make the telencephalic injury were 5 mm in length and 0.1 mm in diameter.

Plasmids

For labeling of ependymoglia cells prior to imaging we used pCS2-TdTomatomem plasmid (Barbosa et al., 2015).

Constitutively active zebrafish AhR construct (caAhR) was cloned in-house. The N-terminal portion of zebrafish ahr2 lacking PAS B domain was amplified by PCR using zebrafish cDNA and was fused by Gibson cloning to the transactivation domain of mouse AhR obtained from mouse liver cDNA. In order to be able to follow caAhR *in vivo* the protein was tagged by a FLAG tag.

Plasmid electroporation and cerebroventricular microinjections of drugs or morpholinos

TdTomatomem plasmid DNA (2.5μg/μl) was diluted in distilled water (Aqua B. Braun) to the final concentration of 1 μg/μl and injected with the dye Fast Green (0.3 mg ml^{-1}; Sigma).

Fish were first anaesthetized in 0.02% MS222 and immobilized in a sponge. A small hole in the skull was made, in the region between the telencephalon and the optic tectum using a microknife (Fine Science Tools). Subsequently, ventricular injections of the plasmid DNA were performed as previously done (Barbosa et al., 2015) using a glass capillary (Harvard Apparatus) and a pressure injector (200hPa, Femtojet®, Eppendorf). Five electrical pulses (amplitude, 65 V; duration, 25 ms; intervals, 1 s) were delivered with a square-wave pulse generator TSS20 Ovodyne (Intracel) or using ECM830 square wave electroporator (BTX Harvard Apparatus).

In the case of CMVI only, we followed the same procedure as above described, however instead of plasmid DNA, drugs or morpholinos were diluted in artificial cerebro-spinal fluid (ACSF) and injected with the dye Fast Green (0.3 mg ml^{-1}; Sigma) in the ventricle using a glass capillary (Harvard Apparatus) and a pressure injector (170hPa, Femtojet®, Eppendorf).

After the electroporation or injection, fish were awakened in the aerated water and kept in their normal husbandry conditions until the first *in vivo* imaging session, FACS or immunohistochemical analysis.

In vivo imaging

For *in vivo* imaging we used only animals with the *brassy* background in order to minimize the interference of the auto-fluorescence from the pigment cells existing in wild-type strains.

Ependymoglia cells were labeled by electroporation (see above) of TdTomatomem plasmid and the first imaging session was made 4 days after electroporation in order to leave enough time for fluorescent protein expression and maturation. Subsequently, fish were imaged repetitively on the daily basis for 5 days. In order to facilitate the detection of fluorescent proteins, the skin above the telencephalon area was removed and the skull was thinned using a micro-driller (Foredom) before first imaging session as we have done previously (Barbosa et al., 2015). Fish were anesthetized using the MS222 concentrations described in Barbosa et al. (2015). 1x MS222 water was prepared by adding 4,2 mL of MS222 stock solution to 100ml of E3 medium. During imaging, fish were continuously intubated by delivering aerated 0.75x MS222 solution prepared based on Xu et al. (2015). After imaging sessions, fish were released from the holder and awakened in fresh aerated tank water to allow free swimming between imaging sessions in normal husbandry conditions (see above).

Imaging was performed with a multi-photon, near-infrared, pulsed MaiTai HP DeepSee laser, tunable from 690nm to 1020nm (Spectra Physics) and a FV10-MRG filter (barrier filter = 495– 540 nm, dichromatic mirror = 570 nm, BA 575–630 nm). A water immersion objective (XL Plan N, 25x, 1.05NA, Olympus) was used as in Barbosa et al.,2015. An excitation wavelength of 1005nm was used to excite simultaneously GFP and Tdtomato fluorophores. Images were acquired using the FW10-ASW 4.0 software (Olympus) with independent laser adjustments for each channel.

The *z*-brightness function was used to adjust laser intensity and detector sensitivity with depth, allowing image capture without changes in brightness. The optical sections were acquired with a resolution in the *x-y* dimension 800 × 800 pixels and in the *z*-dimension at 1,5 or 2 μm interval between single optical sections. The imaged area in each fish was reliably reidentified based on the distribution pattern of electroporated cells.

After the imaging, image analysis was performed using the ImageJ (Fiji) and Imaris V8.4 software (Bitplane). In case that the imaging was performed in the *Tg(gfap:GFP)mi2001* transgenic line, cells with the cell body residing on the surface of the telencephalon, radial process and *gfap*:GFP expression were identified as ependymoglia cells and only these cells were analyzed throughout the 5 daytime course.

In the case of imaging performed in *Tg(HuC:GFP)* transgenic line, ependymoglia cells were identified based on radial morphology. Non-glial cells derived from ependymoglia cells that upegulate HuC/D neuronal marker were classified as HuC/D-positive neurons.

Post-imaging analysis was done using BABB clearing protocol for post-imaging immunohistochemistry for confirmation of the identity of the imaged cells as previously described (Barbosa et al., 2016).

Injected drugs

β-naphthoflavone (BNF, Sigma Cat. N3633) was dissolved in DMSO at the concentration of 20mM. For CMVI it was diluted 1:100 in Artificial Cerebro-Spinal Fluid (ACSF, final concentration 20μM). DMSO used in control experiment (Vehicle) was diluted 1:100 in ACSF.

AhR antagonist (Calbiochem, Cat. 182705) was dissolved in DMSO at the concentration of 3mM. For CMVI it was diluted 1:500 in ACSF (final concentration 6μM). DMSO used in control experiment (Vehicle) was diluted 1:500 in ACSF.

Morpholinos

Zebrafish ahr2 morpholino was designed according to Prasch et al. (2003) and was obtained from Gene Tools (USA). The control morpholino was the standard control morpholino (Gene Tools, USA). Both ahr2-MO and Ctrl-MO were dissolved in sterile water at the concentration of 1mM. Prior to CMVI, they were diluted to final concentration of 0.5 mM in ACSF.

Tissue preparation and immunohistochemistry

Animals were sacrificed by MS222 overdose of tricaine methane sulfonate (MS222, 0,2%) by prolonged immersion. Tissue processing was performed as described previously (Baumgart et al., 2012).

Laser capture microdissection

Telencephalon was dissected from intact and injured brains (2 and 7 days after injury) of animals from the *Tg(gfap:gfp)mi2001* transgenic line. 30 μm thick coronal sections were obtained with a cryostat, mounted on POL-membrane slides, and frozen at −80°C until further processing. Sections were dehydrated by immersion in 75%EtOH for 1.5 minutes, then in 90%EtOH for 1.5 minutes, and finally in 100%EtOH for 2 minutes, dried briefly and immediately used for microdissections with Laser Capture Microscopy system (LMD6000, Leica, Germany). Microdissected areas: dorsal and intermediate subventricular zone (VZ, 50 μm width from the ventricular surface), and the brain parenchyma (DP) avoiding regions close to the injury site. The areas chosen for dissection were cut and catapulted to a collecting tube. VZ and DP areas coming from different sections were collected together for a total collected area ranging from $3x10^5$ to 1 $x10^6$ μm2 for each sample and immediately lysed in RTL buffer from the RNeasy Plus Micro Kit for RNA was extraction. RNA was extracted using the RNeasy Plus Micro Kit according to manufacturer instructions. The Agilent 2100 Bioanalyzer was used to assess RNA quality and only high-quality RNA (RIN $\geq$ 8) was further processed for microarray analysis.

Microarray and Bioinformatics analysis

1 ng total RNA was amplified using the Ovation Pico WTA System V2 in combination with the Encore Biotin Module. Amplified cDNA was hybridized on Zebrafish 1.0 ST arrays. Staining and scanning (GeneChip Scanner 3000 7G) were done according to the Affymetrix expression protocol including minor modifications as suggested in the Encore Biotion protocol. Expression console (v.1.2) was used for quality control and to obtain annotated normalized RNA gene-level data (standard settings including median polish and sketch-quantile normalization). Statistical analyses were performed by utilizing the statistical programming environment R (R Development Core Team, 2009) implemented in CARMAweb (Rainer et al., 2006). Genewise testing for differential expression was done employing the limma t test and probe sets with $p < 0.05$, fold-change > 1.5x and average expression in at least one group per brain region > 10. The genomic positions of all probe sets in the zebrafish microarray were extracted from Affymetrix website (http://www.affymetrix.com/analysis/inex.affx) by applying a Batch Query on the GeneChip Array "Zebrafish Gene 1.x ST" (genome version Zv9, 2011). Zebrafish gene identifiers were derived from Ensembl database by using a custom-written Perl script and the extracted genomic positions of the probe sets, via the Application Programming Interface (API), version 64. Subsequently homologous mouse genes were retrieved by Ensembl Compara database. The identified orthologs were then used for canonical pathway enrichment analyses through the use of QIAGEN's Ingenuity Pathway Analysis. Regulated gene sets as input were selected by filters for (to determine). From significantly enriched pathways (Fishers Exact Test, $p < 0.05$) relevant ones were manually selected.

FACS sorting

The dorsal telencephalon from the *Tg(gfap:gfp)mi2001* transgenic line was dissected from intact brains and 1, 2, 5, 7 and 10 days after injury. Telencephali coming from 2 animals were pulled in one tube before dissociation. A single cell suspension was prepared according to Fischer et al. (2011). Single cells were filtered through a 70μm cell strainer and centrifuged at 1500 rpm for 7 min. After this passage, 2 different procedures were used for intracellular FACS analysis of proliferating cells and FACS sorting of ependymoglial cells.

For FACS analysis of proliferating progenitors ($PCNA^+$, gfap:GFP+ aNSCs), cells were fixed in 70% ice cold ethanol and analyzed according to Barbosa et al. (2015). PCNA staining was performed using anti-PCNA antibody (1:250) coupled with AlexaFluor647 donkey anti mouse IgG secondary antibody (1:800). FACS analysis was performed at a FACS Aria (BD) in BD FACS Flow TM medium. Debris and aggregated cells were gated out by forward scattersideward scatter; single cells were gated in by FSC-W/FSC-A. Gating for fluorophores was done using *brassy* animals for GFP gating and *Tg(gfap:gfp)mi2001* animals stained with secondary antibody only for PCNA staining. Different ependymoglial populations are identified by formation of two clear clusters of cells in contour plot and sorting gates are defined based on the contour plots.

For FACS sorting of ependymoglial GFP^{low} populations, cells were washed in PBS, centrifuged at 1500 rpm for 7 min, re-suspended in PBS and analyzed and sorted according to the gates. GFP gating was done using *brassy* animals. GFP low cells were sorted directly in Extraction Buffer from PicoPure RNA Isolation Kit. After 30 minutes incubation at 42°C, sample were kept at 80°C until further processing for RNA isolation for RNA sequencing or Real Time qPCR.

RNA sequencing and Bioinformatic analysis

Total RNA from FACS-sorted cells was isolated employing PicoPure RNA Isolation Kit including digestion of remaining genomic DNA according to producer's guidelines but final RNA elution was performed with nuclease-free water at 37°C. The Agilent 2100 Bioanalyzer was used to assess RNA quality and only high-quality RNA (RIN > 8) was further processed for cDNA synthesis with SMART-Seq v4 Ultra Low Input RNA Kit according to the manufacturer's instruction. cDNA was fragmented to an average size of 200-500 bp in a Covaris S220 device (5 min; 4°C; PP 175; DF 10; CB 200). Fragmented cDNA was used as input for library preparation with MicroPlex Library Preparation Kit v2 and processed according to the manufacturer's instruction. Deep sequencing was performed on Illumina HiSeq system with 50bp paired-end reads.

FASTQ files were mapped to the Danio rerio genome (danrer10) using STAR (Dobin et al., 2013) with default parameters. Raw read counts were normalized using DeSeq2 (Love et al., 2014) to calculate differential gene expression and to perform the PCA analysis. Genes were ranked according to the log fold change between two conditions. Gene Set Enrichment Analysis (Subramanian et al., 2005) was performed using Hallmark gene sets of the Molecular Signatures Database (Subramanian et al., 2005). A custom gene set for Aryl Receptor Pathway was derived from Ingenuity (Aryl Hydrocarbon Receptor Signaling).

Real time q-PCR

Total RNA from FACS-sorted cells or dissected telencephali was isolated using PicoPure RNA Isolation Kit according to the manufacturer's instruction and genomic DNA was removed. The Agilent 2100 Bioanalyzer was used to assess RNA quality and only high-quality RNA (RIN $\geq$ 8) was further processed for cDNA synthesis. cDNA synthesis was performed using random primers with the Maxima first strand synthesis kit. qRT-PCR was conducted using SYBR Green and a Thermo Fisher Quant Studio 6 machine. The expression of each gene was analyzed in triplicate. Data were processed with the $\Delta\Delta$Ct method (Livak and Schmittgen, 2001). Elf1a was used as a reference gene (McCurley and Callard, 2008). Quantification was performed on three independent samples. Primers are used for the Real Time qPCR are listed in Table S2.

BrdU labeling experiments

BrdU (10mM, Sigma) was used and fish were kept in BrdU containing aerated water for 22 h/day for 5 days. During the 2 hours outside of BrdU water, fish were kept in fresh water and fed. After the treatment, animals were divided in two experimental groups. One group of animals was sacrificed right after the BrdU treatment (5 days BrdU, short term neurogenesis experiment). The second group of animals was sacrificed 9 days after (5 days BrdU + 9 days chase, long term neurogenesis experiment).

Cell death assay (TUNEL)

To assess cell death, we used the ApopTag Red *In Situ* Apoptosis Detection Kit (Merck Millipore, S7165) following user manual.

QUANTIFICATION AND STATISTICAL ANALYSIS

Statistical analyses were performed with GraphPad Prism 7 software by using two-tailed unpaired t test for experiments with normal data distribution and Mann-Whitney if we could not determine the normal data distribution. Statistical tests are indicated in the figure legends. Data are presented as the mean ± standard error of the mean (SEM). Statistical parameters are reported in the respective figures and figure legends.

We did at least 3 repetitions of each experiment and analysis was done blindly.

Ependymoglia surface measuring (quantifications)

Quantification of the ependymoglia-free surface was done in Imaris V8.4 (Bitplane) and ImageJ (Fiji) software. The brains were prepared as whole mount and the measuring was done on the single brain hemispheres. First, surface rendering of each hemisphere of the telencephalon was done using Imaris software applying the same criteria to every sample. Afterward, the obtained surface image was imported in ImageJ and the free area was assessed using threshold analysis. Data are presented as the mean ± standard error of the mean (SEM). Statistical analysis was done using Mann-Whitney test as indicated throughout the manuscript.

DATA AND SOFTWARE AVAILABILITY

Software

All software is freely or commercially available and is listed in the STAR Methods description and Key Resources Table.

Data

The accession number for microarray data is GSE102400 and RNA-seq data GSE121404.

Cell Reports, Volume *25*

Supplemental Information

The Aryl Hydrocarbon Receptor Pathway Defines the Time Frame for Restorative Neurogenesis

Rossella Di Giaimo, Tamara Durovic, Pablo Barquin, Anita Kociaj, Tjasa Lepko, Sven Aschenbroich, Christopher T. Breunig, Martin Irmler, Filippo M. Cernilogar, Gunnar Schotta, Joana S. Barbosa, Dietrich Trümbach, Emily Violette Baumgart, Andrea M. Neuner, Johannes Beckers, Wolfgang Wurst, Stefan H. Stricker, and Jovica Ninkovic

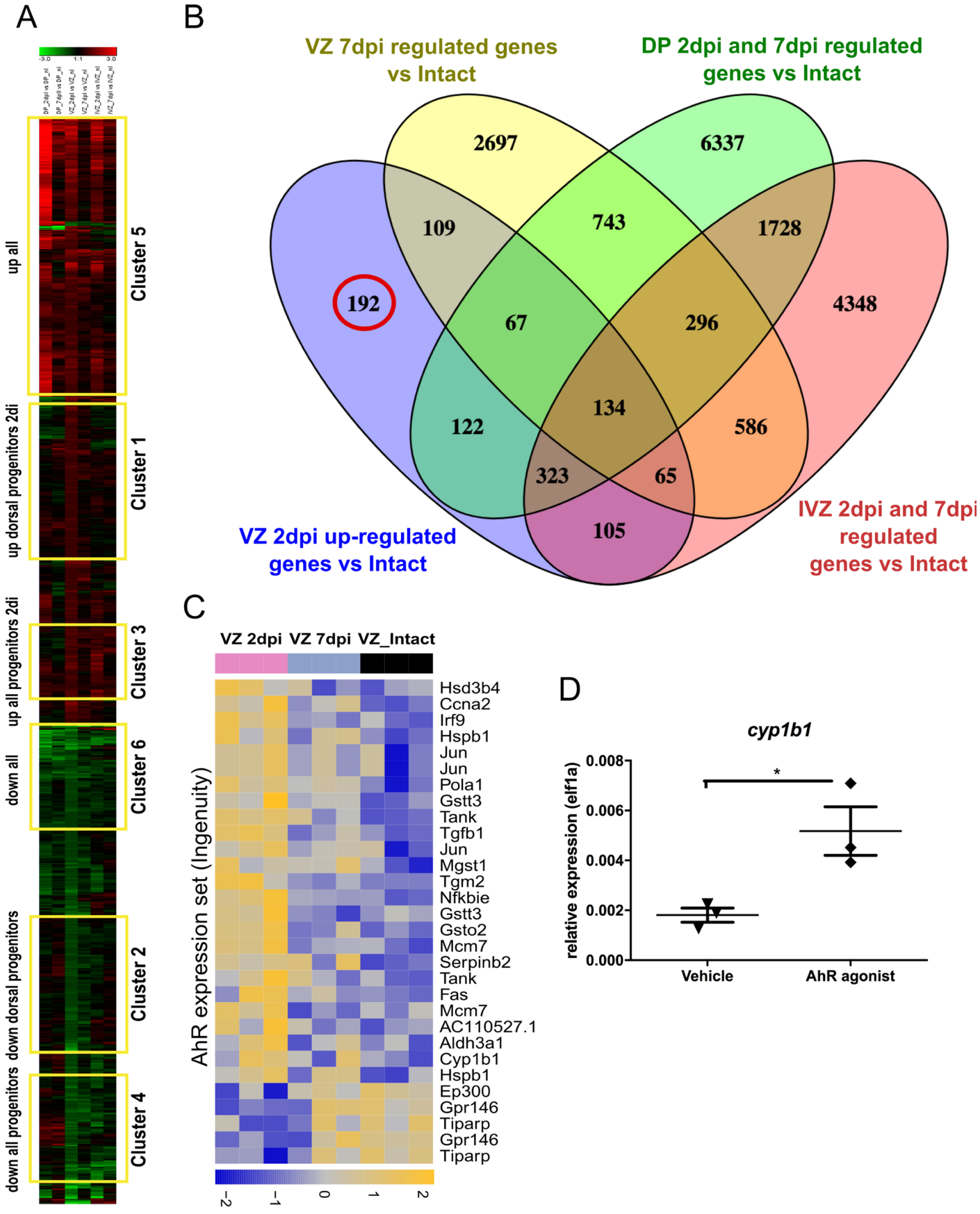

Figure S1. Identification of transcriptome changes in the neurogenic niche after brain injury. Related to Figure 1.
(A) Heatmap depicting clusters of differentially regulated genes in the dorsal ventricular zone (VZ), medial ventricular zone (MVZ) and parenchyma (DP) 2 and 7 days after brain injury compared to intact (nl) brains. Red (green) indicates up (down) regulation. Yellow boxes mark different clusters of co-regulated genes. (B) Venn diagram to identify genes specifically regulated at 2 dpi in the dorsal neurogenic zone (VZ). (C) Heatmap depicting the regulation of AhR target genes in the VZ after brain injury. Yellow (blue) indicates higher (lower) expression levels. (D) Dot plot depicting the expression of Cyp1b1 5 h after ventricular injection (CVMI) of AhR agonist (BNF) or vehicle. Single dots represent individual animals indicating biological replicates. Each biological replicate is the mean value of 4 technical replicates. Lines show mean±SEM. * ≤ 0.05; **≤ 0.01 (unpaired t test).

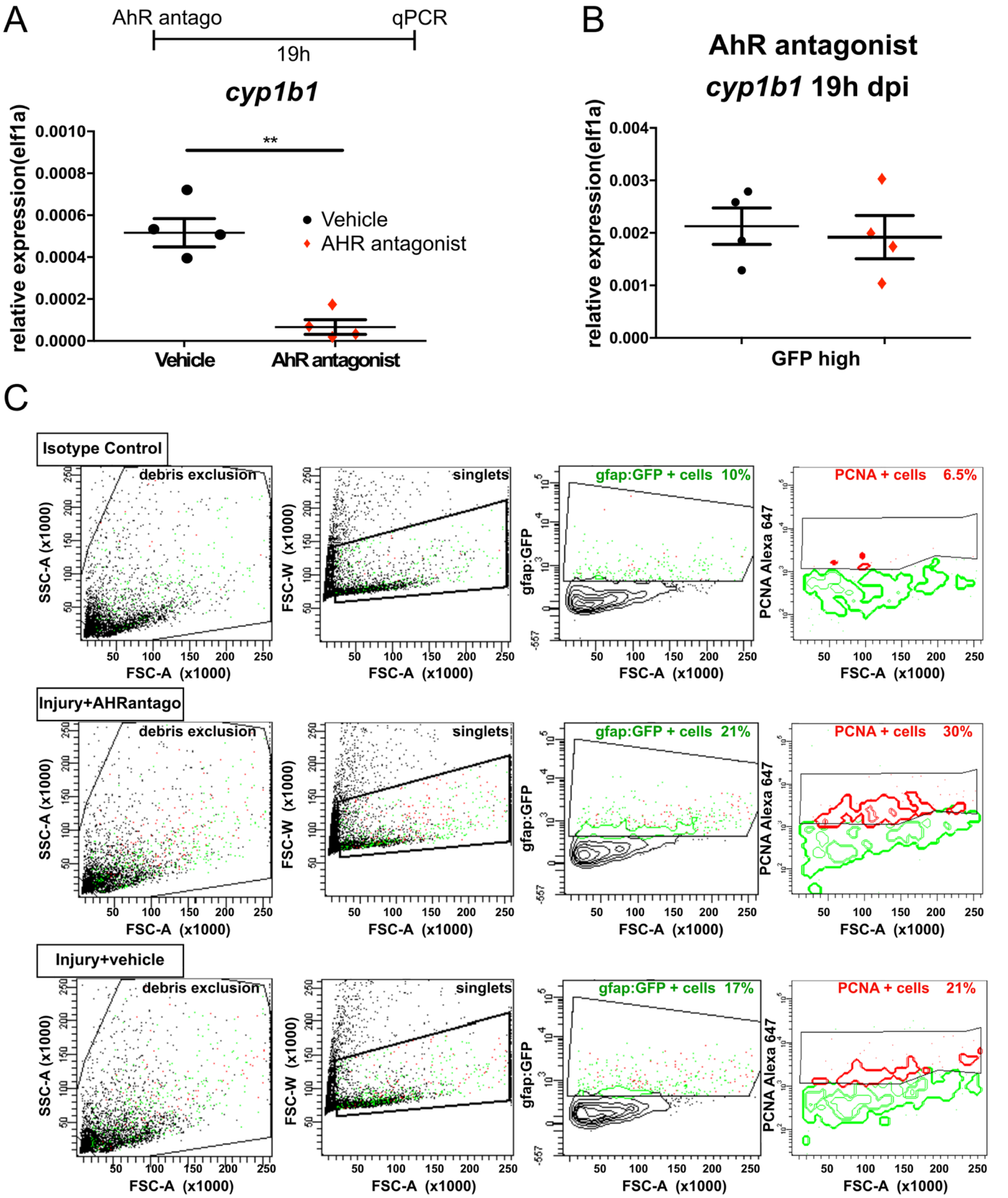

Figure S2. Decrease in AHR signalling promotes ependymoglial proliferation. Related to Figure 2.
(A) Scheme depicting the experimental procedure to assess the efficiency of AhR antagonist and dot plot showing cyp1b1 expression in ependymoglia isolated from Tg(gfap:GFP) transgenic telencephalon 19 h after CVMI of vehicle or AhR antagonist. Single dots represent individual animals indicating biological replicates. Each biological replicate is the mean value of 4 technical replicates. Lines show mean±SEM. **≤ 0.01 (unpaired t test). (B) Dot plot showing real-time qPCR analysis of cyp1b1 expression in GFP+ ependymoglia sorted from the telencephalon of Tg(gfap:GFP) transgenic animals 19 h after CMVI of vehicle or AhR antagonist. Single dots represent individual animals indicating biological replicates. Each biological replicate is the mean value of 4 technical replicates. Lines show mean±SEM. (C) FACS plots depicting the definition of the sorting gates (isotype control) and sorting of PCNA+ and gfap:GFP+ ependymoglia from injured telencephalons after AhR antagonist or vehicle treatment.

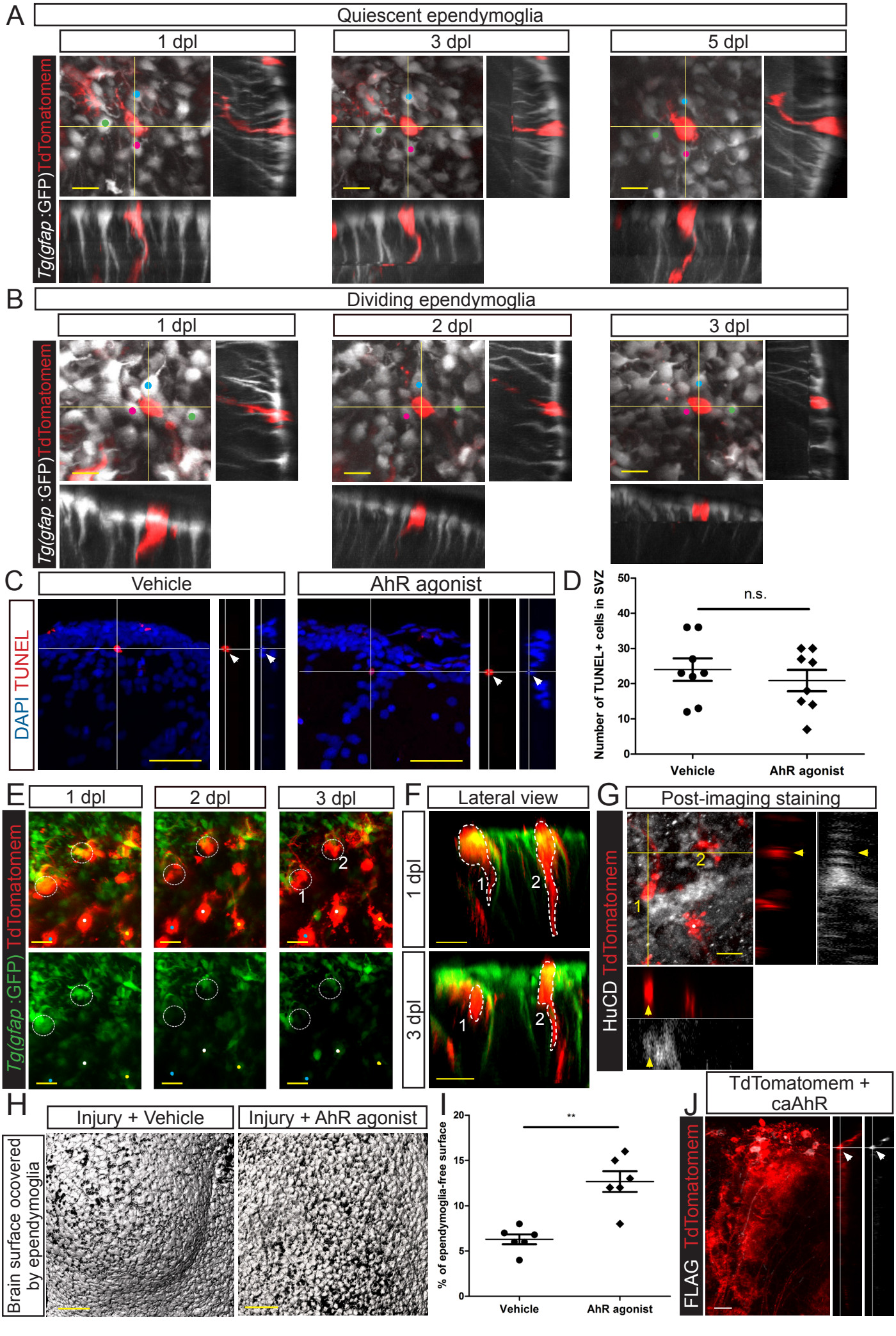
A
Quiescent ependymoglia
1 dpl
3 dpl
5 dpl
Tg(gfap :GFP)TdTomatomem
B
Dividing ependymoglia
1 dpl
2 dpl
3 dpl
Tg(gfap :GFP)TdTomatomem
C
Vehicle
AhR agonist
DAPI TUNEL
D
Number of TUNEL+ cells in SVZ
n.s.
Vehicle
AhR agonist
E
1 dpl
2 dpl
3 dpl
Tg(gfap :GFP) TdTomatomem
F
Lateral view
1 dpl
3 dpl
G
Post-imaging staining
HuCD TdTomatomem
H
Injury + Vehicle
Injury + AhR agonist
Brain surface ocovered by ependymoglia
I
% of ependymoglia-free surface
**
Vehicle
AhR agonist
J
TdTomatomem + caAhR
FLAG TdTomatomem

Figure S3. Live imaging of ependymoglial cells. Related to Figure 3.
(A, B) Micrograph depicting in vivo 2-photon images with orthogonal projections of the same TdTomatomem-labelled quiescent (A) and dividing (B) ependymoglia in the Tg(gfap:GFP) line followed for 5 days. (C) Confocal images with orthogonal projections depicting the TUNEL staining in vehicle- or AhR agonist-treated brains at 3 dpi. (D) Dot plot showing the total number of TUNEL-positive cells in the dorsal ventricular zone (SVZ) in the entire vehicle- or AhR agonist-treated brain. Single dots represent individual animals indicating biological replicates. Lines show mean±SEM (Mann-Whitney test). (E) In vivo 2-photon images following the evolution of TdTomatomem-labelled ependymoglia cells (labelled 1 and 2) in the Tg(gfap:GFP) line throughout 3 days. Lower panels show the downregulation of the gfap marker during imaging time. Dots label the individual cells used as references for the re-identification of tracked cells during imaging time. (F) 3D lateral views of the imaged cells (labelled 1 and 2) in order to assess the loss of radial processes and cell migration towards the parenchyma during direct conversion. Dashed lines define the shape of the cells. (G) Post-imaging immunostainings at 4 dpi for HuC/D and TdTomatomem in whole-brain samples with orthogonal projections confirming the neuronal (HuC/D+) identity of the imaged cells in E and F (yellow arrows). (H) Micrographs depicting the dorsal view on the central part of the hemisphere of the injured zebrafish brain covered with ependymoglia cells 5 days after injury in the Tg(gfap:GFP)mi2001 transgenic line after vehicle and AhR agonist treatment. (I) Dot plot showing the ependymoglia-free surface after treatment with AhR agonist or vehicle. Single dots represent individual animals indicating biological replicates. Lines show mean±SEM. **≤0.01 (Mann-Whitney test). (J) Confocal image with orthogonal projections showing the co-electroporation of TdTomatomem and caAhR constructs confirming the colocalization of both plasmids in the same cells and allowing us to use TdTomatomem as a long-term tracer. Scale bars: 20 μm in A and B, 30 μm in C, 20 μm in E, 30 μm in F, 20 μm in G, 20 μm in H, 50 μm in J.

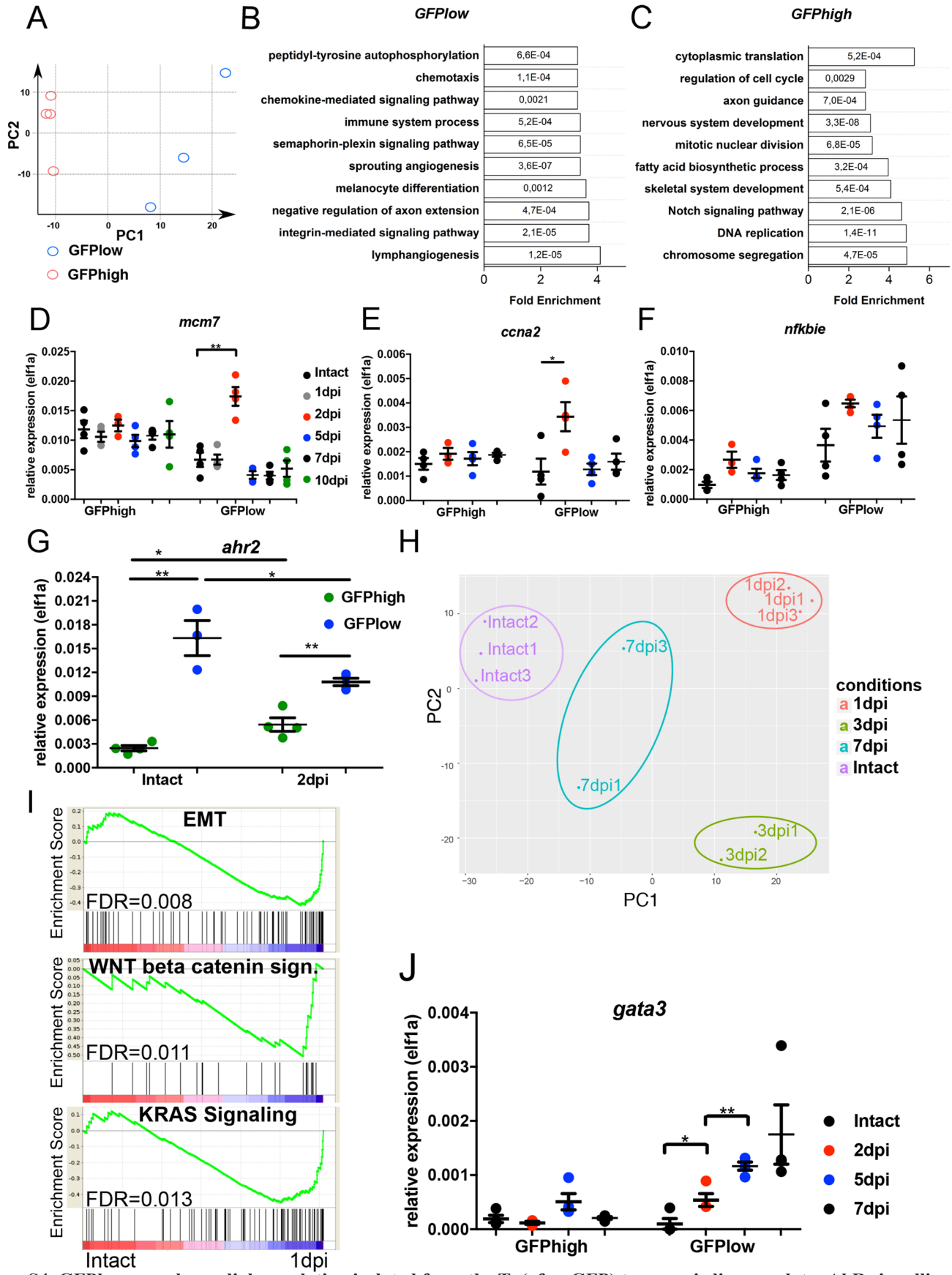

Figure S4. GFPlow ependymoglial population isolated from the Tg(gfap:GFP) transgenic line regulates AhR signalling after injury. Related to Figure 4.

(A) Dot plot depicting principle component analysis based on the total transcriptome of GFPhigh (red circles) and GFPlow (blue circles) ependymoglial population. (B, C) Histograms showing 10 biological processes enriched in GFPlow (B) and GFPhigh (C) transcriptomes based on the Gene Ontology (GO) analysis. (D, E, F, G) Dot plots depicting the expression of AhR-related genes in GFPhigh and GFPlow ependymoglia sorted from intact and injured brains. Single dots represent individual animals indicating biological replicates. Each biological replicate is the mean value of 4 technical replicates. Lines show mean±SEM. * ≤ 0.05; **≤ 0.01 (Unpaired t test). (H) Principal components analysis (PCA) of injury-induced transcriptome changes revealing overall transcriptional changes in the GFPlow ependymoglia in response to injury. (I) Graphs showing overrepresented gene sets in the GFPlow ependymoglia at 1 dpi using GSEA. (J) Dot plots depicting GATA3 expression in two ependymoglial states in intact and injured brains. Single dots represent individual animals indicating biological replicates. Each biological replicate is the mean value of 4 technical replicates. Lines show mean±SEM. * ≤ 0.05; **≤ 0.01 (unpaired t test).

Suppl. Table 2. Primers used for qPCR. Related to STAR Methods.

Gene Name	**Primer forward**	**Primer reverse**	**Reference**
Cyp1b1	AGATATTTTCGGGGCCAGTC	CACTACCCTGTCCACGTCCT	
Elf1a	CTTCTCAGGCTGACTGTGC	CCGCTAGCATTACCCTCC	McCurley and Callard, 2008
GFAP	TTGTGCGAACTGTTGAGACC	AGCAGGGAAAGTTGGTGAGA	
Nestin	GGTCTTTGGAGAGGAGTGGAG	CCCCTCATCAGCAGAATCAT	
Aldh1a2	CGTGAACTCGGAGAGATCGG	CCCACCAAAGGATAACGGCT	
Olig2	TTGCACCTGCTACCGGCAAT	CTTGACGGCGGACAGAAAAAG	
S100b	TAGAGAACTGCCTGGGAACC	CGGTGTCCAAACTTTCCATC	
Aromatb	ACAGTCGGTTCCTCTGGATG	TATGCATTGCAGACCTTTGG	
SOX9b	GCCCAGACGGAGGAAATCAG	TGAGACTGACCGGAGTGTTC	
Ahr2	CCCCATGGCTTGTCAACTAC	TCCTTAAGTGGACGGTTTGC	
Mcm7	GAGATTTACGGCCATGAGGA	GGTGTACTGACTGCGTGGAG	
nfkbie	GCGCAGAACTGGAGAGGTAT	TATGTAACGCCGTCTTCCCG	
Ccna2	TGCGGGAAATGGAGGTCAAG	CTCCCACTTCCACCAACCAG	
Gata3	AACCTGCAAGGTGGAATGAC	AGCTGGAAGTCTGCAAGACAG	Kyritsis et al., 2012

3.2. Aim of the study II

The aim of the study II was to investigate and establish:

The electroporation method and its use for reliable labelling of ependymoglial cells through in vivo delivery of plasmid DNA.

Electroporation is a technique that is used to deliver a reporter containing plasmid, or other charged molecule, into the cell by using an electric field which transiently opens pores on the cell membrane and facilitates delivery of the desired molecules into the cell. This technique was previously, and successfully, used to label ependymoglial cells (Chapouton et al. 2010; Barbosa et al. 2015; Barbosa et al. 2016). However, for the purposes of this thesis, this technique was advanced to be able to label higher numbers of ependymoglial cells more reproducibly among zebrafish (average rate 90-95% of labelled cells) (Durovic and Ninkovic, 2019).

We have been using this electroporation method successfully for most of our experiments and it is used throughout this thesis. In practice, it is mostly used for labeling and following of ependymoglial cells in vivo or counting in fixed tissues. Additionally, this electroporation technique was extremely useful to introduce constitutively active AhR (caAhR construct) specifically in ependymoglial cells and observe its effects. Next, through electroporation, it is possible to co-electroporate two plasmids simultaneously, and therefore we could label ependymoglial cells and their nuclei at the same time with two different colors. This has also been very helpful in concurrent following of both ependymoglia cell bodies and their nuclei and made it possible to observe nuclei division and the exact mode of ependymoglial behavior at the same time.

Electroporation Method for In Vivo Delivery of Plasmid DNA in the Adult Zebrafish Telencephalon

Tamara Durovic, Jovica Ninkovic

Durovic, T., Ninkovic, J. Electroporation Method for In Vivo Delivery of Plasmid DNA in the Adult Zebrafish Telencephalon. J. Vis. Exp. (151), e60066, doi:10.3791/60066 (2019).

https://www.jove.com/video/60066 DOI: doi:10.3791/60066

For this paper I performed all the experiments and analyzed all the data. I wrote all manuscript drafts, which were reviewed and edited by Prof. Dr. Jovica Ninković until finalization of the manuscript version.

Video Article

Electroporation Method for In Vivo Delivery of Plasmid DNA in the Adult Zebrafish Telencephalon

Tamara Durovic[1,2], Jovica Ninkovic[1,3,4]

[1]Institute of Stem Cell Research, Helmholtz Zentrum München

[2]Graduate School of Systemic Neurosciences, Ludwig Maximilian University

[3]Department of Cell Biology and Anatomy, Biomedical Center, Ludwig Maximilian University

[4]Munich Cluster for Systems Neurology (SyNergy)

Correspondence to: Jovica Ninkovic at ninkovic@helmholtz-muenchen.de

URL: https://www.jove.com/video/60066
DOI: doi:10.3791/60066

Keywords: Developmental Biology, Issue 151, electroporation, ependymoglia, in vivo cell labeling, plasmid delivery, zebrafish telencephalon, gene editing

Date Published: 9/13/2019

Citation: Durovic, T., Ninkovic, J. Electroporation Method for In Vivo Delivery of Plasmid DNA in the Adult Zebrafish Telencephalon. *J. Vis. Exp.* (151), e60066, doi:10.3791/60066 (2019).

Abstract

Electroporation is a transfection method in which an electrical field is applied to cells to create temporary pores in a cell membrane and increase its permeability, thereby allowing different molecules to be introduced to the cell. In this paper, electroporation is used to introduce plasmids to ependymoglial cells, which line the ventricular zone of the adult zebrafish telencephalon. A fraction of these cells shows stem cell properties and generates new neurons in the zebrafish brain; therefore, studying their behavior is essential to determine their roles in neurogenesis and regeneration. The introduction of plasmids via electroporation enables long-term labeling and tracking of a single ependymoglial cell. Furthermore, plasmids such as Cre recombinase or Cas9 can be delivered to single ependymoglial cells, which enables gene recombination or gene editing and provides a unique opportunity to assess the cell's autonomous gene function in a controlled, natural environment. Finally, this detailed, step-by-step electroporation protocol is used to obtain successful introduction of plasmids into a large number of single ependymoglial cells.

Video Link

The video component of this article can be found at https://www.jove.com/video/60066/

Introduction

Zebrafish are excellent animal models to examine brain regeneration after a stab wound injury. In comparison to mammals, on the evolutionary ladder, less evolved species such as zebrafish generally show higher rates of constitutive neurogenesis and broader areas of adult neural stem cell residence, leading to constant generation of new neurons throughout most brain areas in the adult life. This feature appears to correlate with significantly higher regenerative capacity of zebrafish in comparison to mammals[1], as zebrafish have remarkable potential to efficiently generate new neurons in most brain injury models studied[2,3,4,5,6,7,8]. Here, the zebrafish telencephalon is studied, since it is a brain area with prominent neurogenesis in adulthood. These zones of adult neurogenesis are homologous to neurogenic zones in the adult mammalian brain[9,10,11].

Abundant neurogenic areas in the zebrafish telencephalon are present due to the existence of radial glia like cells or ependymoglia cells. Ependymoglial cells act as resident adult neural stem cells and are responsible for generation of new neurons in both the intact and regenerating brain[3,5]. Lineage tracing experiments have shown that ventricular ependymoglia react to injury, then proliferate and generate new neuroblasts that migrate to the lesion site[5]. Due to the everted nature of zebrafish telencephalon, ependymoglial cells line the ventricular surface and build the ventral ventricular wall. The dorsal ventricular wall is formed by a dorsal ependymal cell layer (**Figure 1A**). Importantly, zebrafish ependymoglia embody the characteristics of both mammalian radial glia and ependymal cells. Long radial processes are a typical feature of radial glia cells, whereas cellular extensions and tight junctions (as well as their ventricular positions) are typical features of ependymal cells[12,13,14]. Therefore, these cells are referred to as ependymoglial cells.

To follow in vivo behavior of single ependymoglial cells during regeneration, they need to be reliably labeled. Various methods of in vivo cell labeling for fluorescent microscopy have been previously described, such as endogenous reporters or lipophilic dyes[15]. These methods, in contrast to electroporation, may require longer periods of time and often do not offer the possibility of single cell labeling or permanent long-term tracing. Electroporation, however (besides single cell labeling), offers the possibility of introducing new DNA into the host cell. Moreover, compared to other methods of DNA transfer into the cells, electroporation has been demonstrated to be one of the most efficient methods[16,17,18,19].

Presented here is an electroporation protocol that has been refined for the purpose of labeling single ependymoglial cells in the adult zebrafish telencephalon. This protocol allows for the labelling of single ependymoglial cells in order to follow them over a long-term period[20] or to manipulate specific pathways in a cell-autonomous manner[21,22].

Protocol

All animals used in this protocol were kept under standard husbandry conditions, and experiments have been performed according to the handling guidelines and regulations of EU and the Government of Upper Bavaria (AZ 55.2-1-54-2532-0916).

1. Preparation of Plasmid Mixture for Electroporation

1. Dilute the plasmid of interest in sterile water and add fast green stain stock solution [1 mg/mL]. Make sure that the final concentration of the plasmid is #1 µg/µL. Add the stain at a concentration of no more than 3%, as its only purpose is to color the solution and visualize ventricular injection.
2. Once prepared, mix the plasmid solution by pipetting up and down several times or by finger tapping. Store at room temperature (RT) until usage.
   NOTE: For co-electroporation of two plasmids into the same cell, ensure that the concentration of each individual plasmid used in the mixture is at least 0.8 ng/µL with a molar ratio of 1:1 to obtain 80%–90% co-electroporation efficiency.

2. Preparations for Injection and Electroporation Procedure

1. Prepare the glass capillaries (outer diameter 1 mm, inner diameter 0.58 mm) necessary for the injection in the needle pulling apparatus.
2. In order to inject the correct amount of plasmid (see above), pull the capillary at a temperature of 68.5 °C with two light and two heavy weights (see **Table of Materials** for puller specifications).
   NOTE: In case a different puller is used, calibrate the capillary to deliver the appropriate volume of electroporation mix.
3. Manually set the injection device to an injection pressure of 200 hPa (by turning the Pi knob) and constant pressure of 0 hPa. Manually set the injection time to manual mode and control the pressure with foot pedal.
4. Set the electroporation device to “LV mode” with five pulses at 54–57 V (25 ms each with 1 s intervals). Connect the electrodes to the device.
5. Prepare one fish tank with clean fish water, where the fish will be awakened from anesthesia after the electroporation procedure. Aerate the water by keeping the air stone attached to the air pump for the entire recovery period until the fish is fully awakened.
6. Take a regular kitchen sponge and make a longitudinal cut in the sponge to hold fish into during the injection and electroporation procedure (see previous publication[3]).
   NOTE: The kitchen sponge should be regularly washed or exchanged in order to remove potential toxic chemicals.
7. Place a small amount of highly conductive multi-purpose ultrasound gel next to the injection and electroporation setup.
   NOTE: This will ensure adequate electrical conductivity, and consequently, distribution of electroporated cells throughout the entire telencephalon.

3. Zebrafish Anesthesia

1. Prior to anesthetization, prepare a stock solution of anesthesia with 0.2% MS222 in distilled water and adjust the pH to 7 with Tris-HCl buffer. Dilute this stock 1:10 (i.e., to 0.02% MS222) using fish water.
2. Anesthetize the fish by keeping them in this working solution until the movement of the body and gills subsides (typically for a couple of minutes).

4. Plasmid Solution Injection

1. Fill the prepared glass capillary with 10 µL of plasmid solution using microloader tips. Avoid the formation of air bubbles inside the capillary.
2. Press **Menu/Change Capillary** on the injection device. Insert and secure the needle into the needle holder.
3. Under a stereomicroscope with a magnification of 3.2x or 4x, cut only the tip of the capillary using fine-end forceps. Switch the injection device from **Change Capillary** mode into **Inject** mode, then apply pressure with a foot pedal to ensure that the plasmid solution is running easily out of the needle and without hindrance.
4. Transfer the fish from the husbandry tank to the container (plastic box) with anesthetic solution. Wait for a few minutes until movement of the gills subsides.
5. Place fish into the pre-wetted sponge with the dorsal side facing up. Perform all the following injection steps under the stereomicroscope to ensure the accuracy of procedure.
6. Using a dissecting micro-knife from stainless steel with 40 mm cutting edge and 0.5 mm thickness, create a small hole in the fish skull at the posterior side of the telencephalon (**Figure 1B**), just next to the border with optic tectum.
   NOTE: This step should be performed carefully since the hole should be very small and superficial, penetrating solely the skull, to avoid brain damage.
7. Tilt the fish as necessary and orient the tip of the glass capillary towards the skull in the correct angle to facilitate penetration of the capillary tip through the hole.
8. Insert the tip of the capillary through the hole in the skull carefully until it reaches the telencephalic ventricle (see **Figure 1B**). This will require penetration through the dorsal ependymal cell layer. Be especially careful not to insert the capillary too deeply to avoid contact with the brain tissue. Keep the capillary precisely in between the hemispheres, remaining inside the ventricle just after piercing the dorsal ependymal layer.
   NOTE: This is a very delicate step. Accuracy of this procedure is improved using pigmentation mutant lines such as *brassy*[24], allowing better visualization of glass capillary position during injection.

9. With the capillary tip inside of the ventricle, inject the plasmid solution by applying pressure with the foot pedal for about 10 s, which corresponds to approximately 1 µL of plasmid solution.
   NOTE: If changing the needle puller, capillaries or injector, the system should be calibrated in order to always deliver 1 µL of plasmid solution. Calibration can be performed by measuring the diameter of the plasmid droplet expelled into a mineral oil (e.g., paraffin oil) and subsequently calculating the volume of the droplet. After 10 s of injection, there should be ~1 µL of plasmid liquid expelled into the mineral oil.
10. Confirm success of the previous step by observing the spread of liquid throughout the ventricle.

5. Electroporation

1. Remove the fish from the injection set-up while still holding it in the sponge.
2. Immerse the inner side of the tip of the electrodes in the ultrasound gel.
3. Cover the fish telencephalon with a small amount of ultrasound gel.
4. Position the fish head between the electrodes, placing the positive electrode at the ventral side of the fish's head and the negative electrode on the dorsal side (**Figure 1C**), while still holding the fish's body in the sponge. This sets the direction of the flow of the current necessary to electroporate ependymoglia positioned at subventricular zone.
5. Press the electrodes gently and precisely against the telencephalon (**Figure 1C**). Administer the current with the foot pedal. Hold the electrodes in place until all five pulses are finished.

6. Fish Recovery

1. Let the fish recover in the previously prepared, continuously aerated tank until it wakes up. Lidocaine gel could be applied on the skull in order to relieve any possibly developed pain.

Representative Results

The described electroporation method allows delivery of plasmid DNA into ependymoglial cells, which are located superficially in the zebrafish telencephalon and just under the dorsal ependymal cell layer (**Figure 1A**).

If the result of electroporation is positive, labeled single ependymoglial cells (red cells in **Figure 2A,B**) can be observed among other ependymoglial cells (white in **Figure 2A,B**). Depending on the efficiency of the electroporation process, a higher (**Figure 2A**) or lower (**Figure 2B**) number of ependymoglial cells may be labeled. Nevertheless, this protocol yields higher number of labeled cells than previously published[20], which is apparent in **Figure 3A** and **Video 1**. It is worth mentioning that the highest density of labeled cells tends to emerge mostly at the inner, ventricular side of both hemispheres (**Figure 3A**), due to the way in which the injected plasmid liquid distributes between the hemispheres. In **Video 1**, one hemisphere of the zebrafish telencephalon is presented in 3D, and the ependymoglial cells with radial processes can be seen from the side. The cells are co-electroporated and labeled with two plasmids, tdTomato-mem (red fluorescent protein anchored to the cell membrane) and H2B-YFP plasmid (labelling nuclei). Cell division of two nuclei surrounded by yellow circles should be noted.

Unsuccessful electroporation results in very low number or no labeled ependymoglial cells. This outcome can be generally explained by inaccurate injection, in which the tip of the capillary does not penetrate the dorsal ependymal cell layer. In this case, plasmid solution spreads above the dorsal ependymal cell layer instead of filling telencephalic ventricle. This leads to ependymal cells solely being labeled (**Figure 3B**). Dorsal ependymal cells (blue arrows in **Figure 3B**) differ morphologically from ependymoglial cells (yellow arrow in **Figure 3A**). Their soma is larger and cuboid, and they do not possess radial, elongated processes. This is evident from comparing a side view of the ependymoglial cell layer (**Figure 4A,B**). TdTomato-mem labeled cells are most likely ependymal cells, which are located above the layer of ependymoglia (**Figure 4B**). In contrast, in **Figure 4A**, a tdTomato-mem expressing plasmid is introduced to individual ependymoglial cells. Thus, they express tdTomato-mem in addition to their initial labeling (in this case, transgenic *gfap:GFP* fish line, seen here in white).

This protocol enables the labelling and subsequent following of the behaviour of ependymoglial cells in zebrafish telencephalon after injury over a short-[21] or long-term[3] period of time. This is accomplished through live, in vivo imaging and helps address the question of their roles in regeneration and neurogenesis.

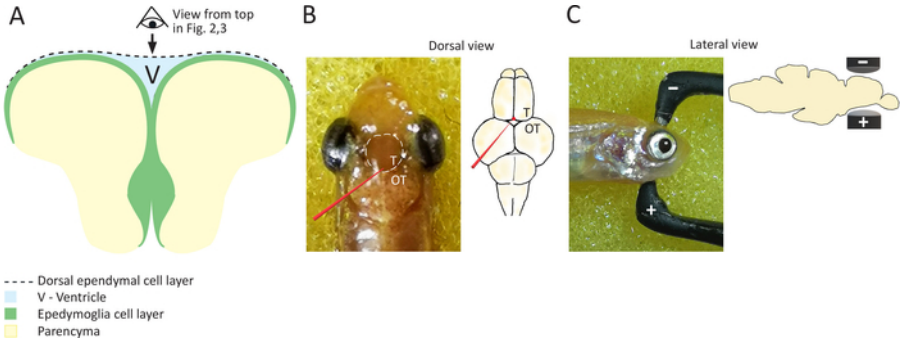

Figure 1: Schematic representation of coronal section of the everted zebrafish telencephalon. (**A**) Scheme of a coronal section of zebrafish telencephalon, highlighting the position of ependymoglial cells, which are lining ventricular surface and building the ventral ventricular wall. Dorsal ependymal layer is bridging the two hemispheres and covering the ventricle (V), located in between two cell layers: ependymoglial and ependymal. Black arrow and the representation of the eye indicate view are shown in **Figures 2** and **Figure 3**. (**B**) On the left, a photograph of the zebrafish head taken from above, highlighting the position of telencephalon with a white dashed line. A glass capillary is depicted in red, along with the target site for capillary insertion. Pictured on the right is a schematic of zebrafish brain showing the position of plasmid injection in red. It should be noted that the glass capillary does not touch the telencephalon and that the plasmid is injected just above the telencephalon into the ventricle. T = telencephalon, OT = optic tectum. (**C**) Depicted on the left is a photograph of the zebrafish head (side view), and on the right is a depiction of the head (side view) showing the position of electrodes in order to target the telencephalon. Please click here to view a larger version of this figure.

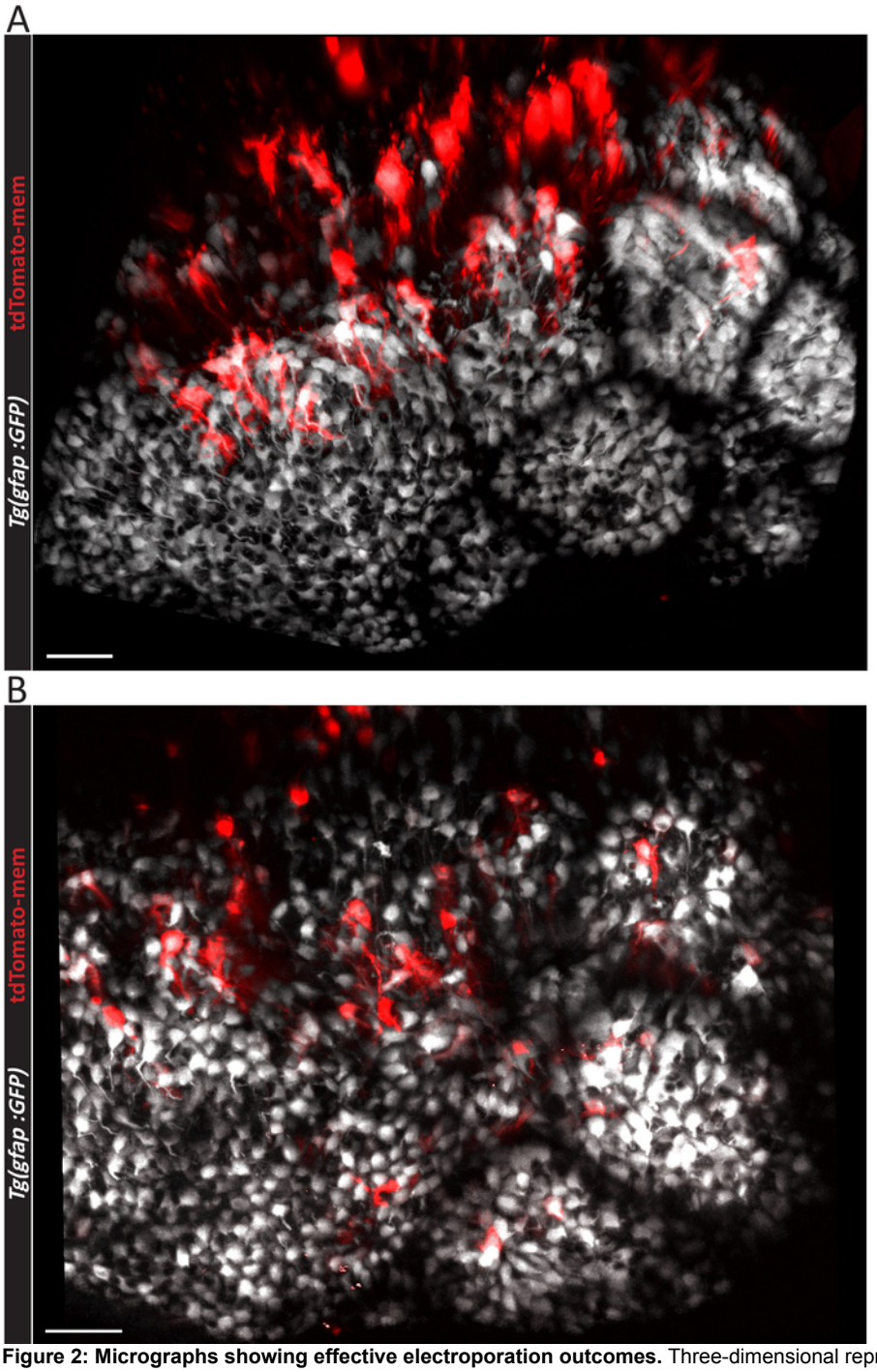

Figure 2: Micrographs showing effective electroporation outcomes. Three-dimensional representation of a (**A**) larger or (**B**) smaller number of electroporated ependymoglial cells in the adult zebrafish telencephalon, as viewed from above. The electroporation were done in Tg (*gfap:GFP*) fish line expressing GFP fluorescent protein (depicted in white) in all ependymoglial cells. Individual electroporated cells are labelled with pCS2-tdTomato-mem plasmid[3]. Scale bars = 50 µm. Please click here to view a larger version of this figure.

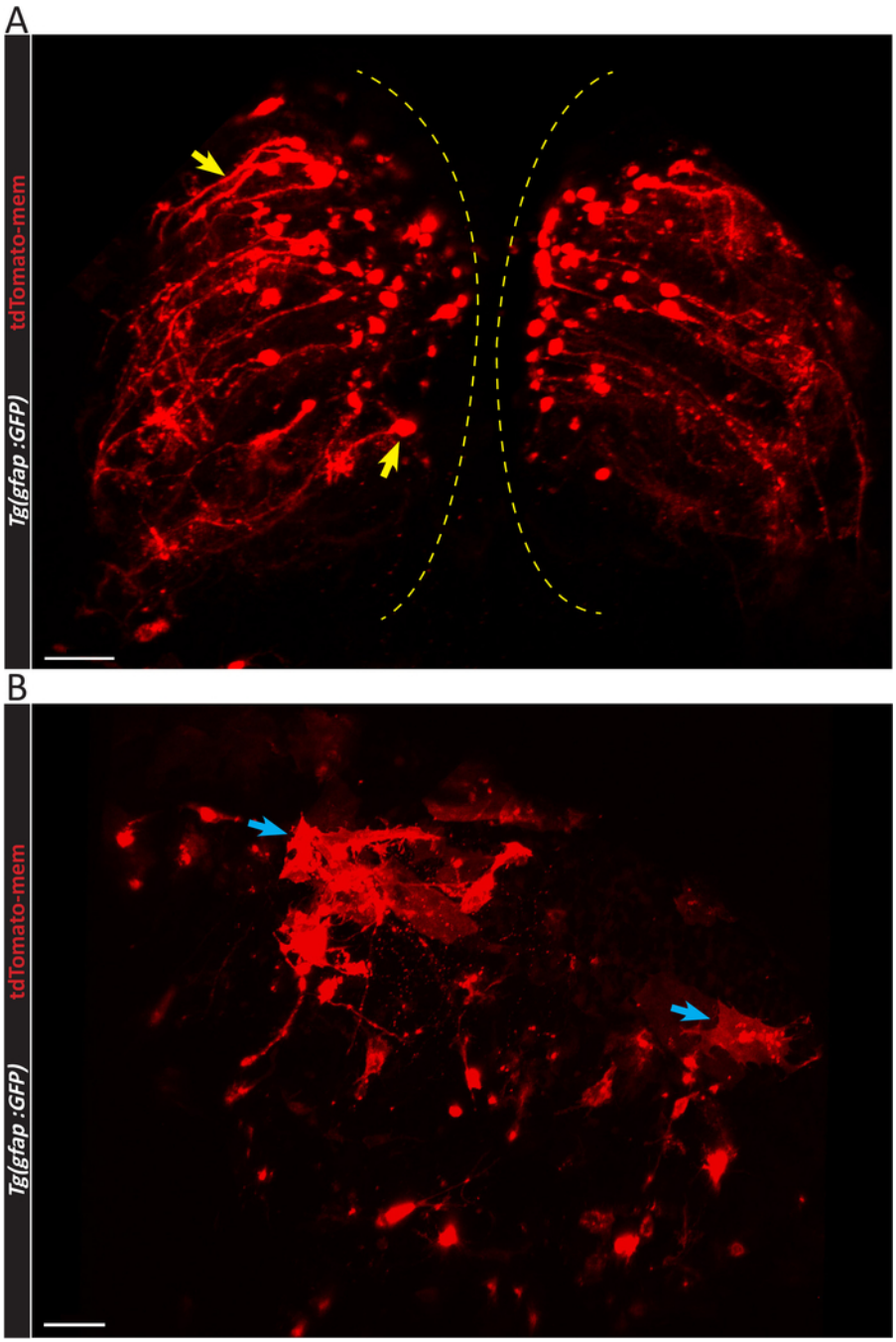

Figure 3: Confocal micrographs depicting the difference between successful and unsuccessful electroporation. (**A**) Three-dimensional confocal image of BABB-cleared zebrafish telencephalon (REF) with a large number of pCS-tdTomato-mem electroporated ependymoglial cells. The morphology of the ependymoglial cells with long, elongated processes (yellow arrows) should be noted. Both telencephalic hemispheres, highlighted with yellow dashed lines, can be observed. (**B**) Confocal image of unsuccessful electroporation of pCS2-tdTomato-mem plasmid. Mostly dorsal ependymal cells are labelled, and few ependymoglial cells express tdTomato-mem plasmid. The clear difference in the morphology of ependymal cells (blue arrows) should be noted. Scale bars = 50 µm. Please click here to view a larger version of this figure.

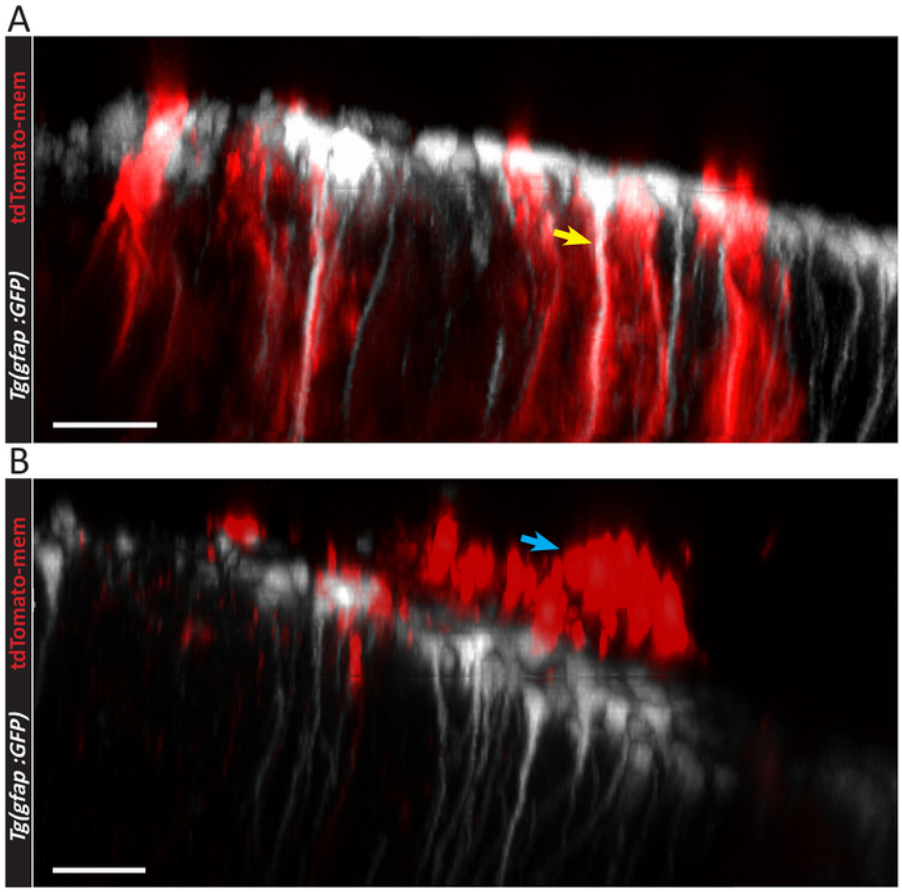

Figure 4: 3D lateral views of electroporated and non-electroporated ependymoglial cells. (**A**) Three-dimensional lateral representation electroporated ependymoglial cells, positive for both Tg(*gfap:GFP*) and pCS2-tdTomato-mem (yellow arrow). (**B**) 3D lateral representation of unsuccessful electroporation. The location of pCS2-tdTomato-mem positive cells above the Tg(*gfap:GFP*) ependymoglia layer should be noted. Most likely dorsal ependymal layer cells were electroporated (blue arrow). Scale bars = 30 µm. Please click here to view a larger version of this figure.

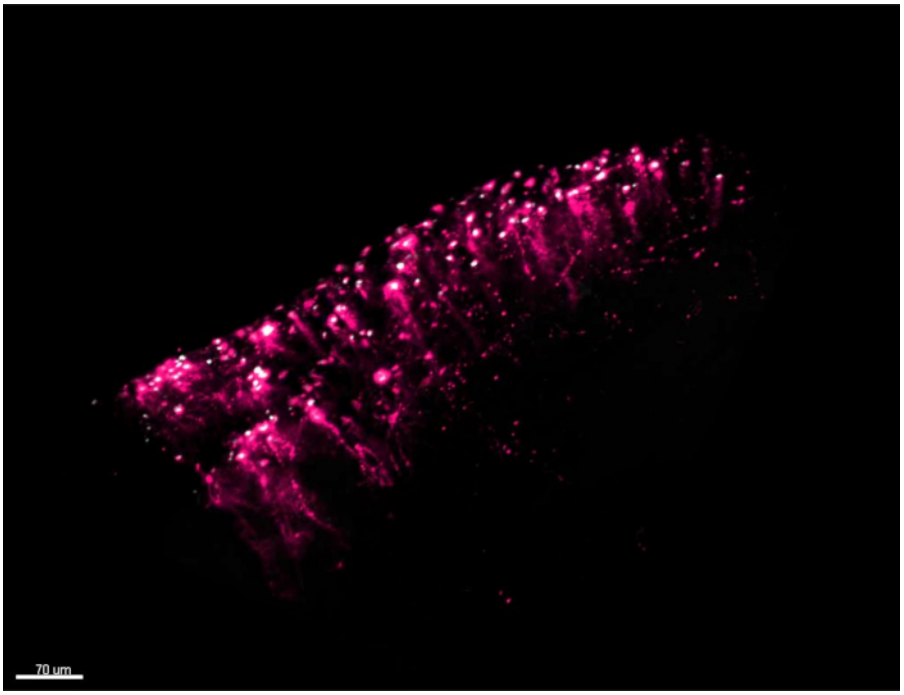

Video 1: 3D movie of zebrafish telencephalon and electroporated ependymoglial cells. Video shows one hemisphere of the zebrafish telencephalon in 3D. Ependymoglial cells are co-electroporated with two plasmids: tdTomato-mem (red fluorescent protein anchored to the cell membrane) and H2B-YFP plasmid (labelling nuclei). Individually labelled ependymoglia with radial processes that can be observed from aside. Yellow circles highlight ependymoglial cell with mitotic figure visualized by H2B-YFP labelled chromatin. Please click here to view this video. (Right-click to download.)

Discussion

This electroporation protocol is a reliable in vivo method of labelling individual ependymoglial cells. The protocol may need a further adaptation to label other cell types such as neurons or oligodendrocytes. To achieve successful labelling, plasmids containing different promoters can be used. Chicken-beta actin promoter, eF1alpha, CMV and ubiquitin promoter have been previously used to drive the expression of different transgenes in ependymoglia and their progeny[23]. However, different kinetics of transgene expression was observed which should be taken into the account. For example, CMV promoter driven transgene expression is very fast (expression could be seen after 24 h), while eF1alpha takes longer. Apart from labeling, the electroporation protocol can be used as a fast and straightforward platform of gene editing with the use of Cre recombinase or CRISPR Cas9 techniques[22]. Moreover, the use of flip-cassette[25]-containing plasmids and their electroporation in cell type-specific Cre lines may serve as a clear extension of a method allowing labelling or gene-editing in the ependymoglial progeny generated after electroporation.

This protocol has several critical steps. First, during the injection step, the experimental needs to be careful that the injected plasmid amount is equal for each individual fish, such that the number of labelled cells remains comparably similar. This can be achieved by controlling the size of the glass capillary opening, meaning that the cut of each tip should be constant among different capillaries or calibration should be performed for each individual capillary. Additionally, the duration of injection, regulated by a foot pedal, should be the same for each individual injection. Second, the proper position of a hole in the skull made with the micro-knife is crucial for the proper dispersion of the plasmid liquid throughout the telencephalon. It is equally important to penetrate the dorsal ependymal cell layer with the capillary tip, as stated in the protocol. Moreover, it is also essential that the hole created is not too large to prevent the plasmid mixture and cerebrospinal fluid from leaking out of the telencephalon. Another critical step is the strength of the applied electrical current. It is important to make sure that the electroporation device is operating as precisely as possible, such that the strength of the applied current does not deviate much from the voltage appearing on the screen, which is not always accurate. If these values are not consistent, it is necessary to adjust the strength of the current on the electroporation device, since an administered current higher than the recommended 54-57 V may compromise fish survival.

Compared to the other methods for a plasmid delivery and cell labelling commonly used in the field, electroporation has obvious advantages. Despite the critical steps mentioned above, it happens very rarely that no electroporated cells can be observed or that the dorsal ependymal cells are mistakenly electroporated. Generally, the success rate of this electroporation protocol is 90%-95% and we observe almost no TUNEL+ cells after electroporation. In contrast to lipofection for example, during electroporation, cationic liposomes (e.g., lipofectamine) are not used and thus toxicity connected with its usage is completely avoided[26]. It was previously reported that lipofection and electroporation have equal efficiency rates (20-50 cells per telencephalon)[27]. However, this optimized protocol generally yields 100-200 cells per telencephalon. In comparison to viral vectors, biosafety is not an issue with electroporation.

In addition, commonly used AAVs or lentiviruses fail to produce detectable expression of transgenes in zebrafish brain[17,28]. Finally, although the Cre-lox system is nowadays commonly used in zebrafish, plasmid electroporation is faster since it does not require long waiting times necessary for fish breeding and growing and allows individual cell labelling and tracing. However, such a technique requires highly skilled scientists to achieve successful electroporation and high survival rates of experimental animals (we typically experience survival rates of ~70%-80%). This

rate also tends to fluctuate depending on the experimenter. Learning the procedure requires practice and typically takes three trials. However, this is dependent on the manual dexterity of the individual and may take longer in some cases.

The presented electroporation protocol is a fast, highly efficient method for electroporating a large number of ependymoglial cells with the necessary precautions to obtain optimal results. Electroporation of the adult zebrafish telencephalon is crucial for visualizing individual ependymoglial cells and studying their roles in neurogenesis and regeneration processes. Recently, success has been achieved in the simultaneous disruption of multiple genes of the adult zebrafish telencephalon through gene editing via the electroporation and StagR-Cas9 techniques[22]. This opens many possibilities and future applications of electroporation for a broad range of genetic manipulations.

Disclosures

Authors have nothing to disclose.

Acknowledgments

Special thanks to James Copti for editing of the manuscript. We also gratefully acknowledge funding to JN from the German Research foundation (DFG) by the SFB 870 and SPP “Integrative Analysis of Olfaction” and SPP 1738 “Emerging roles of non-coding RNAs in nervous system development, plasticity & disease”, SPP1757 “Glial heterogeneity”, and Excellence Strategy within the framework of the Munich Cluster for Systems Neurology (EXC 2145 SyNergy – ID 390857198).

References

1. Kaslin, J., Ganz, J., Brand, M. Proliferation, neurogenesis and regeneration in the non-mammalian vertebrate brain. *Philosophical Transactions of the Royal Society of London Series B Biological Sciences.* **363** (1489), 101-122 (2008).
2. Baumgart, E. V., Barbosa, J. S., Bally-Cuif, L., Gotz, M., Ninkovic, J. Stab wound injury of the zebrafish telencephalon: a model for comparative analysis of reactive gliosis. *Glia.* **60** (3), 343-357 (2012).
3. Barbosa, J. et al. Live imaging of adult neural stem cell behavior in the intact and injured zebrafish brain. *Science.* **346** (6236), 789-793 (2015).
4. Kishimoto, N., Shimizu, K., Sawamoto, K. Neuronal regeneration in a zebrafish model of adult brain injury. *Disease Model and Mechanisms.* **5** (2), 200-209 (2012).
5. Kroehne, V., Freudenreich, D., Hans, S., Kaslin, J., Brand, M. Regeneration of the adult zebrafish brain from neurogenic radial glia-type progenitors. *Development.* **138** (22), 4831-4841 (2011).
6. Marz, M., Schmidt, R., Rastegar, S., Strahle, U. Regenerative response following stab injury in the adult zebrafish telencephalon. *Developmental Dynamics.* **240** (9), 2221-2231 (2011).
7. Ayari, B., Elhachimi, K. H., Yanicostas, C., Landoulsi, A., Soussi-Yanicostas, N. Prokineticin 2 expression is associated with neural repair of injured adult zebrafish telencephalon. *Journal of Neurotrauma.* (2010).
8. Skaggs, K., Goldman, D., Parent, J. M. Excitotoxic brain injury in adult zebrafish stimulates neurogenesis and long-distance neuronal integration. *Glia.* **62** (12), 2061-2079 (2014).
9. Schmidt, R., Strahle, U., Scholpp, S. Neurogenesis in zebrafish - from embryo to adult. *Neural Development.* **8** (3) (2013).
10. Alunni, A., Bally-Cuif, L. A comparative view of regenerative neurogenesis in vertebrates. *Development.* **143** (5), 741-753 (2016).
11. Kizil, C., Kaslin, J., Kroehne, V., Brand, M. Adult neurogenesis and brain regeneration in zebrafish. *Developmetal Neurobiology.* **72** (3), 429-461 (2012).
12. Than-Trong, E., Bally-Cuif, L. Radial glia and neural progenitors in the adult zebrafish central nervous system. *Glia.* **63** (8), 1406-1428 (2015).
13. Lyons, D. A., Talbot, W. S. Glial cell development and function in zebrafish. *Cold Spring Harbor Perspectives in Biology.* **7** (2), a020586 (2014).
14. Obermann, J. et al. The Surface Proteome of Adult Neural Stem Cells in Zebrafish Unveils Long-Range Cell-Cell Connections and Age-Related Changes in Responsiveness to IGF. *Stem Cell Reports.* **12** (2), 258-273 (2019).
15. Progatzky, F., Dallman, M. J., Lo Celso, C. From seeing to believing: labelling strategies for in vivo cell-tracking experiments. *Interface Focus.* **3** (3), 20130001 (2013).
16. Kusumanto, Y. H. et al. Improvement of in vivo transfer of plasmid DNA in muscle: comparison of electroporation versus ultrasound. *Drug Delivery.* **14** (5), 273-277 (2007).
17. Zou, M., De Koninck, P., Neve, R. L., Friedrich, R. W. Fast gene transfer into the adult zebrafish brain by herpes simplex virus 1 (HSV-1) and electroporation: methods and optogenetic applications. *Frontiers in Neural Circuits.* **8,** (41) (2014).
18. Van Tendeloo, V. F. et al. Highly efficient gene delivery by mRNA electroporation in human hematopoietic cells: superiority to lipofection and passive pulsing of mRNA and to electroporation of plasmid cDNA for tumor antigen loading of dendritic cells. *Blood.* **98** (1), 49-56 (2001).
19. Mars, T. et al. Electrotransfection and lipofection show comparable efficiency for in vitro gene delivery of primary human myoblasts. *The Journal of Membrane Biology.* **248** (2), 273-283 (2015).
20. Barbosa, J. S., Di Giaimo, R., Gotz, M., Ninkovic, J. Single-cell in vivo imaging of adult neural stem cells in the zebrafish telencephalon. *Nature Protocols.* **11** (8), 1360-1370 (2016).
21. Di Giaimo, R. et al. The Aryl Hydrocarbon Receptor Pathway Defines the Time Frame for Restorative Neurogenesis. *Cell Reports.* **25** (12), 3241-3251.e3245 (2018).
22. Breunig, C. T. et al. One step generation of customizable gRNA vectors for multiplex CRISPR approaches through string assembly gRNA cloning (STAgR). *PLoS One.* **13** (4), e0196015 (2018).
23. Barbosa, J. S. In vivo single cell analysis reveals distinct behavior of neural stem and progenitor cells in homeostasis and regeneration in the adult brain. *Doctoral dissertation. University of Coimbra.* (2014).
24. Kelsh, R. N. et al. Zebrafish pigmentation mutations and the processes of neural crest development. *Development.* **123,** 369-389 (1996).

25. Torper, O. et al. In Vivo Reprogramming of Striatal NG2 Glia into Functional Neurons that Integrate into Local Host Circuitry. *Cell Reports.* **12** (3), 474-481 (2015).
26. Nguyen, L. T., Atobe, K., Barichello, J. M., Ishida, T., Kiwada, H. Complex formation with plasmid DNA increases the cytotoxicity of cationic liposomes. *Biological and Pharmaceutical Bulletin.* **30** (4), 751-757 (2007).
27. Chapouton, P., Godinho, L. Neurogenesis. Chapter IV in The Zebrafish: Cellular and Developmental Biology, Part A Developmental Biology. (Vol **100**). *Edited by Detrich III, H. W., Westerfield, M., & Zon, L. Academic Press.* (2010).
28. Zhu, P. et al. Optogenetic Dissection of Neuronal Circuits in Zebrafish using Viral Gene Transfer and the Tet System. *Frontiers in Neural Circuits.* **3** (21) (2009).

3.3. Aim of the study III

The aim of the study III was to investigate and establish:

The StagR technique, a single step method enabling packaging of multiple (up to eight) gRNAs in single vector, and its functional utilization for gene ablation in adult zebrafish telencephalon in vivo.

The StagR (String assembly gRNA cloning) technique, developed by Breunig et al. 2018, is a modification of well-known CRISPR/Cas9 technique. CRISPR/Cas9 is an intelligent natural defense mechanism derived from bacteria which acts as a self-protection mechanism from invading DNAs of other bacteriophages and plasmids. The machinery is based on CRISPR (clustered regularly interspaced short palindromic repeats) and Cas9 (CRISPR associated protein) (Wang et al., 2016).

CRISPR/Cas9 system has been widely used and modified as a very useful, cost-efficient, genome editing tool. This modified version is based on single guide RNA (sgRNA or gRNA), consisting of around 20 base pairs (bps) and the Cas9 protein, meaning that only around 20 bps are necessary to target practically any DNA loci site currently, thus making CRISPR/Cas9 a highly efficient and easily customizable tool. Various other modifications of CRISPR/Cas have been made and are modernly applied for many purposes, such as sequence-specific gene editing, gene knockout and knock-in or site specific sequence mutagenesis and correction (Wang et al., 2016).

Due to widespread usage of CRISPR/Cas as a genome editing tool, it has been adopted as an engineering tool in zebrafish as well, in particular for gene knock-ins, knock-outs or genome manipulations (Albadri et al., 2017; Li et al., 2016). Nevertheless, gene modifications were mostly done in zebrafish zygotes, that need up two generations of waiting time for knock-out or reporter animal lines to be created (Li et al., 2016). On the other hand, StagR technique, developed by Breunig et al., 2018, is a reliable and largely customizable tool, packing multiple (up to eight) gRNAs into one expression vector. This technique allows simultaneous and direct gene knock-out in the ependymoglial cells in the adult zebrafish telencephalon.

Throughout this thesis, we used electroporation to introduce the StagR construct into ependymoglial cells. This new method of gene manipulation opens a wide range of possibilities for applications due to its effectiveness and simplicity. To our knowledge, a method such as this one, which combines electroporation with StagR constructs to introduce gene editing to adult zebrafish brain, has not been used in the field so far. The additional advantage of the StagR technique is the possibility to target specifically ependymoglial cells, due to their position at the ventricular surface of the zebrafish telencephalon.

One step generation of customizable gRNA vectors for multiplex CRISPR approaches through string assembly gRNA cloning (STAgR)

Christopher T. Breunig, **Tamara Durovic**, Andrea M. Neuner, Valentin Baumann, Maximilian F. Wiesbeck, Anna Köferle, Magdalena Götz, Jovica Ninkovic, Stefan H. Stricker.

Breunig CT, Durovic T, Neuner AM, Baumann V, Wiesbeck MF, Köferle A, et al. (2018) One step generation of customizable gRNA vectors for multiplex CRISPR approaches through string assembly gRNA cloning (STAgR). PLoS ONE 13 (4): e0196015.

https://doi.org/10.1371/journal. pone.0196015

For this paper I was involved in experiments with the zebrafish, testing the efficiency of the StagR-Cas9 construct in vivo in the zebrafish telencephalon, and describing the electroporation procedure in the manuscript. The contribution of other authors is outlined in the paper.

PLOS ONE

RESEARCH ARTICLE

One step generation of customizable gRNA vectors for multiplex CRISPR approaches through string assembly gRNA cloning (STAgR)

Christopher T. Breunig[1,2], Tamara Durovic[3,4], Andrea M. Neuner[1], Valentin Baumann[1,3], Maximilian F. Wiesbeck[1], Anna Köferle[1], Magdalena Götz[5,6], Jovica Ninkovic[4,6], Stefan H. Stricker[1,2]*

1 MCN Junior Research Group, Munich Center for Neurosciences, Ludwig-Maximilian-Universität, BioMedical Center, Planegg-Martinsried, Germany, **2** Epigenetic Engineering, Institute of Stem Cell Research, Helmholtz Zentrum, German Research Center for Environmental Health, Planegg-Martinsried, Germany, **3** Graduate School of Systemic Neurosciences, Ludwig-Maximilians-University, Munich, Germany, **4** Neurogenesis and Regeneration, Institute of Stem Cell Research, Helmholtz Zentrum, German Research Center for Environmental Health, Neuherberg, Germany, **5** Neural stem cells, Institute of Stem Cell Research, Helmholtz Zentrum, German Research Center for Environmental Health, Neuherberg, Germany, **6** Physiological Genomics, BioMedical Center, Ludwig-Maximilian-Universität, Planegg-Martinsried, Germany

* stricker@biologie.uni-muenchen.de

OPEN ACCESS

Citation: Breunig CT, Durovic T, Neuner AM, Baumann V, Wiesbeck MF, Köferle A, et al. (2018) One step generation of customizable gRNA vectors for multiplex CRISPR approaches through string assembly gRNA cloning (STAgR). PLoS ONE 13 (4): e0196015. https://doi.org/10.1371/journal.pone.0196015

Editor: Knut Stieger, Justus Liebig Universitat Giessen, GERMANY

Received: January 14, 2018

Accepted: April 4, 2018

Published: April 27, 2018

Data Availability Statement: Plasmids for STAgR cloning can be obtained from Addgene and sequences from figshare using the following URL: https://figshare.com/projects/One_step_generation_of_customizable_gRNA_vectors_for_multiplex_CRISPR_approaches_through_string_assembly_gRNA_cloning_STAgR_/31046. The Addgene ID numbers are STAGR_SAMScaffold_hH1 (ID 102847), STAGR_SAMScaffold_h7SK (ID 102846), STAGR_SAMScaffold_mU6 (ID 102845),

Abstract

Novel applications based on the bacterial CRISPR system make genetic, genomic, transcriptional and epigenomic engineering widely accessible for the first time. A significant advantage of CRISPR over previous methods is its tremendous adaptability due to its bipartite nature. Cas9 or its engineered variants define the molecular effect, while short gRNAs determine the targeting sites. A majority of CRISPR approaches depend on the simultaneous delivery of multiple gRNAs into single cells, either as an essential precondition, to increase responsive cell populations or to enhance phenotypic outcomes. Despite these requirements, methods allowing the efficient generation and delivery of multiple gRNA expression units into single cells are still sparse. Here we present STAgR (String assembly gRNA cloning), a single step gRNA multiplexing system, that obtains its advantages by employing the N20 targeting sequences as necessary homologies for Gibson assembly. We show that STAgR allows reliable and cost-effective generation of vectors with high numbers of gRNAs enabling multiplexed CRISPR approaches. Moreover, STAgR is easily customizable, as vector backbones as well as gRNA structures, numbers and promoters can be freely chosen and combined. Finally, we demonstrate STAgR's widespread functionality, its efficiency in multi-targeting approaches, using it for both, genome and transcriptome editing, as well as applying it in vitro and in vivo.

STAGR_gRNAScaffold_mU6 (ID 102844), STAGR_SAMScaffold_hU6 (ID 102843), STAGR_gRNAScaffold_h7SK (ID 102842), STAGR_gRNAScaffold_hH1 (ID 102841), STAGR_gRNAScaffold_hU6 (ID 102840), mCherry (ID 102993), STAgR_Neo (ID 102992).

Funding: CB, AN, VB, MW, AK and SHS were supported by Deutsche Forschungsgemeinschaft (STR 1385/1-1) (http://www.dfg.de/). The funders had no role in study design, data collection and analysis, decision to publish, or preparation of the manuscript.

Competing interests: The authors have declared that no competing interests exist.

Introduction

The adaptation of CRISPR as a molecular tool has been the most recent revolution in synthetic biology [1], since several groups have transformed components of this prokaryotic immune system to acquire programmable genomic targeting [2–4]. The nuclease Cas9, the only protein component in CRISPR, has the extraordinary feature of finding and binding those sequences in the genome, that are encoded in a small RNA, the guide or gRNA. While originally developed to induce double strand brakes on single sites [4], several refinements and modifications of both the protein as well as the RNA part allow at present a large spectrum of experimental strategies ranging from epigenome engineering to transcriptional activation/ repression [5, 6]. Many of these are, however, strictly dependent on the simultaneous delivery and expression of multiple gRNAs. This includes, for example, the use of Cas9 nickases [7], the induction of translocations [8, 9], medium scale deletions [10], larger genomic alterations [11, 12], CRISPR mediated generation of conditional alleles [10, 13], generation of concomitant mutations [14] and long term lineage tracing using CRISPR [15]. Furthermore, a large number of CRISPR strategies rely on multiple targeting sites, sometimes in proximity to each other, to obtain maximal effect sizes; for example when fusion proteins of the enzymatically dead dCas9 with transcriptional activators [16–18] or chromatin enzymes [19] are used for transcriptional engineering, epigenome editing [20] or cellular reprogramming [16, 21]. However, combining multiple individual gRNA expression vectors to achieve expression of multiple gRNAs in single cells has its limits, in vitro, as well as in vivo, as the fraction of cells expressing a complete set of gRNAs is decreasing with the number of gRNAs used, and those that do, rarely receive stoichiometric levels. Besides these approaches, which are strictly depending on the availability of multiple gRNAs in single cells, there is also a more general need for quick and cost-effective vector generation. Due to differences in targeting efficiencies and chromatin topology, testing a significant number of potential gRNA sequences is advisable for most experimental setups. Thus, the availability of customization strategies would constitute decisive advantages. Here we report a simple and cost-effective one step method to generate functional expression vectors for multiple gRNA delivery with high reliability and a large number of options for customization.

Materials and methods

A detailed protocol for STAgR cloning is available supplementary (S1 File). HeLa cells (gift from Stephan Beck) were cultured in DMEM medium (Dulbecco's modified eagle medium) supplemented with 10% (v/v) FCS and 1% penicillin/streptomycin (10000 U/ml penicillin, 10000 μg/ml streptomycin). Cells were grown in a monolayer in cell culture dishes at 37˚C and 5% CO2. P19 (obtained from ATCC) were cultured in identical conditions, but supplemented with 1% NEAAs (Gibco). For each transfection 250,000 cells/well were seeded into 6-well plates. 2 μg of each STAgR and control plasmid was transfected per sample using Lipofecatmin2000 according to the manufacturer's instructions. Seven days after the transfection cells were analysed by flow cytometry or qPCR respectively. For flow analysis, cells have been trypsinized, washed once with PBS and directly analyzed on a FACSAriaIII™(Becton Dickinson) flow cytometer. For each sample, GFP signal of 10000 cells has been recorded. RNA was extracted from P19 cells using the Quiagen RNAeasy Mini Kit according the manufacturer's instructions. 100 ng RNA was reverse transcribed using the Thermo Fisher cDNA first strand kit. qPCR reactions were performed on an Applied Biosystems™ QuantStudio™ 6 Flex Real-Time PCR System. Each 10-μl reaction consisted of 5 μl of cDNA, 5μl PowerUp™ SYBR™ Green Master Mix (Thermo Scientific), and appropriate amount of primers. The amount of the target transcript was quantified relative to Gapdh as a reference. Each sample was assayed at least in triplicates.

For *in vivo* experiments STAgR plasmids and a wildtype Cas9 expression construct were mixed with Fast Green dye (0.3 mg ml^{-1}; Sigma). 400ng (STAgR plasmids) and 800ng (Expression plasmid containing a Cas9 expression cassette derived from [22]) in 1 μl artificial CSF solution have been injected per fish representing a molar plasmid ratio of approximately 1:1. To conduct the injections fish were anaesthetized in 0.02% MS222 and immobilized in a sponge. A small hole was generated in the skull using a micro-knife to expose the brain tissue between the telencephalon and the optic tectum (Fine Science Tools). Subsequently, ventricular injections of the plasmid DNA were performed as previously described [23] using a glass capillary (Harvard Apparatus) and a pressure injector (200hPa, Femtojet®, Eppendorf). Five electrical pulses (amplitude: 65V; duration: 25ms; intervals: 1s) were delivered with a square-wave pulse generator TSS20 Ovodyne (Intracel) or by using the ECM830 square wave electroporator (BTX Harvard Apparatus). After the electroporation, fish were awakened in aerated water and kept in their normal husbandry conditions for 7 days until sacrifice and immunohistochemical analysis. All included animal work (and protocols) have been approved by the Goverment of Upper Bavaria (AZ 55.2-1-54-2532-09-16). For anesthesia, 0.02% MS222 and for euthanasia, an MS222 overdose (as approved in the above mentioned protocol) was used.

Results and discussion

An optimal method for the routine generation of multiplex gRNA vectors would combine simplicity with speed, would be cost-effective, efficient and highly customizable. Aiming to meet these requirements we designed a cloning strategy (STAgR) based on enzymatic assembly of short gRNA expression units, amplified from a single DNA fragment as a template, the String (S1 Fig). To avoid the need to purchase new strings for each individual gRNA, we omitted the N20 targeting sequence on the DNA fragment, containing only the gRNA hairpin, a transcriptional stop signal (poly dT) and a human U6 promoter. Instead, we provide the individual N20 sequences by short overhang primers used to amplify the String by PCR (Fig 1). In contrast to existing cloning strategies STAgR provides three distinct advantages: (1) any chosen gRNA expression unit can be amplified from the same DNA String; (2) any specific number or chosen combination of gRNA transcription units can be cloned using one single String, since the N20 targeting sequences provides the necessary homology for Gibson assembly [24]; (3) substitution and combination of different Strings as PCR template allows straight-forward customization to different Cas9- or expression-systems.

First, we tested the feasibility of STAgR by aiming to clone three different sets of four individual gRNAs into a standard gRNA expression vector, pgRNA1 [25, 26]. Following a standard PCR and Gibson assembly protocol (S1 File, S1 Fig), we routinely achieved hundreds of bacterial Ampicillin resistant colonies, indicating a large number of transformation events. To avoid unnecessary time- and cost-consuming vector preparation and sequencing, we devised a robust PCR strategy to quickly characterize the accuracy of the transformed vectors in individual bacterial colonies (S1 File, Fig 2A). This enabled us not only to concentrate downstream analysis on a distinct set of vectors, but also to comprehensively characterize STAgR efficiencies. The quantification presented in Fig 2B and the example of an analytical gel in Fig 2A shows that the tested STAgR strategy is successful in generating individual multiplexed gRNA vectors. Indeed, over a third (34%, (n = 130)) of bacterial clones possessed the envisaged four gRNA expression units, which, as confirmed by subsequent Sanger sequencing, have been matching the in silico designed gRNA vector perfectly in most tested cases (90%, 5 clones each sequenced in 8 independent experiments; n = 40). This indicated that likely a small number of bacterial clones are sufficient to routinely retrieve immediately at least one impeccable plasmid.

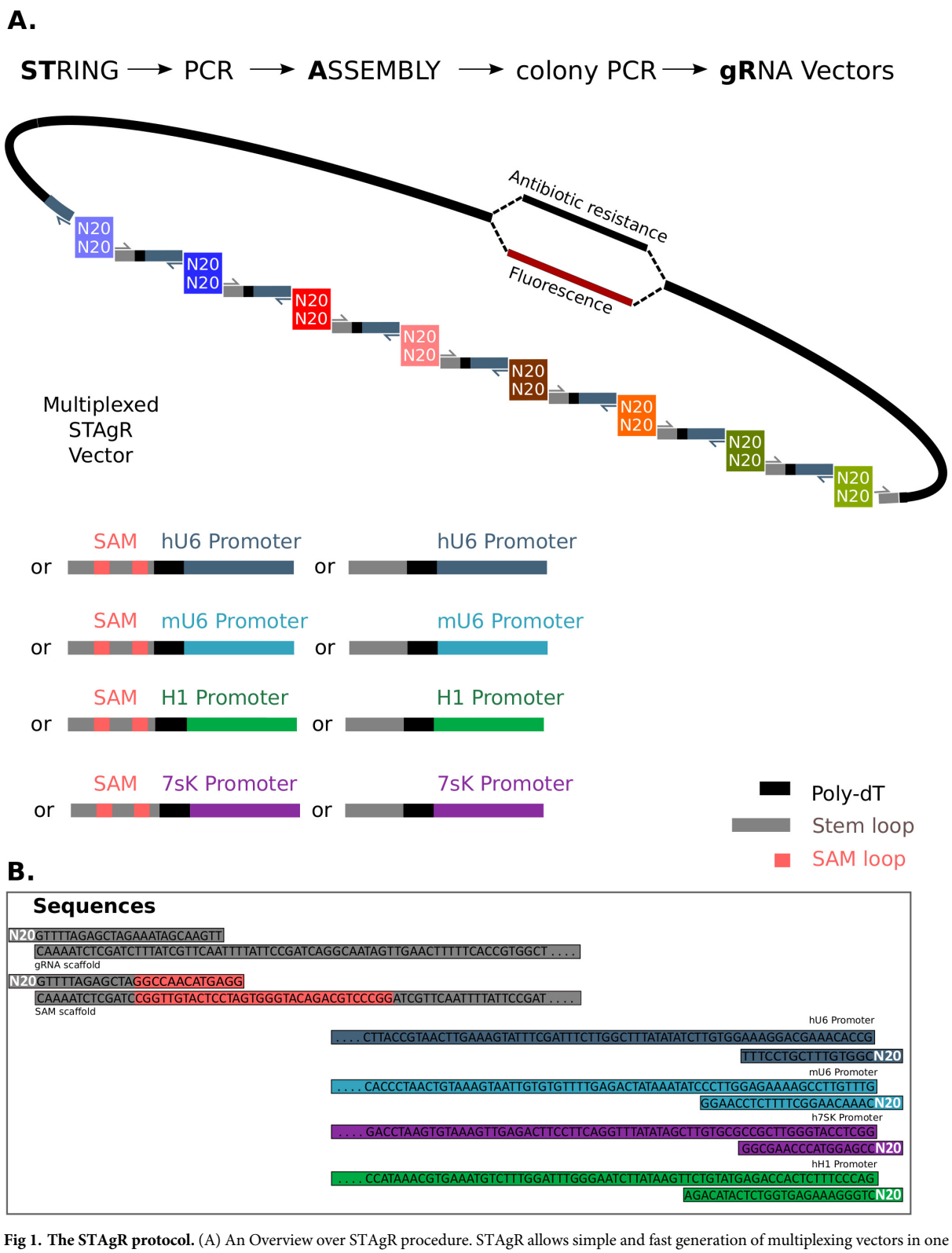

Fig 1. The STAgR protocol. (A) An Overview over STAgR procedure. STAgR allows simple and fast generation of multiplexing vectors in one overnight reaction. STAgR is also highly customizable as diverse strings and vectors can be used to assemble expression cassettes with different promoters and gRNA scaffolds. (B) Sequences of overhang primers used for generation of STAgR vectors.

https://doi.org/10.1371/journal.pone.0196015.g001

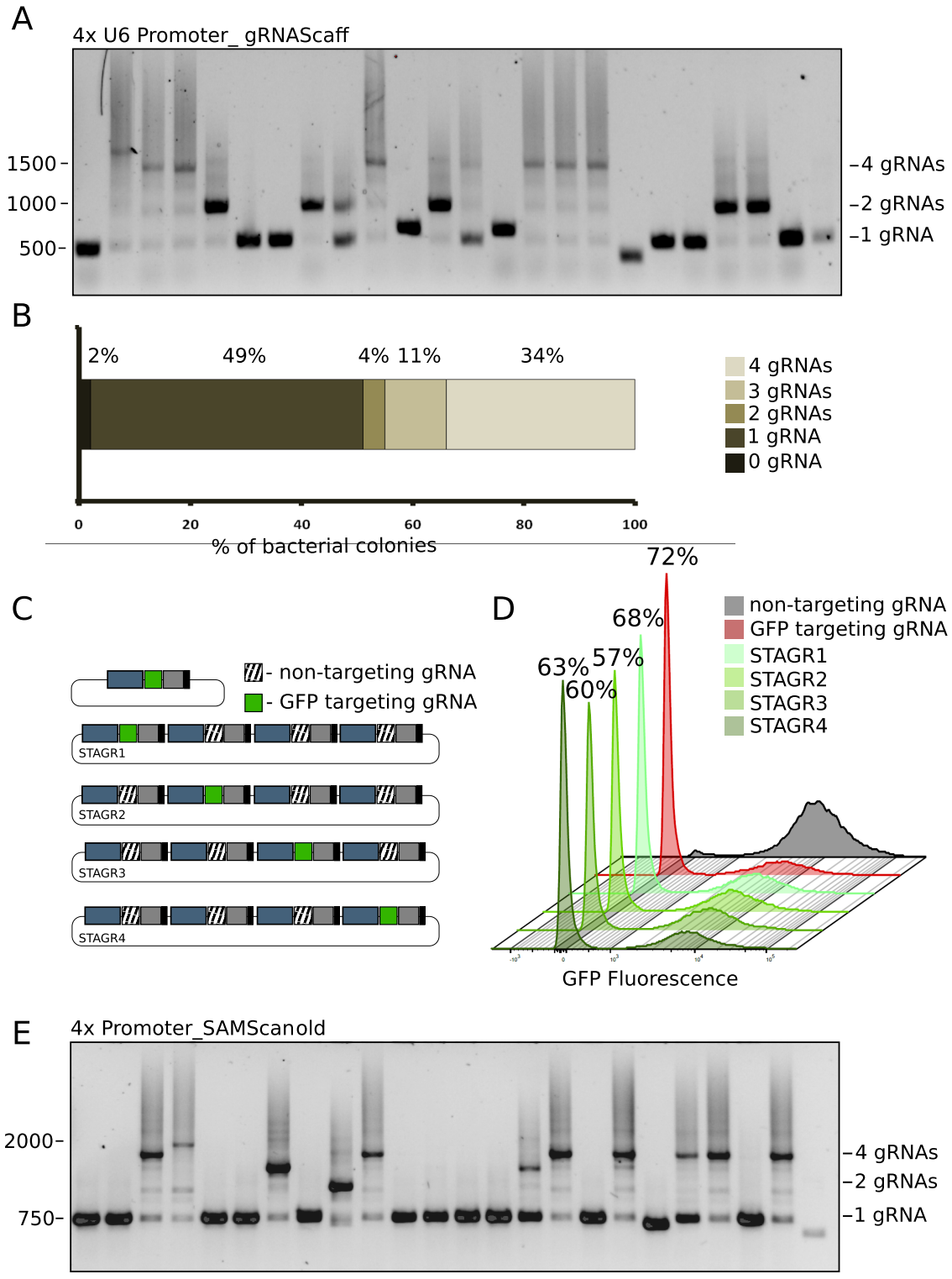

Fig 2. Functional validation of STAgR. (A) Colony PCR of a 4xSTAgR reaction (using a string sequence containing a hU6 promoter and a canonical gRNA scaffold). 24 bacterial colonies are shown, of which six present the amplicon size indicative of the full length reaction (1596 bp). Additionally marked are amplicon sizes indicative of two (823 bp) and single gRNAs (458 bp). (B) Quantification of cloning efficiencies from three different 4xSTAgR reactions (n = 130). (C) A schematic showing constructs used for functional validation of STAgR gRNAs. A gRNA targeting the GFP ORF was either delivered in a single gRNA expression vector or on each of four different positions in STAgR vectors. (D) Functional validation of STAgR vectors shown in Fig 2C. HeLa cells stably

expressing d2GFP and Cas9 have been transfected with vectors depicted above. Flow cytometry indicates that STAgR constructs are similarly efficient in mutating the ORF of GFP compared to a single gRNA vector. (E) Colony PCR of a 4xSTAgR reaction using four different promoters and SAM loop scaffolds. 24 bacterial colonies are shown, of which seven colonies incorporated the amplicon size indicative of the full length reaction (2043 bp). Shorter amplicons are indicative of gRNA subsets, which vary in size, depending on the incorporated promoter.

https://doi.org/10.1371/journal.pone.0196015.g002

Vectors containing multiple gRNA expression cassettes in close proximity are crucially dependent on efficient promoter and terminator sequences as transcriptional interference and/or transcriptional run-through hamper the functionality of individual gRNA sequences. Since it is still a complicated task to characterize these undesirable effects, as well as to determine the integrity and expression of individual gRNAs directly, we instead employed instead a genetic assay to quantify whether the effectiveness of a gRNA cassette changes with its position on an otherwise identical STAgR plasmid. We incorporated a single GFP-targeting gRNA into four STAgR plasmids and compared them directly to standard vectors containing only one single gRNA expression unit. We chose the assembly in such a way, that the GFP-targeting gRNA becomes incorporated on four different positions between three non-GFP-targeting control gRNA units (Fig 2C and 2D). We transfected human HeLa cells, stably expressing Cas9 and GFP, with the above mentioned gRNA expression plasmids and found that when using a single gRNA expression vector 72% of cells lost GFP expression after eight days, indicating the creation of detrimental ORF mutations. Reassuringly, STAgR plasmids containing the same GFP targeting gRNA on any of the four positions (next to non-GFP-targeting control gRNAs) triggered comparable GFP loss in site-by-site experiments, indicating similar functionality to single gRNA expression plasmids and suggesting absence of transcriptional interference or read-through in the STAgR vectors.

To demonstrate the customizability of the presented STAgR protocol, we generated a series of Strings to be used as alternative templates (Fig 1). We tested not only the adaptability of STAgR to different promoters, but also structurally different gRNA sequences. Shown as an example in Fig 2E is the assembly of four gRNAs, driven by four different promoter (human U6, mouse U6, 7SK and H1) and each containing additional RNA structures (one or two SAM loops) 3' from the gRNA hairpin to allow the targeting of MS2-fusion proteins to chosen genomic sites in addition to Cas9 fusion proteins [27]. One step STAgR assembly of this highly customized and combinatorial strategy proofed to be of similar efficiency as the STAgR strategy described before (ca. 30%, Fig 2E) and indicates a decisive advantage for the use of this method when combining different Cas9 variants, MS2 fusion proteins or dCas9 effectors

To further investigate the limits of the STAgR protocol we increased the number of gRNA cassettes to be incorporated in one single reaction step. As depicted in Fig 3A, increasing the number of individual gRNA cassettes to six did not change the efficiency of the STAgR approach. A significant proportion of bacterial colonies were indicative of full gRNA incorporation in the PCR assay (30%, n = 24) and all those tested were revealing perfect assembly when sequenced (S2A Fig). Following the STAgR protocol we routinely generate vectors with up to eight expression units, the maximum number of units we have tested so far (Fig 3B) and to our knowledge amongst the highest number of gRNA units generated on single CRISPR vectors by any method. Moreover, colony PCRs also reveal, that those STAgR clones, which apparently do not contain all gRNA expression units in completion, possess mostly insert sizes representing integer multiples of single gRNA expression units, something we have observed in each experiment we have conducted so far (Figs 2A, 2E and 3A). Thus we employed Sanger sequencing to investigate, the origin of the assembly failure and the sequences of the resulting plasmids. Interestingly, nearly all (87%, n = 15) of those truncated plasmids contained in silico designed sequences without a cloning scar, breakage points or sequence repetition, but were

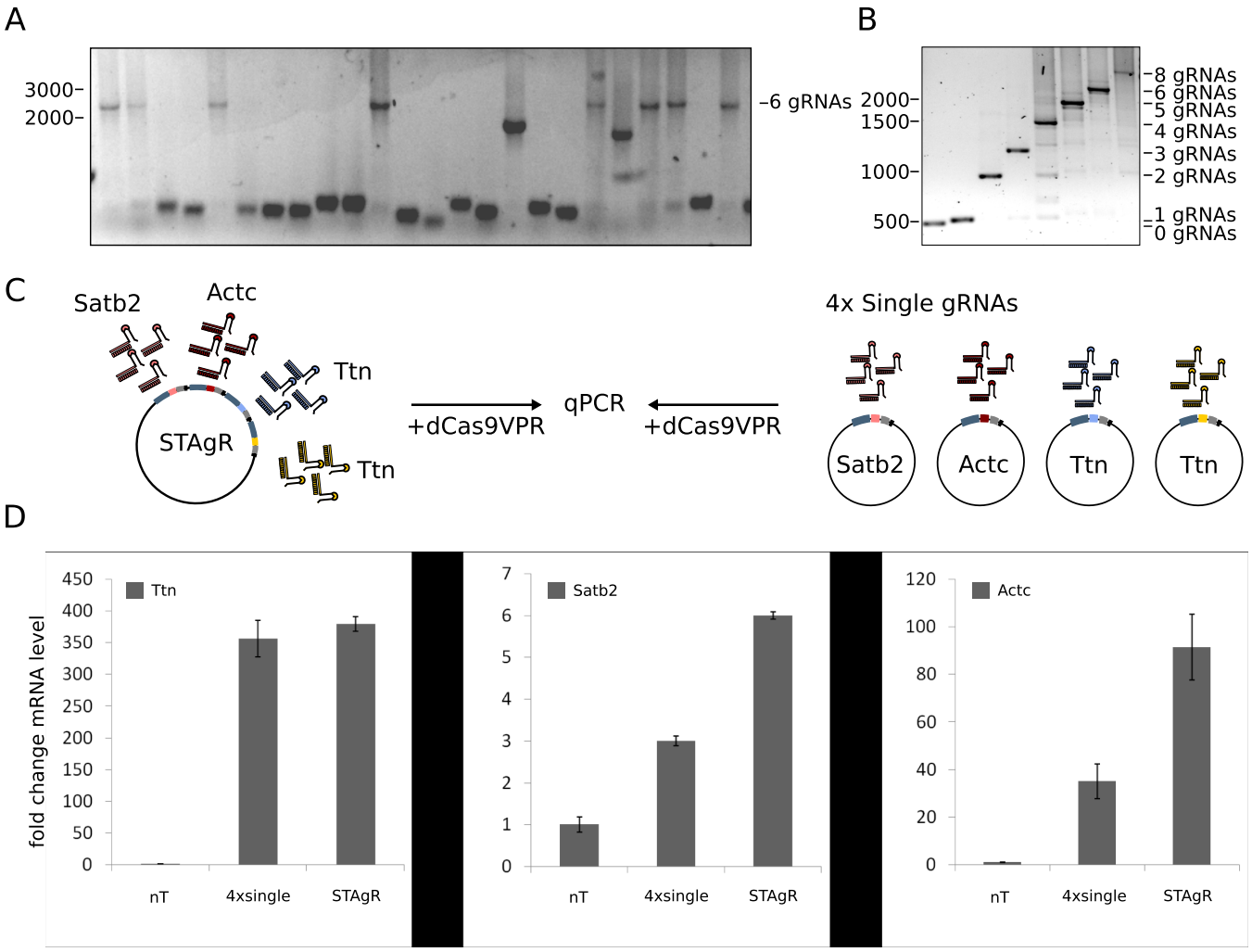

Fig 3. Application of STAgR. (A) Colony PCR of a 6xSTAgR reaction using two different promoters as well as both, the canonical and the SAM loop gRNA scaffold. The gel shows a colony PCR of 22 bacterial colonies, of which seven showed the amplicon indicative of the full length STAgR reaction (2444bp). (B) Exemplary colony PCR of STAgR constructs with 0 to 8 gRNA expression cassettes. (C) A STAgR plasmid containing four gRNAs or a mixture of four single gRNA plasmids have been transfected into P19 Cells expressing dCas9-VPR. (D) After 7 days mRNA was extracted and transcript levels of target genes have been compared via qPCR. Error bars depict standard errors of the mean.

https://doi.org/10.1371/journal.pone.0196015.g003

entirely lacking one or more gRNA expression units (for examples see S2B–S2E Fig). This surprising result is due to a low-probability alignment of String sequences during assembly and offers the unexpected possibility to use STAgR not only for the generation of multiplex gRNA vectors, but also for the simultaneous obtainment of gRNA subsets.

To demonstrate the added value of combining multiple gRNAs on single vectors, we produced a STAgR plasmid containing four gRNAs, of which one is targeting the promoter of the neuronal gene Satb2, one is targeting the promoter of the cardiac muscle actin gene Actc1 and the last two are binding the promoter region of the gene Ttn1 (Fig 3C). dCas9-VPR expressing P19 cells transfected with this STAgR plasmid upregulate two of three of these genes substantially stronger than cells receiving only a mixture of single gRNAs, indicating a distinct advantage for the use of STAgR in transcript activation over conventional approaches (Fig 3D).

To test whether the in vivo use of STAgR plasmids allows efficient simultaneous disruption of multiple genes in individual cells, we employed expression vectors commonly used in

zebrafish and used the protocol at hand to incorporate three gRNAs targeting GFP and Sox2 or a control STAgR vector. Subsequently, we electroporated ependymoglia in the brains of three and a half months old GFAP-GFP transgenic zebrafish, Tg(gfap:GFP) (n = 6), as previously done [28, 29] in three independent experiments using STAgR plasmids and a wildtype Cas9 expression construct (Fig 4 [22]). Seven days later we analyzed the outcome, which proved to be highly reproducible over animals and experiments. As depicted in Fig 4, a large number of ependymoglia lost GFP and Sox2 expression, while in the control electroporated brains ependymoglia cells continuously express both proteins. To our knowledge this represents the first CRISPR mediated gene knockout in adult fish brains. Moreover, most cells negative for one protein were also devoid of the other, certifying an efficient accomplishment of multiple gene targeting using STAgR in vivo.

Conclusions

Efficient multi-gene and–locus targeting provides a critical bottleneck for the implementation of the ever increasing toolbox of CRISPR based methods. Combinations of a large number of gRNA expression vectors have the disadvantage that only a subset of cells receives all gRNA sequences. Furthermore, the limited number of available antibiotic and fluorescent selection markers makes this subset not even accessible for selective analysis. The synthesis of multi-gRNA expression vectors is slow and expensive and thus impedes the comprehensive validation of different targeting efficiencies and gRNA sequences, as well as a straight forward customization of vector backbones and CRISPR systems for most experimental setups. In contrast to this, STAgR is fast, cheap and highly efficient. Employing the protospacer sequences of the gRNAs as sources of homology for Gibson assembly enables simple and customizable vector generation for multi-gene and multi-locus targeting. Following the attached protocol, vectors allowing the simultaneous targeting of high numbers of genes or loci can be generated efficiently in one over-night reaction. Moreover, the STAgR protocol does not depend on expensive or restricted materials or skill sets; its simplicity makes the application universally available (see detailed supplementary manual, S1 File). Only few strategies have been published so far which allow the multiplexed generation of multiple gRNA vectors [30–34]. These methods have much practical value, but they either lack the simplicity of vector generation in a single step, the high number of individual gRNA expression cassettes that can be combined, the customizability and/or the independence from purchasing new large DNA fragments for each individual gRNA sequence. STAgR, a one-step method for the generation of functional gRNA vectors, is reliable, highly customizable, simple and efficient, to prove its effectiveness we used it to generate the first in vivo gene targeting in the adult fish brain.

Accession numbers

Plasmids for STAgR cloning can be obtained from Addgene and sequences from figshare (https://figshare.com/projects/One_step_generation_of_customizable_gRNA_vectors_for_multiplex_CRISPR_approaches_through_string_assembly_gRNA_cloning_STAgR_/31046). The ID numbers are pcDNA_STAGR_SAMScaffold_hH1 (ID 102847), pcDNA_STAGR_SAMScaffold_h7SK (ID 102846), pcDNA_STAGR_SAMScaffold_mU6 (ID 102845), pcDNA_STAGR_gRNAScaffold_mU6 (ID 102844), pcDNA_STAGR_SAMScaffold_hU6 (ID 102843), pcDNA_STAGR_gRNAScaffold_h7SK (ID 102842), pcDNA_STAGR_gRNAScaffold_hH1 (ID 102841), pcDNA_STAGR_gRNAScaffold_hU6 (ID 102840), STAgR_mCherry (ID 102993), STAgR_Neo (ID 102992).

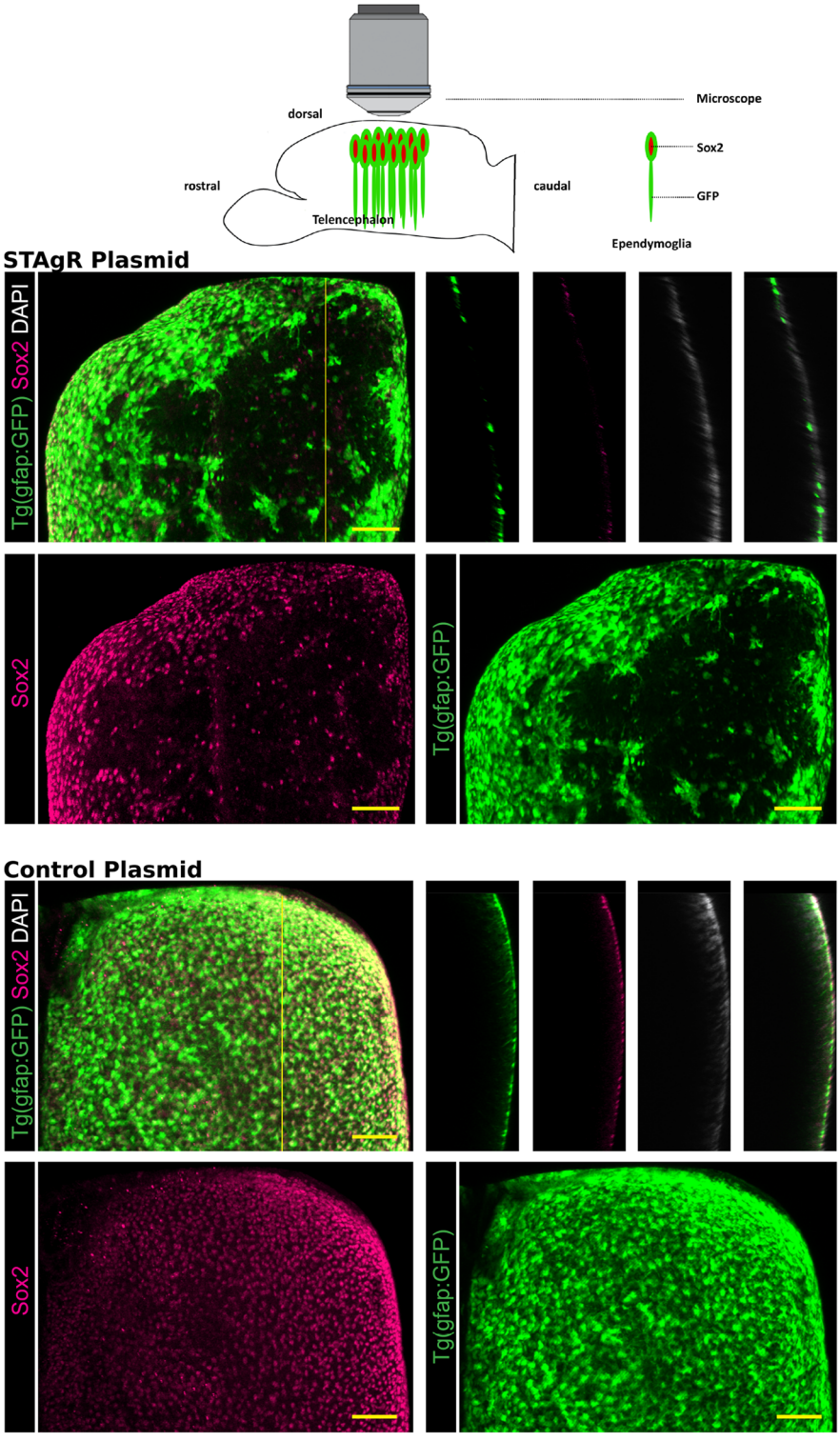

Fig 4. In vivo application of STAgR. STAgR constructs allow simultaneous genetic deletions in vivo. Above: Imaging setup from whole mount adult zebrafish brains. Below: 3D reconstructions of whole mount Tg(gfap:GFP) zebrafish telencephali (depicted from above). GFP+ and Sox2+ ependymoglia have been electroporated with STAgR targeting GFP and Sox2 (above) or a vector control (below) together with a Cas9 expression vector. Scale bar represents 50μm.

https://doi.org/10.1371/journal.pone.0196015.g004

Supporting information

S1 Fig. Overview of the STAgR protocol.
(EPS)

S2 Fig. Sanger sequencing of five clones acquired in one single 6xSTAgR reaction. Upper left: scheme depicting complete and partial incorporations. Upper right: colony PCRs of five random clones sequenced. Shown below are sequences obtained demonstrating accurate incorporation of 6 (A), 4 (B), 3 (C), 2 (D) or 1 (E) gRNA cassettes.
(TIFF)

S1 File. A detailed protocol for STAgR cloning.
(PDF)

Acknowledgments

The authors would like to thank Prof. Dr. Stephan Beck for his input, help and support in developing the STAgR method.

Author Contributions

Conceptualization: Christopher T. Breunig, Anna Köferle, Jovica Ninkovic, Stefan H. Stricker.

Data curation: Christopher T. Breunig, Tamara Durovic, Andrea M. Neuner, Valentin Baumann, Maximilian F. Wiesbeck.

Formal analysis: Christopher T. Breunig.

Funding acquisition: Magdalena Götz, Stefan H. Stricker.

Investigation: Christopher T. Breunig, Tamara Durovic, Andrea M. Neuner, Valentin Baumann, Maximilian F. Wiesbeck, Anna Köferle.

Methodology: Christopher T. Breunig, Tamara Durovic, Andrea M. Neuner, Anna Köferle, Jovica Ninkovic, Stefan H. Stricker.

Project administration: Magdalena Götz, Stefan H. Stricker.

Resources: Stefan H. Stricker.

Supervision: Christopher T. Breunig, Magdalena Götz, Jovica Ninkovic, Stefan H. Stricker.

Validation: Christopher T. Breunig.

Visualization: Christopher T. Breunig, Tamara Durovic.

Writing – original draft: Christopher T. Breunig, Stefan H. Stricker.

Writing – review & editing: Stefan H. Stricker.

References

1. Ledford H. CRISPR: gene editing is just the beginning. Nature. 2016; 531(7593):156–9. https://doi.org/10.1038/531156a PMID: 26961639.
2. Cong L, Ran FA, Cox D, Lin S, Barretto R, Habib N, et al. Multiplex genome engineering using CRISPR/Cas systems. Science. 2013; 339(6121):819–23. https://doi.org/10.1126/science.1231143 PMID: 23287718
3. Jinek M, East A, Cheng A, Lin S, Ma E, Doudna J. RNA-programmed genome editing in human cells. eLife. 2013; 2:e00471. https://doi.org/10.7554/eLife.00471 PMID: 23386978

4. Jinek M, Chylinski K, Fonfara I, Hauer M, Doudna JA, Charpentier E. A programmable dual-RNA-guided DNA endonuclease in adaptive bacterial immunity. Science. 2012; 337(6096):816–21. https://doi.org/10.1126/science.1225829 PMID: 22745249.
5. Köferle A, Stricker SH, Beck S. Brave new epigenomes: the dawn of epigenetic engineering. Genome Med. 2015; 7(1):59. https://doi.org/10.1186/s13073-015-0185-8 PMID: 26089986
6. Chavez A, Scheiman J, Vora S, Pruitt BW, Tuttle M, E PRI, et al. Highly efficient Cas9-mediated transcriptional programming. Nat Methods. 2015; 12(4):326–8. https://doi.org/10.1038/nmeth.3312 PMID: 25730490
7. Shen B, Zhang W, Zhang J, Zhou J, Wang J, Chen L, et al. Efficient genome modification by CRISPR-Cas9 nickase with minimal off-target effects. Nat Methods. 2014; 11(4):399–402. https://doi.org/10.1038/nmeth.2857 PMID: 24584192.
8. Lekomtsev S, Aligianni S, Lapao A, Burckstummer T. Efficient generation and reversion of chromosomal translocations using CRISPR/Cas technology. BMC Genomics. 2016; 17(1):739. https://doi.org/10.1186/s12864-016-3084-5 PMID: 27640184
9. Jiang J, Zhang L, Zhou X, Chen X, Huang G, Li F, et al. Induction of site-specific chromosomal translocations in embryonic stem cells by CRISPR/Cas9. Scientific reports. 2016; 6:21918. https://doi.org/10.1038/srep21918 PMID: 26898344
10. Yang H, Wang H, Shivalila CS, Cheng AW, Shi L, Jaenisch R. One-step generation of mice carrying reporter and conditional alleles by CRISPR/Cas-mediated genome engineering. Cell. 2013; 154(6):1370–9. https://doi.org/10.1016/j.cell.2013.08.022 PMID: 23992847
11. Wang L, Shao Y, Guan Y, Li L, Wu L, Chen F, et al. Large genomic fragment deletion and functional gene cassette knock-in via Cas9 protein mediated genome editing in one-cell rodent embryos. Scientific reports. 2015; 5:17517. https://doi.org/10.1038/srep17517 PMID: 26620761
12. Zhang L, Jia R, Palange NJ, Satheka AC, Togo J, An Y, et al. Large genomic fragment deletions and insertions in mouse using CRISPR/Cas9. PLoS One. 2015; 10(3):e0120396. https://doi.org/10.1371/journal.pone.0120396 PMID: 25803037
13. Yang H, Wang H, Jaenisch R. Generating genetically modified mice using CRISPR/Cas-mediated genome engineering. Nat Protoc. 2014; 9(8):1956–68. https://doi.org/10.1038/nprot.2014.134 PMID: 25058643.
14. Wang H, Yang H, Shivalila CS, Dawlaty MM, Cheng AW, Zhang F, et al. One-step generation of mice carrying mutations in multiple genes by CRISPR/Cas-mediated genome engineering. Cell. 2013; 153(4):910–8. https://doi.org/10.1016/j.cell.2013.04.025 PMID: 23643243
15. Kalhor R, Mali P, Church GM. Rapidly evolving homing CRISPR barcodes. Nat Methods. 2017; 14(2):195–200. https://doi.org/10.1038/nmeth.4108 PMID: 27918539
16. Balboa D, Weltner J, Eurola S, Trokovic R, Wartiovaara K, Otonkoski T. Conditionally Stabilized dCas9 Activator for Controlling Gene Expression in Human Cell Reprogramming and Differentiation. Stem Cell Reports. 2015; 5(3):448–59. https://doi.org/10.1016/j.stemcr.2015.08.001 PMID: 26352799
17. Chakraborty S, Ji H, Kabadi AM, Gersbach CA, Christoforou N, Leong KW. A CRISPR/Cas9-based system for reprogramming cell lineage specification. Stem Cell Reports. 2014; 3(6):940–7. https://doi.org/10.1016/j.stemcr.2014.09.013 PMID: 25448066
18. Maeder ML, Linder SJ, Cascio VM, Fu Y, Ho QH, Joung JK. CRISPR RNA-guided activation of endogenous human genes. Nat Methods. 2013; 10(10):977–9. https://doi.org/10.1038/nmeth.2598 PMID: 23892898
19. Hilton IB, D'Ippolito AM, Vockley CM, Thakore PI, Crawford GE, Reddy TE, et al. Epigenome editing by a CRISPR-Cas9-based acetyltransferase activates genes from promoters and enhancers. Nat Biotechnol. 2015. https://doi.org/10.1038/nbt.3199 PMID: 25849900.
20. Stricker SH, Koferle A, Beck S. From profiles to function in epigenomics. Nat Rev Genet. 2017; 18(1):51–66. https://doi.org/10.1038/nrg.2016.138 PMID: 27867193.
21. Black JB, Adler AF, Wang HG, D'Ippolito AM, Hutchinson HA, Reddy TE, et al. Targeted Epigenetic Remodeling of Endogenous Loci by CRISPR/Cas9-Based Transcriptional Activators Directly Converts Fibroblasts to Neuronal Cells. Cell Stem Cell. 2016; 19(3):406–14. https://doi.org/10.1016/j.stem.2016.07.001 PMID: 27524438
22. Ran FA, Hsu PD, Wright J, Agarwala V, Scott DA, Zhang F. Genome engineering using the CRISPR-Cas9 system. Nat Protoc. 2013; 8(11):2281–308. https://doi.org/10.1038/nprot.2013.143 PMID: 24157548
23. Kizil C, Brand M. Cerebroventricular microinjection (CVMI) into adult zebrafish brain is an efficient misexpression method for forebrain ventricular cells. PLoS One. 2011; 6(11):e27395. https://doi.org/10.1371/journal.pone.0027395 PMID: 22076157

24. Gibson DG, Young L, Chuang RY, Venter JC, Hutchison CA 3rd, Smith HO. Enzymatic assembly of DNA molecules up to several hundred kilobases. Nat Methods. 2009; 6(5):343–5. https://doi.org/10.1038/nmeth.1318 PMID: 19363495.

25. Koferle A, Worf K, Breunig C, Baumann V, Herrero J, Wiesbeck M, et al. CORALINA: a universal method for the generation of gRNA libraries for CRISPR-based screening. BMC Genomics. 2016; 17 (1):917. https://doi.org/10.1186/s12864-016-3268-z PMID: 27842490

26. Koferle A, Stricker SH. A universal protocol for large-scale gRNA library production from any DNA source. Journal of Visualized Experiments. in press.

27. Konermann S, Brigham MD, Trevino AE, Joung J, Abudayyeh OO, Barcena C, et al. Genome-scale transcriptional activation by an engineered CRISPR-Cas9 complex. Nature. 2014. https://doi.org/10.1038/nature14136 PMID: 25494202.

28. Barbosa JS, Sanchez-Gonzalez R, Di Giaimo R, Baumgart EV, Theis FJ, Gotz M, et al. Neurodevelopment. Live imaging of adult neural stem cell behavior in the intact and injured zebrafish brain. Science. 2015; 348(6236):789–93. https://doi.org/10.1126/science.aaa2729 PMID: 25977550.

29. Barbosa JS, Di Giaimo R, Gotz M, Ninkovic J. Single-cell in vivo imaging of adult neural stem cells in the zebrafish telencephalon. Nat Protocols. 2016; 11(8):1360–70. https://doi.org/10.1038/nprot.2016.077 PMID: 27362338

30. Xie K, Minkenberg B, Yang Y. Boosting CRISPR/Cas9 multiplex editing capability with the endogenous tRNA-processing system. Proc Natl Acad Sci U S A. 2015; 112(11):3570–5. https://doi.org/10.1073/pnas.1420294112 PMID: 25733849

31. Kabadi AM, Ousterout DG, Hilton IB, Gersbach CA. Multiplex CRISPR/Cas9-based genome engineering from a single lentiviral vector. Nucleic Acids Res. 2014; 42(19):e147. https://doi.org/10.1093/nar/gku749 PMID: 25122746

32. Sakuma T, Nishikawa A, Kume S, Chayama K, Yamamoto T. Multiplex genome engineering in human cells using all-in-one CRISPR/Cas9 vector system. Scientific reports. 2014; 4:5400. https://doi.org/10.1038/srep05400 PMID: 24954249

33. Port F, Bullock SL. Augmenting CRISPR applications in Drosophila with tRNA-flanked sgRNAs. Nat Methods. 2016; 13(10):852–4. https://doi.org/10.1038/nmeth.3972 PMID: 27595403

34. Ferreira R, Skrekas C, Nielsen J, David F. Multiplexed CRISPR/Cas9 Genome Editing and Gene Regulation Using Csy4 in Saccharomyces cerevisiae. ACS Synth Biol. 2017. https://doi.org/10.1021/acssynbio.7b00259 PMID: 29161506.

4. DISCUSSION

Within the scope of this thesis, in summary, AhR receptor was found to be implicated in the temporal control of ependymoglia behavior after injury. More specifically, we observed that levels of AhR signaling dropped at 2dpi and rose back to basal levels at 7dpi. This change in the signaling levels of AhR was followed by a specific mode of ependymoglia behavior. Namely, when AhR signaling levels were low, ependymoglial cells were prone to proliferate and conversely, high levels of AhR acted like a cue for ependymoglia to directly convert. Additionally, we discovered two ependymoglial subpopulations, based on levels of GFP transgene in *gfap:GFP* transgenic zebrafish line: GFP high and GFP low. Both GFP high and GFP low ependymoglial cells can have fluctuating levels of GFP, meaning that the GFP high subpopulation can become GFP low and vice versa. Nevertheless, more than 90% of ependymoglial cells had GFP low phenotype immediately before direct conversion (Di Giaimo, Durovic et al., 2018). GFP low cells express higher AhR levels and show stronger downregulation of AhR upon injury, compared to GFP high. Additionally, the transcriptome of GFP low cells, after injury, is mainly enriched for biological processes connected to chemotaxis, cell migration, morphological changes, and differentiation, whereas transcriptome of GFP high cells shows cell cycle regulation, mitotic nuclear division, and DNA replication processes as dominant.

These new findings open many interesting questions and hypotheses to explore. Noteworthy, our data would be in line with the findings of Baumgart et al., 2012, regarding the time frame of the activation of ependymoglial cells after an injury. Concretely, they observed that the dynamics of ependymoglial proliferation after injury, based on gfap:GFP transgenic line and BrdU staining, follows the trend as depicted on the Figure 8; ependymoglia start proliferating between 1 and 2 days post injury to reach the highest level of proliferation at 7 dpi (as observed within the scope of the 7 day time frame).

These data correspond to our observation about AhR signaling dynamics, specifically the fact that low AhR levels, which occur at 2 dpi, promote ependymoglia proliferation and/or self-renewal. However, as AhR levels go back to basal levels at 7 dpi, GFP low population, being mostly affected by AhR signaling, goes through the process of direct conversion, as we observed that high AhR levels act as a signal to allow neurogenesis through direct conversion to take place (Di Giaimo, Durovic et al., 2018).

Our observation is further in line with the study of Barbosa et al. 2015 using in vivo imaging after injury for up to one month. Live imaging analysis revealed direct conversions largely after 7 days post injury.

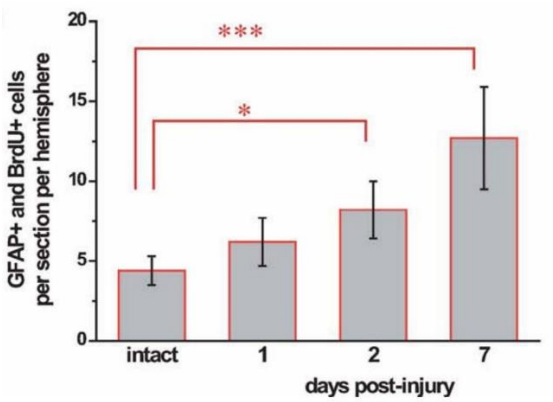

Figure 8. Proliferative dynamics of ependymoglial cells as a reaction to injury (Baumgart et al., 2012)**.** Adapted by copyright permission from John Willey and Sons and Copyright Clearance Center: *GLIA* 60 (3): 343–57. (Baumgart et al. 2012). License No: 4763050090615. (2012). https://doi.org/10.1002/glia.22269

Moreover, live imaging demonstrated that the direct conversion process is a faster neurogenesis mode to produce new neurons, especially when compared to neuronal production through intermediate progenitor step. This implies that too fast production of new neurons through direct conversion would lead to hampered survival of these neurons, as we could see from our experiments (Di Giaimo, Durovic et al., 2018). As expected, in the first couple of days after injury the environment around the injury site is under inflammation conditions, due to accumulation and proliferation of microglia, oligodendroglia, endothelial cells and leukocytes (Kroehne et al., 2011). This environment is not optimal for survival and integration of new neurons, leading to their impaired survival. Therefore, the general kinetics of AhR signaling serves as a guarding mechanism against premature neurogenesis through direct conversion. Proper timing of neurogenesis is crucial, such that it starts only after the wound healing period is over. This idea is represented on the simplified schematic on Figure 9.

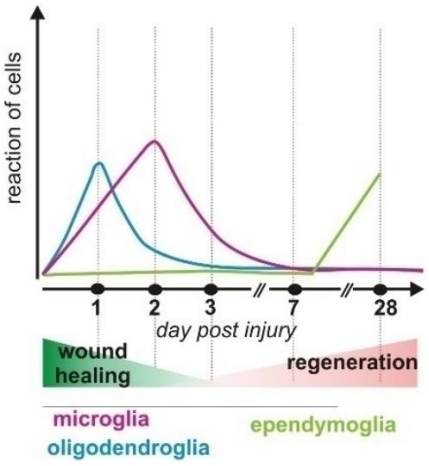

Figure 9. Proliferative dynamics of ependymoglial cells as a reaction to injury. With the permission of Prof. Dr. Jovica Ninkovic.

Additionally, it has been shown that acute inflammation is necessary and sufficient for activation of ependymoglia division (Kyritsis et al., 2012), meaning that it is preceding ependymoglia activation. We have also observed many inflammatory agents, such as Irf9, NF-kB or TGF-ß1, being activated at 2dpi. However, this is not merely enough for ependymoglia to become active and divide in order for proper regeneration to occur, as we could learn from mammalian brain. After an injury in mammals, infiltrating macrophages/microglia and astrocytes are activated and remain present for months after the injury. This generated inflammatory environment leads to scar formation, and results in inhibited survival and integration of newborn neurons (Dimou and Gotz, 2014). Therefore, the advantage of zebrafish is in its superior regulation of post-injury inflammation - especially given that inflammation is not long-lasting and ceases a few days after the injury, which is coupled with precise timing of ependymoglial activation.

Thus, the relationship between AhR signaling level and inflammatory system is very interesting to explore further. AhR is considered to be highly ``promiscuous`` in the field, since it has broad spectrum of agonists and ligands. Being an environmental sensor, and thus keeping homeostasis, AhR is found to be widely implicated in many molecular pathways connected to immune system, and it plays an important role in immunological barrier organs, such as skin, the gut and the lungs (Stockinger et al., 2014). Overall, the action of the AhR receptor seems to be complex and highly context dependent. For instance, besides xenobiotics, some of the endogenous ligands of AhR have been reported, such as essential amino acid tryptophan metabolites, kynurenine, or indoles. Indoles can be additionally derived from metabolism of some foods, particularly cruciferous vegetables. Other promising ligands include 6-formylindolo[3,2-b] carbazole (FICZ), present in humans, mainly in the skin (Stockinger et al., 2014), and even glucose has been described as AhR ligand (Dabir et al., 2008). Nevertheless, the strongest endogenous candidate of AhR seems to be kynurenine (Bersten et al., 2013; Stockinger et al., 2014). Kynurenine is produced in the kynurenine pathway, a metabolic pathway of the essential amino acid tryptophan degradation. Tryptophan can be found in the blood, bound to albumin and can be transported into the brain through blood-brain barrier (Yan et al., 2015). Inside the brain, mainly neurons, microglia, infiltrating macrophages and astrocytes can metabolize tryptophan to kynurenine. Kynurenine is not the end product of degradation pathway, but can be further metabolized into different components, such as kynurenic acid or neurotoxic quinolinic acid (Yan et al., 2015). In the context of AhR pathway activation, kynurenine promotes mast cell activation through the AhR receptor (Kawasaki et al., 2014). Within the scope of brain insult research, interestingly, it has been found that L-kynurenine/AhR pathway has detrimental effects in the acute phase after cerebral ischemia stroke in mouse model, and that the pathway becomes activated mainly in neurons (Cuartero et al., 2014). Additionally, kynurenine pathway has been described to be activated upon traumatic brain injury in humans in microglia through interferon γ (IFN-γ) (Yan et al., 2015) or in cultured microglia by TNFα or IL-1β (Wang et al.,

2010). Likewise, it has been shown that AhR can be induced by lipopolysaccharides (LPS) in macrophages and that it negatively regulates inflammatory responses (Kimura et al., 2009).

Another intriguing finding demonstrated activation of AhR by INF type 1 in mouse astrocytes throughout the course of inflammatory diseases, such as multiple sclerosis and autoimmune encephalomyelitis. INF-β works through JAK/STAT pathway, and together with IRF9, this complex binds IFN-response elements on the AhR promoter (Rothhammer et al., 2016). AhR activation would subsequently act in an anti-inflammatory manner and limit CNS inflammation. On the contrary, AhR deletion would promote increased number of inflammatory infiltrating monocytes and activation of microglia, due to activation of NF-kB in astrocytes. The rationale is that Nf-kB would bind to genes connected with monocyte infiltration, whereas AhR expression would interfere with this process (Rothhammer et al., 2016). Interestingly, AhR has been found to be increased in proliferating juxtavascular astrocytes, potentially acting as a repressor of further inflammation and monocyte infiltration in the stab would injury model (Frik et al., 2018).

Curiously, the upregulation of IRF9 and Nf-kB cytokines that we observed after injury, simultaneously with AhR downregulation, might point towards the connection between these key players even in our injury model. Considering the similarities between the roles of astrocytes and ependymoglial cells in zebrafish, kynurenine mediated activation of AhR should not be excluded as the potential candidate in ependymoglia cells after injury.

Interestingly, there is another possibility of resolution of post-injury effects and stem cell activation, given that AhR might not exert its effects directly on ependymoglial cells. This hypothesis would point towards the indirect effect of inflammatory cells on ependymoglia behavior after injury (Kizil et al., 2015). Specifically, tissue damage after injury causes the activation of tissue resident microglia and macrophages. As a reaction, these cells initiate acute inflammation through secretion of pro-inflammatory cytokines and chemokines. This reaction cascade subsequently calls upon peripheral immune cells that secret even more proinflammatory factors, which would influence stem cells to become activated and for instance, proliferate (Kizil et al., 2015).

Given the discoveries of Rothhammer et al. 2016, and the effects AhR asserts in astrocytes through interaction with inflammatory system, it is not implausible to consider that AhR might have an indirect role on regenerative neurogenesis and stem cell behavior in zebrafish too. Namely, they observed that AhR expression in astrocytes has a limiting effect on CNS inflammation, whereas AhR deletion increases the expression of chemokines, cytokines, and is associated with an increased number of infiltrating monocytes.

If we would translate this effect on our injury model and our findings, the logical bridge poses the next question - would it be possible that low AhR upon injury influences infiltration of immune cells in the brain, and pro- or anti- inflammatory molecules these cells produce,

consequently influence the behavior of ependymoglia (mainly proliferation)? In contrast, high AhR levels, occurring around 7 dpi, would help limiting inflammation and would prompt final production of a last, faster-emerging, batch of new neurons (mainly through direct conversion).

Finally, we did check the number of infiltrating cells upon prolonged AhR downregulation, however, we did not observe any difference compared to control animals (preliminary data, not shown). Additionally, we have shown that the effects that AhR asserts on ependymoglial cells indeed are cell autonomous. Nevertheless, this still does not completely exclude the previously mentioned hypothesis, especially not potential communication between ependymoglial cells and immune cells. Therefore, further experiments might concentrate on the opposite mechanism of action, namely ablation of infiltrating immune cells and investigation of the outcome.

Taking everything into consideration, the relevance of our work lies in the finding that the AhR receptor is the key molecule in the zebrafish model, being involved in timely regulation of ependymoglial activation post-injury, while simultaneously ´´sensing´´ the injury environment and inflammatory condition. This is particularly interesting in the light of the similarities shared between zebrafish ependymoglia and mouse astrocytes, especially since AhR is expressed in mouse astrocytes in inflammatory conditions as well (Frik et al., 2018; Rothhammer et al., 2016). However, not enough is known about AhR dynamics in astrocytes upon injury in the mammalian brain and if specific manipulation of AhR would lead to improved regeneration. Focus of further regeneration research should include better characterization of the role of AhR in astrocytes and its relationship with the post-injury inflammation.

4.1. AhR and the stemness

Since AhR is expressed in ependymoglial cells, which are acting as the stem cells in the zebrafish brain, it is interesting to further explore its role in cell differentiation and pluripotency. Recent reports are showing a lot of relevant evidence for AhR being involved in stemness and cell differentiation. In mouse embryonic stem cells, AhR is transcriptionally repressed by traditional pluripotency factors OCT3/4, NANOG, SOX2 and polycomb proteins. This repression is reversible, and therefore AhR upregulation may quickly lead to embryonic stem cell differentiation (Ko et al., 2016). In this way, AhR is involved in maintenance of embryonic stem cell pool, and Ko et al., 2016 state that the timely expression of AhR during stem cell differentiation secures exit from pluripotency in the proper time and promotion of cardiogenesis. Accordingly, we observed depletion of stem cell pools upon misregulation of AhR signaling and premature potentiation. Likewise, these interesting findings correlate with

our observation about the importance of punctual AhR activation upon injury and cell fate that will be consequently promoted.

Furthermore, another study showed that AhR downregulation by antagonist binding facilitates the expansion of human hematopoietic stem cells ex vivo, whereas AhR expression keeps them in unexpansive state (Boitano et al., 2010). Similarly, another finding showed that Musashi-2, a RNA-binding protein, downregulates components of AhR pathway and thus promotes expansion of umbilical cord blood-derived hematopoietic stem cells (Rentas et al., 2016).

In agreement with these findings, recent findings observed that AhR expression regulated by TCDD hindered the long-term self-renewal of hematopoietic stem cells in the fetus throughout pregnancy (Laiosa et al., 2016). Additionally, AhR knockout embryonic mice are frequently not able to survive throughout the gestation period, and if they are born, they have multi-organ dysfunctions. The mice that survive likely have an aberrant developmental program, presumably due to changes in the pluripotency of the inner cell mass (ICM) cells, which leads to imbalanced pluripotency (Ko and Puga, 2017).

Based on the aforementioned research, AhR is implicated in regulation of proliferation, differentiation, and pluripotency. Specifically, AhR downregulation seems to promote self-renewal, whereas AhR expression leads to cell differentiation. Curiously, this is an identical mechanism of AhR behavior as we observed after the injury. Given that AhR is expressed in many cell types, it additionally suggests that, not only the expression, but also distinct signaling, has a role on the cell fate.

Nevertheless, the difference in response of AhR compared to other established self-renewing pathways, such as Notch or WNT, remains to be determined. Interestingly, there are some findings suggesting the connection between AhR and Notch for instance, where AhR works through Notch signaling (Lee et al., 2011), probably through binding to dioxin responsive elements, on the upstream regulatory region of the Notch genes (Stevens et al., 2009). Looking at this finding in the context of the role of Notch in the balance between quiescence and proliferation of ependymoglia cells (Chapouton et al. 2010), it is very interesting to see that AhR might be implicated in Notch signaling and additionally regulate stem cell activation and maintenance of stem cell pool throughout this pathway.

Regarding WNT signaling, one study demonstrated the effect of AhR signaling on inhibition of fin regeneration, through misregulation of Wnt/β-catenin signaling (Mathew et al., 2009). In this study, they observed that TCDD-elicited AhR response activates R-Spondin1, which is a Wnt ligand. On the other hand, this signaling pathway axis negatively regulates Sox 9, an inhibitor of β-catenin signaling. Together, these events lead to uncontrolled upregulation of Wnt signaling and mis-regulation of multiple β-catenin target genes. Noteworthy, our data show upregulation of Wnt signaling pathway in GFP low ependymoglia cells. These cells

undergo direct conversion, and we might say, variation of epithelial to mesenchymal transition, by directly transforming from ependymoglial cells to neurons. Strikingly, R-Spondin1 and Wnt/β-catenin are observed to be involved in epithelial-mesenchymal transition, mostly studied in the light of cancer cell signaling (Basu et al., 2018; Hu et al., 2019), suggesting that this might be one of the main pathways responsible for the direct conversion of GFP low cells. Additionally, and only to point out, we did find Sox9 to be expressed in GFP low cells in contrast to GFP high, for instance.

Lastly, emergence of new data gives support to the wide-spread role of AhR as one of the crucial components of inflammatory and regenerative processes. Our previous knowledge of AhR was limited and only recently, has it received increasingly deserved attention. All above mentioned findings open a new avenue in regeneration approaches, with AhR being one of the strongest candidates for manipulation.

4.2. Closing remarks

Bearing in mind all the data that were acquired throughout this thesis, a couple of overall closing remarks can be made. Broadly, the findings about AhR could be summarized in the following schematic:

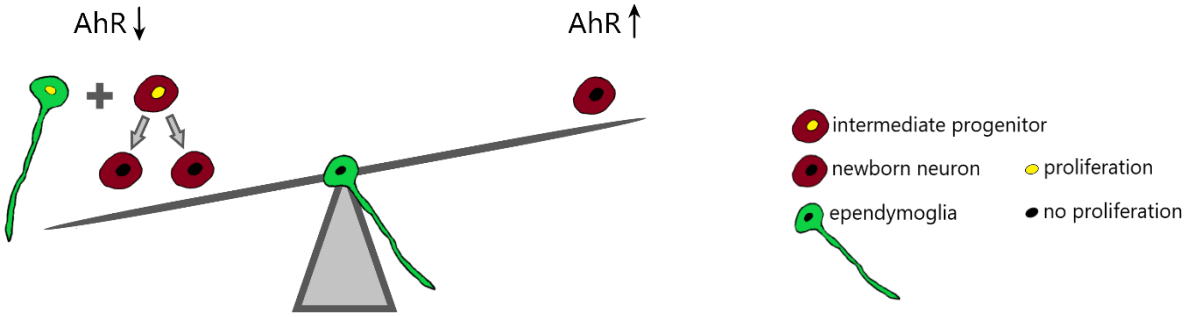

Figure 10. The balance between low and high AhR levels and ependymoglia behavior. *When AhR levels are low after the injury, we can observe proliferation of ependymoglial cells. After the wound healing period is finished, AhR levels go back to basal levels and promote direct conversion of ependymoglial cells (mostly GFP low).*

The AhR defines the time frame of restorative neurogenesis in zebrafish after injury and doesn´t allow for the premature neurogenesis to take place before the wound healing

period is over. We found two subpopulations of ependymoglial cells that react differently to AhR, GFP high and GFP low. GFP low is the subpopulation that expresses higher levels of AhR and downregulates it specifically after injury. We found this subpopulation to be mostly responsible for direct conversion.

Our findings, together with previous research, open many questions regarding the role of AhR in both physiological and regenerative conditions. Of high importance is the role AhR plays in regulating both cell stemness and differentiation, suggests that it can be legitimately placed among crucial pluripotency factors. However, more research needs to be done to elucidate its exact role in different biological systems. Considering all the above-mentioned discoveries, AhR may be regarded as a novel candidate responsible for coordination of cell states in different systems and conditions. Orchestration of balance between stemness and differentiation is necessary in order to ensure both homeostasis and repair.

5. REFERENCES

Adolf, B., Chapouton, P., Lam, C.S., Topp, S., Tannhauser, B., Strahle, U., Gotz, M., and Bally-Cuif, L. (2006). Conserved and acquired features of adult neurogenesis in the zebrafish telencephalon. Dev Biol *295*, 278–293.

Albadri, S., Del Bene, F., and Revenu, C. (2017). Genome editing using CRISPR/Cas9-based knock-in approaches in zebrafish. Methods *121–122*, 77–85.

Altman, J., and Das, G.D. (1965). Autoradiographic and histological evidence of postnatal hippocampal neurogenesis in rats. J Comp Neurol *124*, 319–335.

Alunni, A., and Bally-Cuif, L. (2016). A comparative view of regenerative neurogenesis in vertebrates. Development (Cambridge, England) *143*, 741–753.

Alunni, A., Krecsmarik, M., Bosco, A., Galant, S., Pan, L., Moens, C.B., and Bally-Cuif, L. (2013). Notch3 signaling gates cell cycle entry and limits neural stem cell amplification in the adult pallium. Development *140*, 3335–3347.

Alvarez-Buylla, A., and Garcia-Verdugo, J.M. (2002). Neurogenesis in adult subventricular zone. J Neurosci *22*, 629–634.

Anderson, M.A., Burda, J.E., Ren, Y., Ao, Y., O'Shea, T.M., Kawaguchi, R., Coppola, G., Khakh, B.S., Deming, T.J., and Sofroniew, M.V. (2016). Astrocyte scar formation aids central nervous system axon regeneration. Nature *532*, 195–200.

Arvidsson, A., Collin, T., Kirik, D., Kokaia, Z., and Lindvall, O. (2002). Neuronal replacement from endogenous precursors in the adult brain after stroke. Nature Medicine *8*, 963–970.

Ayari, B., Elhachimi, K.H., Yanicostas, C., Landoulsi, A., and Soussi-Yanicostas, N. (2010). Prokineticin 2 expression is associated with neural repair of injured adult zebrafish telencephalon. J Neurotrauma.

Barbosa, J., Gonzalez-Sanchez, R., Di Giaimo, R., Baumgardt Violette, E., Theis, F., Götz, M., and Ninkovic, J. (2015). Live imaging of adult neural stem cell behavior in the intact and injured zebrafish brain. Science *in press*.

Barbosa, J.S., Di Giaimo, R., Gotz, M., and Ninkovic, J. (2016). Single-cell in vivo imaging of adult neural stem cells in the zebrafish telencephalon. Nat. Protocols *11*, 1360–1370.

Basu, S., Cheriyamundath, S., and Ben-Ze'ev, A. (2018). Cell–cell adhesion: linking Wnt/β-catenin signaling with partial EMT and stemness traits in tumorigenesis. F1000Res *7*.

Baumgart, E.V., Barbosa, J.S., Bally-Cuif, L., Gotz, M., and Ninkovic, J. (2012). Stab wound injury of the zebrafish telencephalon: a model for comparative analysis of reactive gliosis. Glia *60*, 343–357.

Becker, C.G., and Becker, T. (2008). Adult zebrafish as a model for successful central nervous system regeneration. Restor Neurol Neurosci *26*, 71–80.

Bendel, O., Bueters, T., von Euler, M., Ögren, S.O., Sandin, J., and von Euler, G. (2005). Reappearance of Hippocampal CA1 Neurons after Ischemia is Associated with Recovery of Learning and Memory. J Cereb Blood Flow Metab *25*, 1586–1595.

Bernier, P.J., Bédard, A., Vinet, J., Lévesque, M., and Parent, A. (2002). Newly generated neurons in the amygdala and adjoining cortex of adult primates. Proc Natl Acad Sci U S A *99*, 11464–11469.

Bersten, D.C., Sullivan, A.E., Peet, D.J., and Whitelaw, M.L. (2013). bHLH–PAS proteins in cancer. Nature Reviews Cancer *13*, 827–841.

Bhardwaj, R.D., Curtis, M.A., Spalding, K.L., Buchholz, B.A., Fink, D., Bjork-Eriksson, T., Nordborg, C., Gage, F.H., Druid, H., Eriksson, P.S., et al. (2006). Neocortical neurogenesis in humans is restricted to development. Proc Natl Acad Sci U S A *103*, 12564–12568.

Boitano, A.E., Wang, J., Romeo, R., Bouchez, L.C., Parker, A.E., Sutton, S.E., Walker, J.R., Flaveny, C.A., Perdew, G.H., Denison, M.S., et al. (2010). Aryl Hydrocarbon Receptor Antagonists Promote the Expansion of Human Hematopoietic Stem Cells. Science *329*, 1345–1348.

Bond, A.M., Ming, G., and Song, H. (2015). Adult Mammalian Neural Stem Cells and Neurogenesis: Five Decades Later. Cell Stem Cell *17*, 385–395.

Breunig, C.T., Durovic, T., Neuner, A.M., Baumann, V., Wiesbeck, M.F., Koferle, A., Gotz, M., Ninkovic, J., and Stricker, S.H. (2018). One step generation of customizable gRNA vectors for multiplex CRISPR approaches through string assembly gRNA cloning (STAgR). PloS One *13*, e0196015.

Brill, M.S., Ninkovic, J., Winpenny, E., Hodge, R.D., Ozen, I., Yang, R., Lepier, A., Gascon, S., Erdelyi, F., Szabo, G., et al. (2009). Adult generation of glutamatergic olfactory bulb interneurons. Nat Neurosci *12(12)*, 1524–1533.

Buffo, A., Rite, I., Tripathi, P., Lepier, A., Colak, D., Horn, A.P., Mori, T., and Gotz, M. (2008). Origin and progeny of reactive gliosis: A source of multipotent cells in the injured brain. Proc Natl Acad Sci U S A *105*, 3581–3586.

Burda, J.E., and Sofroniew, M.V. (2014). Reactive gliosis and the multicellular response to CNS damage and disease. Neuron *81*, 229–248.

Burda, J.E., Bernstein, A.M., and Sofroniew, M.V. (2016). Astrocyte roles in traumatic brain injury. Exp Neurol *275*, 305–315.

Casado, F.L. (2016). The Aryl Hydrocarbon Receptor Relays Metabolic Signals to Promote Cellular Regeneration. Stem Cells Int *2016*, 4389802.

Chang, E.H., Adorjan, I., Mundim, M.V., Sun, B., Dizon, M.L.V., and Szele, F.G. (2016). Traumatic Brain Injury Activation of the Adult Subventricular Zone Neurogenic Niche. Front Neurosci *10*.

Chapouton, P., Adolf, B., Leucht, C., Tannhauser, B., Ryu, S., Driever, W., and Bally-Cuif, L. (2006). her5 expression reveals a pool of neural stem cells in the adult zebrafish midbrain. Development (Cambridge, England) *133*, 4293–4303.

Chapouton, P., Skupien, P., Hesl, B., Coolen, M., Moore, J.C., Madelaine, R., Kremmer, E., Faus-Kessler, T., Blader, P., Lawson, N.D., et al. (2010). Notch Activity Levels Control the Balance between Quiescence and Recruitment of Adult Neural Stem Cells. The Journal of Neuroscience *30*, 7961–7974.

Chen, W.-C., Chang, L.-H., Huang, S.-S., Huang, Y.-J., Chih, C.-L., Kuo, H.-C., Lee, Y.-H., and Lee, I.-H. (2019). Aryl hydrocarbon receptor modulates stroke-induced astrogliosis and neurogenesis in the adult mouse brain. Journal of Neuroinflammation *16*, 187.

Cosacak, M.I., Papadimitriou, C., and Kizil, C. (2015). Regeneration, Plasticity, and Induced Molecular Programs in Adult Zebrafish Brain. Biomed Res Int *2015*, 769763.

Cuartero, M.I., Ballesteros, I., de la Parra, J., Harkin, A.L., Abautret-Daly, A., Sherwin, E., Fernández-Salguero, P., Corbí, A.L., Lizasoain, I., and Moro, M.A. (2014). L-kynurenine/aryl hydrocarbon receptor pathway mediates brain damage after experimental stroke. Circulation *130*, 2040–2051.

Dabir, P., Marinic, T.E., Krukovets, I., and Stenina, O.I. (2008). Aryl hydrocarbon receptor is activated by glucose and regulates the thrombospondin-1 gene promoter in endothelial cells. Circ. Res. *102*, 1558–1565.

Davalos, D., Grutzendler, J., Yang, G., Kim, J.V., Zuo, Y., Jung, S., Littman, D.R., Dustin, M.L., and Gan, W.-B. (2005). ATP mediates rapid microglial response to local brain injury in vivo. Nat. Neurosci. *8*, 752–758.

Di Giaimo, R., Durovic, T., Barquin, P., Kociaj, A., Lepko, T., Aschenbroich, S., Breunig, C.T., Irmler, M., Cernilogar, F.M., Schotta, G., et al. (2018). The Aryl Hydrocarbon Receptor Pathway Defines the Time Frame for Restorative Neurogenesis. Cell Reports *25*, 3241-3251.e5.

Dimou, L., and Gotz, M. (2014). Glial cells as progenitors and stem cells: new roles in the healthy and diseased brain. Physiol Rev *94*, 709–737.

Diotel, N., Vaillant, C., Gueguen, M.-M., Mironov, S., Anglade, I., Servili, A., Pellegrini, E., and Kah, O. (2010). Cxcr4 and Cxcl12 expression in radial glial cells of the brain of adult zebrafish. Journal of Comparative Neurology *518*, 4855–4876.

Doetsch, F., and Alvarez-Buylla, A. (1996). Network of tangential pathways for neuronal migration in adult mammalian brain. Proc. Natl. Acad. Sci. U.S.A. *93*, 14895–14900.

Dray, N., Bedu, S., Vuillemin, N., Alunni, A., Coolen, M., Krecsmarik, M., Supatto, W., Beaurepaire, E., and Bally-Cuif, L. (2015). Large-scale live imaging of adult neural stem cells in their endogenous niche. Development *142*, 3592–3600.

Durovic, and Ninkovic, (last) (2019). Electroporation Method for In Vivo Delivery of Plasmid DNA in the Adult Zebrafish Telencephalon. JoVE e60066.

Edelmann, K., Glashauser, L., Sprungala, S., Hesl, B., Fritschle, M., Ninkovic, J., Godinho, L., and Chapouton, P. (2013). Increased radial glia quiescence, decreased reactivation upon injury and unaltered neuroblast behavior underlie decreased neurogenesis in the aging zebrafish telencephalon. J Comp Neurol *521*, 3099–3115.

Ehninger, D., and Kempermann, G. (2003). Regional effects of wheel running and environmental enrichment on cell genesis and microglia proliferation in the adult murine neocortex. Cereb. Cortex *13*, 845–851.

Ernst, A., Alkass, K., Bernard, S., Salehpour, M., Perl, S., Tisdale, J., Possnert, G., Druid, H., and Frisen, J. (2014). Neurogenesis in the striatum of the adult human brain. Cell *156*, 1072–1083.

Faiz, M., Sachewsky, N., Gascón, S., Bang, K.W.A., Morshead, C.M., and Nagy, A. (2015). Adult Neural Stem Cells from the Subventricular Zone Give Rise to Reactive Astrocytes in the Cortex after Stroke. Cell Stem Cell *17*, 624–634.

Folgueira, M., Bayley, P., Navratilova, P., Becker, T.S., Wilson, S.W., and Clarke, J.D. (2012). Morphogenesis underlying the development of the everted teleost telencephalon. Neural Dev *7*, 32.

Frik, J., Merl-Pham, J., Plesnila, N., Mattugini, N., Kjell, J., Kraska, J., Gómez, R.M., Hauck, S.M., Sirko, S., and Götz, M. (2018). Cross-talk between monocyte invasion and astrocyte proliferation regulates scarring in brain injury. EMBO Rep *19*.

Fukuzaki, Y., Shin, H., Kawai, H.D., Yamanoha, B., and Kogure, S. (2015). 532 nm Low-Power Laser Irradiation Facilitates the Migration of GABAergic Neural Stem/Progenitor Cells in Mouse Neocortex. PLoS One *10*.

Furness, S.G.B., Lees, M.J., and Whitelaw, M.L. (2007). The dioxin (aryl hydrocarbon) receptor as a model for adaptive responses of bHLH/PAS transcription factors. FEBS Letters *581*, 3616–3625.

Ganz, J., Kaslin, J., Hochmann, S., Freudenreich, D., and Brand, M. (2010). Heterogeneity and Fgf dependence of adult neural progenitors in the zebrafish telencephalon. Glia *58*, 1345–1363.

Glaser, T., Brose, C., Franceschini, I., Hamann, K., Smorodchenko, A., Zipp, F., Dubois-Dalcq, M., and Brustle, O. (2007). Neural cell adhesion molecule polysialylation enhances the sensitivity of embryonic stem cell-derived neural precursors to migration guidance cues. STEM CELLS *25*, 3016–3025.

Götz, M., Hartfuss, E., and Malatesta, P. (2002). Radial glial cells as neuronal precursors: a new perspective on the correlation of morphology and lineage restriction in the developing cerebral cortex of mice. Brain Res. Bull. *57*, 777–788.

Gould, E., Vail, N., Wagers, M., and Gross, C.G. (2001). Adult-generated hippocampal and neocortical neurons in macaques have a transient existence. PNAS *98*, 10910–10917.

Grade, S., and Götz, M. (2017). Neuronal replacement therapy: previous achievements and challenges ahead. NPJ Regen Med *2*, 29.

Grandel, H., Kaslin, J., Ganz, J., Wenzel, I., and Brand, M. (2006). Neural stem cells and neurogenesis in the adult zebrafish brain: origin, proliferation dynamics, migration and cell fate. Dev Biol *295*, 263–277.

Hanisch, U.-K., and Kettenmann, H. (2007). Microglia: active sensor and versatile effector cells in the normal and pathologic brain. Nat Neurosci *10*, 1387–1394.

Hu, W., Wang, Z., Zhang, S., Lu, X., Wu, J., Yu, K., Ji, A., Lu, W., Wang, Z., Wu, J., et al. (2019). IQGAP1 promotes pancreatic cancer progression and epithelial-mesenchymal transition (EMT) through Wnt/β-catenin signaling. Sci Rep *9*, 1–12.

Inta, D., Cameron, H.A., and Gass, P. (2015). New neurons in the adult striatum: from rodents to humans. Trends Neurosci *38*, 517–523.

Kálmán, M. (2002). GFAP expression withdraws--a trend of glial evolution? Brain Research Bulletin *57*, 509–511.

Kawasaki, H., Chang, H.-W., Tseng, H.-C., Hsu, S.-C., Yang, S.-J., Hung, C.-H., Zhou, Y., and Huang, S.-K. (2014). A tryptophan metabolite, kynurenine, promotes mast cell activation through aryl hydrocarbon receptor. Allergy *69*, 445–452.

Kimura, A., Naka, T., Nakahama, T., Chinen, I., Masuda, K., Nohara, K., Fujii-Kuriyama, Y., and Kishimoto, T. (2009). Aryl hydrocarbon receptor in combination with Stat1 regulates LPS-induced inflammatory responses. J Exp Med *206*, 2027–2035.

Kishimoto, N., Shimizu, K., and Sawamoto, K. (2012). Neuronal regeneration in a zebrafish model of adult brain injury. Dis Model Mech *5*, 200–209.

Kizil, C., Kaslin, J., Kroehne, V., and Brand, M. (2012a). Adult neurogenesis and brain regeneration in zebrafish. Developmental Neurobiology *72*, 429–461.

Kizil, C., Dudczig, S., Kyritsis, N., Machate, A., Blaesche, J., Kroehne, V., and Brand, M. (2012b). The chemokine receptor cxcr5 regulates the regenerative neurogenesis response in the adult zebrafish brain. Neural Development *7*, 27.

Kizil, C., Kyritsis, N., Dudczig, S., Kroehne, V., Freudenreich, D., Kaslin, J., and Brand, M. (2012c). Regenerative neurogenesis from neural progenitor cells requires injury-induced expression of Gata3. Developmental Cell *23*, 1230–1237.

Kizil, C., Kyritsis, N., and Brand, M. (2015). Effects of inflammation on stem cells: together they strive? EMBO Rep *16*, 416–426.

Ko, C.-I., and Puga, A. (2017). Does the Aryl Hydrocarbon Receptor Regulate Pluripotency? Curr Opin Toxicol *2*, 1–7.

Ko, C.-I., Fan, Y., de Gannes, M., Wang, Q., Xia, Y., and Puga, A. (2016). Repression of the Aryl Hydrocarbon Receptor Is Required to Maintain Mitotic Progression and Prevent Loss of Pluripotency of Embryonic Stem Cells. Stem Cells *34*, 2825–2839.

Koketsu, D., Mikami, A., Miyamoto, Y., and Hisatsune, T. (2003). Nonrenewal of Neurons in the Cerebral Neocortex of Adult Macaque Monkeys. J. Neurosci. *23*, 937–942.

Kornack, D.R., and Rakic, P. (2001). Cell Proliferation Without Neurogenesis in Adult Primate Neocortex. Science *294*, 2127–2130.

Kroehne, V., Freudenreich, D., Hans, S., Kaslin, J., and Brand, M. (2011). Regeneration of the adult zebrafish brain from neurogenic radial glia-type progenitors. Development (Cambridge, England) *138*, 4831–4841.

Kuge, A., Takemura, S., Kokubo, Y., Sato, S., Goto, K., and Kayama, T. (2009). Temporal profile of neurogenesis in the subventricular zone, dentate gyrus and cerebral cortex following transient focal cerebral ischemia. Neurological Research *31*, 969–976.

Kyritsis, N., Kizil, C., Zocher, S., Kroehne, V., Kaslin, J., Freudenreich, D., Iltzsche, A., and Brand, M. (2012). Acute inflammation initiates the regenerative response in the adult zebrafish brain. Science *338*, 1353–1356.

Laiosa, M.D., Tate, E.R., Ahrenhoerster, L.S., Chen, Y., and Wang, D. (2016). Effects of Developmental Activation of the Aryl Hydrocarbon Receptor by 2,3,7,8-Tetrachlorodibenzo-p-dioxin on Long-term Self-renewal of Murine Hematopoietic Stem Cells. Environ Health Perspect *124*, 957–965.

Lange, C., Rost, F., Machate, A., Reinhardt, S., Lesche, M., Weber, A., Kuscha, V., Dahl, A., Rulands, S., and Brand, M. (2020). Single cell sequencing of radial glia progeny reveals the diversity of newborn neurons in the adult zebrafish brain. Development *147*.

Lanham, K.A., Prasch, A.L., Weina, K.M., Peterson, R.E., and Heideman, W. (2011). A Dominant Negative Zebrafish Ahr2 Partially Protects Developing Zebrafish from Dioxin Toxicity. PLoS One *6*.

Latchney, S.E., Hein, A.M., O'Banion, M.K., DiCicco-Bloom, E., and Opanashuk, L.A. (2013). Deletion or activation of the aryl hydrocarbon receptor alters adult hippocampal neurogenesis and contextual fear memory. J Neurochem *125*, 430–445.

Lee, J., Cella, M., McDonald, K., Garlanda, C., Kennedy, G.D., Nukaya, M., Mantovani, A., Kopan, R., Bradfield, C.A., Newberry, R., et al. (2011). AHR drives the development of gut ILC22 cells and postnatal lymphoid tissues via pathways dependent on and independent of Notch. Nat Immunol *13*, 144–151.

Li, M., Zhao, L., Page-McCaw, P.S., and Chen, W. (2016). Zebrafish Genome Engineering Using the CRISPR-Cas9 System. Trends Genet. *32*, 815–827.

Lindsey, B.W., Darabie, A., and Tropepe, V. (2012). The cellular composition of neurogenic periventricular zones in the adult zebrafish forebrain. J. Comp. Neurol. *520*, 2275–2316.

Liu, R.-X., Ma, J., Wang, B., Tian, T., Guo, N., and Liu, S.-J. (2020). No DCX-positive neurogenesis in the cerebral cortex of the adult primate. Neural Regen Res *15*, 1290–1299.

Lois, C., and Alvarez-Buylla, A. (1993). Proliferating subventricular zone cells in the adult mammalian forebrain can differentiate into neurons and glia. Proc Natl Acad Sci U S A *90*, 2074–2077.

Luzzati, F., De Marchis, S., Fasolo, A., and Peretto, P. (2006). Neurogenesis in the Caudate Nucleus of the Adult Rabbit. J. Neurosci. *26*, 609–621.

Madsen, T.M., Yeh, D.D., Valentine, G.W., and Duman, R.S. (2005). Electroconvulsive Seizure Treatment Increases Cell Proliferation in Rat Frontal Cortex. Neuropsychopharmacol *30*, 27–34.

Magavi, S.S., Leavitt, B.R., and Macklis, J.D. (2000). Induction of neurogenesis in the neocortex of adult mice. Nature *405*, 951–955.

Magnusson, J.P., Goritz, C., Tatarishvili, J., Dias, D.O., Smith, E.M., Lindvall, O., Kokaia, Z., and Frisen, J. (2014). A latent neurogenic program in astrocytes regulated by Notch signaling in the mouse. Science *346*, 237–241.

März, M., Chapouton, P., Diotel, N., Vaillant, C., Hesl, B., Takamiya, M., Lam, C.S., Kah, O., Bally-Cuif, L., and Strähle, U. (2010). Heterogeneity in progenitor cell subtypes in the ventricular zone of the zebrafish adult telencephalon. Glia *58*, 870–888.

März, M., Schmidt, R., Rastegar, S., and Strähle, U. (2011). Regenerative response following stab injury in the adult zebrafish telencephalon. Dev. Dyn. *240*, 2221–2231.

Mathew, L.K., Simonich, M.T., and Tanguay, R.L. (2009). AHR-dependent misregulation of Wnt signaling disrupts tissue regeneration. Biochem Pharmacol *77*, 498–507.

Mueller, T., Dong, Z., Berberoglu, M.A., and Guo, S. (2011). The Dorsal Pallium in Zebrafish, Danio rerio (Cyprinidae, Teleostei). Brain Res *1381*, 95–105.

Mulero-Navarro, S., and Fernandez-Salguero, P.M. (2016). New Trends in Aryl Hydrocarbon Receptor Biology. Front Cell Dev Biol *4*, 45.

Nakatomi, H., Kuriu, T., Okabe, S., Yamamoto, S., Hatano, O., Kawahara, N., Tamura, A., Kirino, T., and Nakafuku, M. (2002). Regeneration of Hippocampal Pyramidal Neurons after Ischemic Brain Injury by Recruitment of Endogenous Neural Progenitors. *110*, 429–441.

Nato, G., Caramello, A., Trova, S., Avataneo, V., Rolando, C., Taylor, V., Buffo, A., Peretto, P., and Luzzati, F. (2015). Striatal astrocytes produce neuroblasts in an excitotoxic model of Huntington's disease. Development *142*, 840–845.

Nemirovich-Danchenko, N.M., and Khodanovich, M.Yu. (2019). New Neurons in the Post-ischemic and Injured Brain: Migrating or Resident? Front Neurosci *13*.

Nimmerjahn, A., Kirchhoff, F., and Helmchen, F. (2005). Resting microglial cells are highly dynamic surveillants of brain parenchyma in vivo. Science *308*, 1314–1318.

Ohira, K., Furuta, T., Hioki, H., Nakamura, K.C., Kuramoto, E., Tanaka, Y., Funatsu, N., Shimizu, K., Oishi, T., Hayashi, M., et al. (2010). Ischemia-induced neurogenesis of neocortical layer 1 progenitor cells. Nat. Neurosci. *13*, 173–179.

Oyarce, K., Bongarzone, E.R., and Nualart, F. (2014). Unconventional Neurogenic Niches and Neurogenesis Modulation by Vitamins. J Stem Cell Res Ther *4*, 184.

van Praag, H., Schinder, A.F., Christie, B.R., Toni, N., Palmer, T.D., and Gage, F.H. (2002a). Functional neurogenesis in the adult hippocampus. Nature *415*, 1030–1034.

van Praag, H., Schinder, A.F., Christie, B.R., Toni, N., Palmer, T.D., and Gage, F.H. (2002b). Functional neurogenesis in the adult hippocampus. Nature *415*, 1030–1034.

Rentas, S., Holzapfel, N., Belew, M.S., Pratt, G., Voisin, V., Wilhelm, B.T., Bader, G.D., Yeo, G.W., and Hope, K.J. (2016). Musashi-2 Attenuates AHR Signaling to Expand Human Hematopoietic Stem Cells. Nature *532*, 508–511.

Rothenaigner, I., Krecsmarik, M., Hayes, J.A., Bahn, B., Lepier, A., Fortin, G., Gotz, M., Jagasia, R., and Bally-Cuif, L. (2011). Clonal analysis by distinct viral vectors identifies bona fide neural stem cells in the adult zebrafish telencephalon and characterizes their division properties and fate. Development (Cambridge, England) *138*, 1459–1469.

Rothhammer, V., Mascanfroni, I.D., Bunse, L., Takenaka, M.C., Kenison, J.E., Mayo, L., Chao, C.C., Patel, B., Yan, R., Blain, M., et al. (2016). Type I interferons and microbial metabolites of tryptophan modulate astrocyte activity and central nervous system inflammation via the aryl hydrocarbon receptor. Nature Medicine *22*, 586–597.

Schmidt, R., Strahle, U., and Scholpp, S. (2013). Neurogenesis in zebrafish - from embryo to adult. Neural Development *8*, 3.

Spalding, K.L., Bhardwaj, R.D., Buchholz, B.A., Druid, H., and Frisén, J. (2005). Retrospective birth dating of cells in humans. Cell *122*, 133–143.

Stevens, E.A., Mezrich, J.D., and Bradfield, C.A. (2009). The aryl hydrocarbon receptor: a perspective on potential roles in the immune system. Immunology *127*, 299–311.

Stocchetti, N., and Zanier, E.R. (2016). Chronic impact of traumatic brain injury on outcome and quality of life: a narrative review. Crit Care *20*.

Stockinger, B., Di Meglio, P., Gialitakis, M., and Duarte, J.H. (2014). The aryl hydrocarbon receptor: multitasking in the immune system. Annu. Rev. Immunol. *32*, 403–432.

Sun, D. (2014). The potential of endogenous neurogenesis for brain repair and regeneration following traumatic brain injury. Neural Regen Res *9*, 688–692.

Thored, P., Arvidsson, A., Cacci, E., Ahlenius, H., Kallur, T., Darsalia, V., Ekdahl, C.T., Kokaia, Z., and Lindvall, O. (2006). Persistent production of neurons from adult brain stem cells during recovery after stroke. STEM CELLS *24*, 739–747.

Viales, R.R., Diotel, N., Ferg, M., Armant, O., Eich, J., Alunni, A., Marz, M., Bally-Cuif, L., Rastegar, S., and Strahle, U. (2015). The helix-loop-helix protein id1 controls stem cell proliferation during regenerative neurogenesis in the adult zebrafish telencephalon. Stem Cells *33*, 892–903.

Wang, Lawson, M.A., Dantzer, R., and Kelley, K.W. (2010). LPS-induced indoleamine 2,3-dioxygenase is regulated in an interferon-c- 3 independent manner by a JNK signaling pathway in primary murine microglia. Brain Behav Immun *24*, 201.

Wang, H., La Russa, M., and Qi, L.S. (2016). CRISPR/Cas9 in Genome Editing and Beyond. Annu. Rev. Biochem. *85*, 227–264.

Xie, Y., and Dorsky, R.I. (2017). Development of the hypothalamus: conservation, modification and innovation. Development *144*, 1588–1599.

Yamashita, T., Ninomiya, M., Hernández Acosta, P., García-Verdugo, J.M., Sunabori, T., Sakaguchi, M., Adachi, K., Kojima, T., Hirota, Y., Kawase, T., et al. (2006). Subventricular zone-derived neuroblasts migrate and differentiate into mature neurons in the post-stroke adult striatum. J. Neurosci. *26*, 6627–6636.

Yan, E.B., Frugier, T., Lim, C.K., Heng, B., Sundaram, G., Tan, M., Rosenfeld, J.V., Walker, D.W., Guillemin, G.J., and Morganti-Kossmann, M.C. (2015). Activation of the kynurenine pathway and increased production of the excitotoxin quinolinic acid following traumatic brain injury in humans. J Neuroinflammation *12*, 110.

Zambusi, A., and Ninkovic, J. (2020). Regeneration of the central nervous system-principles from brain regeneration in adult zebrafish. World Journal of Stem Cells *12*, 8–24.

Zupanc, G.K., Hinsch, K., and Gage, F.H. (2005). Proliferation, migration, neuronal differentiation, and long-term survival of new cells in the adult zebrafish brain. J Comp Neurol *488*, 290–319.

Publications

- Di Giaimo, R.*, **Durovic, T**.*, Barquin, P., Kociaj, A., Lepko, T., Aschenbroich, S., Breunig, C.T., Irmler, M., Cernilogar, F.M., Schotta, G., et al. (2018). **The Aryl Hydrocarbon Receptor Pathway Defines the Time Frame for Restorative Neurogenesis**. *Cell Reports*. 2018 Dec 18; 25(12): 3241-3251.e5. doi: 10.1016/j.celrep.2018.

  * authors contributed equally to the manuscript

- **Durovic T**., Ninkovic, J. **Electroporation Method for In Vivo Delivery of Plasmid DNA in the Adult Zebrafish Telencephalon**. *J. Vis. Exp.* 2019 Sep 13; (151), e60066, doi:10.3791/60066 (2019).

- Breunig, C.T., **Durovic, T**., Neuner, A.M., Baumann, V., Wiesbeck, M.F., Koferle, A., Götz, M., Ninkovic, J., and Stricker, S.H. **One step generation of customizable gRNA vectors for multiplex CRISPR approaches through string assembly gRNA cloning (STAgR)**. *PloS One.* 2018 Apr 27; 13(4):e0196015. doi: 10.1371/journal.pone.0196015.

Author contributions

The Aryl Hydrocarbon Receptor Pathway Defines the Time Frame for Restorative Neurogenesis

Rossella Di Giaimo *, **Tamara Durovic ***, Pablo Barquin, Anita Kociaj, Tjasa Lepko, Sven Aschenbroich, Christopher T. Breunig, Martin Irmler, Filippo M. Cernilogar, Gunnar Schotta, Joana S. Barbosa, Dietrich Trumbach, Emily Violette Baumgart, Andrea M. Neuner, Johannes Beckers, Wolfgang Wurst, Stefan H. Stricker, and Jovica Ninkovic.

* The authors contributed equally to the manuscript

The contribution of autors is as follows:

R.D.G. and J.N. conceived the project and experiments. R.D.G., T.D., A.K.,M.I., F.M.C., J.B., E.V.B., P.B., C.T.B., A.M.N., and S.H.S. performed the experiments and analysed the data; M.I., G.S., and D.T. performed the bioinformatics analyses. R.D.G., J.N., and T.D. wrote the manuscript with inputs from P.B., A.K., M.I., F.M.C., G.S., J.B., D.T., E.V.B., J.S.B., and W.W

For this paper I performed one half of all experiments and analysed all the data coming from those experiments. The other half of the experiments and data analyses was done by Prof. Dr. Rossella Di Giaimo, with whom I share first co-authorship. I also contributed to writing process, together with Prof. Dr. Jovica Ninkovic and Prof. Dr. Rossella Di Giaimo.

Confirmation of author contributions:

Prof. Dr. Rossella DiGiaimo

Tamara Đurović

Prof. Dr. Jovica Ninković

Electroporation Method for In Vivo Delivery of Plasmid DNA in the Adult Zebrafish Telencephalon

Tamara Durovic, Jovica Ninkovic

For this paper I performed all the experiments and analysed all the data. I wrote manuscript drafts, which were reviewed and edited by Prof. Dr. Jovica Ninkovic until final manuscript version.

I obtained explicit written permission to reuse my JoVE article in my thesis, as long as I ensure that JoVE is properly attributed and cited throughout.

Confirmation of author contribution:

Prof. Dr. Jovica Ninković	Tamara Đurović

One step generation of customizable gRNA vectors for multiplex CRISPR approaches through string assembly gRNA cloning (STAgR)

Christopher T. Breunig, **Tamara Durovic**, Andrea M. Neuner, Valentin Baumann, Maximilian F. Wiesbeck, Anna Köferle, Magdalena Götz, Jovica Ninkovic and Stefan H. Stricker.

The contribution of autors is as follows:

Conceptualization: Christopher T. Breunig, Anna Köferle, Jovica Ninkovic,Stefan H.Stricker. **Data curation**: Christopher T.Breunig, **Tamara Durovic**, Andrea M.Neuner, Valentin Baumann, Maximilian F.Wiesbeck. Formal analysis: Christopher T. Breunig. **Funding acquisition**: Magdalena Götz, Stefan H. Stricker. **Investigation**: Christopher T. Breunig, Tamara Durovic, Andrea M. Neuner, Valentin Baumann, Maximilian F. Wiesbeck, Anna Köferle. **Methodology**: Christopher T. Breunig, **Tamara Durovic**, Andrea M. Neuner, Anna Köferle, Jovica Ninkovic, Stefan H. Stricker. **Project administration**: Magdalena Götz, Stefan H. Stricker. **Resources**: Stefan H. Stricker. **Supervision**: Christopher T. Breunig, Magdalena Götz, Jovica Ninkovic, Stefan H. Stricker. **Validation**: Christopher T. Breunig. Visualization:

Christopher T. Breunig, **Tamara Durovic**. **Writing-original draft**: Christopher T. Breunig, Stefan H. Stricker. **Writing - review & editing**: Stefan H. Stricker

For this paper I was solely involved in experiments with zebrafish, testing the efficiency of StagR-Cas9 construct in vivo in zebrafish telencephalon, and describing electroporation procedure in the manuscript.

Confirmation of author contribution:

Prof. Dr. Jovica Ninković

Tamara Đurović

Acknowledgements

Firstly, I would particularly like to thank my supervisor, Prof. Dr. Jovica Ninković for giving me the opportunity to carry out my thesis in his group. I owe my deepest gratitude to Jovica for the supervision, knowledge and guidance he provided during the whole duration of my PhD thesis and for his availability and time whenever I needed his suggestion, advice or a sense of direction concerning my project. His exceptional scientific ideas and great enthusiasm were a leading light for successful completion of this thesis, which I am truly grateful for. Most importantly, I wholeheartedly appreciate his understanding and support during the times of personal crisis, which cannot be forgotten, since it helped me overcome the difficulties and regain motivation. Without Jovica´s guidance and persistent help this dissertation would not have been materialized.

Next, I have greatly benefited from the help of Dr. Rosario Sanchez Gonzales, whether it was work related or personal. I would like to offer my special thanks to her, for all the insightful scientific discussion, generous feedback, comments and suggestions throughout my PhD studies. But above all, I am deeply grateful for the personal support and encouragement she was offering. Her advice and comments were valuable, even when they were not gently presented or what I wanted to hear. All of this enormously helped me to progress, advance and develop.

I'd also like to extend my gratitude to Dr. Joana Santos Barbosa for her generous help with my beginnings, patience and for teaching me many crucial techniques that were necessary basis of my further work. I also had a pleasure of working with Emily Violette Baumgart, and I am very grateful for her support, patience and great amount of assistance throughout my beginnings. I gratefully acknowledge scientific contribution, experience and insights provided by Prof. Dr. Magdalena Götz, which greatly helped to shape and improve my work. Additionally, I am very thankful for the amazing scientific environment Magdalena created on our Department. This Department was and is full of amazing people, who altogether were big professional help and many of them became also dear friends (special thanks to Sonia, Bob and Allwyn). Great atmosphere that was created and fun and enjoyable times we shared inside and outside of the lab, strongly influenced my fondness of coming to work every day and considerably eased less good days. My deepest appreciation goes for all those people and moments we shared together during the whole length of my PhD. I would additionally like to recognize and thank Sven Falk for teaching me basis of confocal microscopy, for transferring valuable knowledge and for his support with sharing the responsibilities of ´´confocal responsible´´ persons. I must also thank Christopher Breunig for his help and collaboration on our papers and for being a friend in the tough moments.

I am extending my warmest thanks also to all ´´old´´ and ´´new´´ PhD students and members of Ninković group, without listing all the names, for each person was helpful in various occasions. I am very grateful for the fun working atmosphere we always had, help they

extended whenever needed and for all the good and not so good moments we shared together.

I also had great pleasure of being GSN student and I very much appreciate everything that being GSN student meant. I´d like to extend my gratitude for all the lovely GSN employees, who were always extremely helpful, for all the useful courses, for all the financial help to attend the conferences, for the entertaining and enjoyable social events and for many other benefits I received throughout my studies as a part of the GSN. I would like to thank members of my TAC committee as well, for taking their time, for practical help and valuable advice and for always being very supportive.

I owe my heartfelt appreciation to all my friends in Munich who extended generous emotional support and encouragement in various moments throughout my PhD – Paul, Lisa, Pablo, Elena, Isabel, Nina and Anna, whose help cannot be overestimated and who never wavered in their support. Here I would like to include my roommates as well – Severin, Anna and Julia, for being the easiest going flat mates ever and with whom living together was a pleasure.

Unconditional love of my family, my sister, father and especially my mother was essential throughout the whole period of my studies, and I cannot begin to express my gratitude for enormous amounts of support, encouragement and understanding that I have received from them, despite the distance.

Finally, I am indebted to my boyfriend Daniel for great amounts of emotional and practical support, for never failing to be there whenever I needed and for regularly feeding me all those extremely busy days of my PhD and thesis writing. I am deeply grateful and lucky for his love.